

**DIMERIZATION OF TRANSCRIPTION FACTORS IN GENE EXPRESSION  
MODELS: THE CONTROL OF HMP SYNTHESIS BY NSRR AS A CASE STUDY**

**MOHAMMAD HAMIDI**  
**Master of Science in Physical Chemistry, Azad University, 2014**

A thesis submitted  
in partial fulfilment of the requirements for the degree of

**MASTER OF SCIENCE**

in

**BIOCHEMISTRY**

Department of Chemistry and Biochemistry  
University of Lethbridge  
LETHBRIDGE, ALBERTA, CANADA

© Mohammad Hamidi, 2022

DIMERIZATION OF TRANSCRIPTION FACTORS IN GENE EXPRESSION  
MODELS: THE CONTROL OF HMP SYNTHESIS BY NSRR AS A CASE STUDY

MOHAMMAD HAMIDI

Date of Defence: December 20, 2022

Dr. M. Roussel Thesis Supervisor	Professor	Ph.D.
-------------------------------------	-----------	-------

Dr. S. Wetmore Thesis Examination Committee Member	Professor	Ph.D.
---	-----------	-------

Dr. T. Patel Thesis Examination Committee Member	Associate Professor	Ph.D.
---	---------------------	-------

Dr. M. Gerken Chair, Thesis Examination Committee	Professor	Ph.D.
--	-----------	-------

# Dedication

This thesis is dedicated to my wife, who is super supportive throughout my whole life.

# Abstract

Many transcription factors act as dimers or higher oligomers. The effects of dimerization of transcription factors in gene expression models are not well studied. However, explicit consideration of dimers and, especially, of their regulation, may affect the dynamical behavior of a model. In the present work, I study how the effects of dimerization of transcriptional factors impact gene expression and compare the results between models for the control of transcription assuming monomeric or dimeric transcription factors. NsrR is a nitric oxide (NO) sensor and a key regulator of NO metabolism in a number of bacterial species. NsrR uses an iron-sulfur cluster to sense NO. NsrR binds to gene promoters as a dimer. In *Streptomyces*, NsrR acts a repressor to regulate only two independent copies of the *hmp* gene and the *nsrR* gene. Nitrosylation of an iron-sulfur cluster in each NsrR monomer affects the ability of NsrR to bind to the promoters of these genes. Hmp catalyzes the detoxifying reaction of NO to the less toxic nitrate ion. In this study, I have built a base model in which NsrR acts as a (theoretical) monomer, and then I have generated two models where NsrR is a dimer that differ in the assumed effects of uneven nitrosylation of the two monomers in a dimer. Most of the parameters were estimated from the literature. The model equations for the three models were generated by using the rule-based modelling software BioNetGen. The monomer and dimer models behave essentially identically either at the default parameters estimated from the literature, or with changes in most of the parameters. However, by changing binding parameters for NsrR-promoter complexes or the rate of recycling of nitrosylated NsrR to the intact holo-protein, the monomer and dimer models can be made to behave differently.

# Acknowledgments

First and foremost, I am deeply grateful to my supervisor, Marc Roussel, whose guidance and encouragement has made this thesis possible. He has been an inspiration and molded my perspective on biochemistry. He truly embodied the role of an advisor as he pushed me to develop my own thoughts and abilities in order to make me a better, more well rounded researcher. I am grateful for all the knowledge and experience I have gained under Marc's supervision.

I would like to thank my thesis committee: Stacey and Trushar for giving me all their valuable comments.

I would also like to thank Professor James R. Faeder of the University of Pittsburgh for answering my questions about BioNetGen.

# Contents

<b>Dedication</b>	<b>iii</b>
<b>Abstract</b>	<b>iv</b>
<b>Acknowledgments</b>	<b>v</b>
<b>List of Tables</b>	<b>viii</b>
<b>List of Figures</b>	<b>ix</b>
<b>1 Introduction</b>	<b>1</b>
1.1 Biological Background . . . . .	1
1.1.1 Biological roles of nitric oxide . . . . .	1
1.1.2 Antibiotics and resistance . . . . .	2
1.1.3 Eliminating the toxicity of NO . . . . .	3
1.1.4 Regulation of NO-responsive genes . . . . .	3
1.2 Statement of the problem . . . . .	5
1.3 Previous work . . . . .	5
1.4 Justifying a study based on <i>Streptomyces</i> . . . . .	6
1.5 Rule-based modeling . . . . .	7
1.5.1 Modeling . . . . .	8
1.6 Plan of thesis . . . . .	9
<b>2 Methods</b>	<b>10</b>
<b>3 Dimerization of transcription factors in gene expression models: the control of Hmp synthesis by NsrR as a case study</b>	<b>12</b>
<b>Abstract</b>	<b>13</b>
3.1 Introduction . . . . .	14
3.2 Description of the models . . . . .	16
3.2.1 Hmp kinetics . . . . .	16
3.2.2 Monomeric model of NsrR dynamics (MM model) . . . . .	20
3.2.3 Dimer model 1 (DM1) . . . . .	24
3.2.4 Dimer model 2 (DM2) . . . . .	28
3.2.5 Parameter estimates . . . . .	29
3.3 Methods and software . . . . .	31
3.4 Results . . . . .	32

---

3.4.1	Dynamical behavior of the models at the default parameters . . . . .	33
3.4.2	Conditions making the models behave differently . . . . .	41
3.5	Discussion and conclusion . . . . .	46
<b>4</b>	<b>Conclusion</b>	<b>51</b>
4.1	Summary . . . . .	51
4.2	Future directions . . . . .	52
	<b>Bibliography</b>	<b>55</b>
<b>A</b>	<b>BioNetGen code</b>	<b>63</b>
A.1	Monomer (MM) . . . . .	63
A.2	Dimer model 1 (DM1) . . . . .	66
A.3	Dimer model 2 (DM2) . . . . .	69
<b>B</b>	<b>Differential equations</b>	<b>74</b>
B.1	Monomer (MM) . . . . .	74
B.2	Dimer model 1 (DM1) . . . . .	76
B.3	Dimer model 2 (DM2) . . . . .	82

# List of Tables

3.1 Default model parameters. . . . . 32

# List of Figures

1.1	Structures of NADPH and NADH. . . . .	4
3.1	Bifurcation diagram for model MM at the default parameters values. . . . .	34
3.2	Two-parameter phase diagram showing a cusp bifurcation. . . . .	35
3.3	Bifurcation diagrams for models DM1 and DM2. . . . .	36
3.4	NsrR family dimer concentrations vs [NO] at the default parameters for DM1	38
3.5	NsrR family dimer concentrations vs [NO] for model DM1 when $k_{AB} =$ $k_{BC} = k_{CD} = k_{DE} = k_{EF} = 1 \mu\text{M}^{-1}\text{s}^{-1}$ , other parameters being at their de- fault values. . . . .	40
3.6	Bifurcation diagram for model MM with all parameters as in Table 3.1 except $[\text{O}_2] = 16 \mu\text{M}$ . . . . .	41
3.7	Bifurcation diagrams for the three models at $k_r = 0.001 \text{ s}^{-1}$ . . . . .	43
3.8	Limit cycles for model DM2 at $k_r = 0.001 \text{ s}^{-1}$ . . . . .	44
3.9	Active promoter concentrations vs [NO] . . . . .	45
3.10	Bifurcation diagram for models MM, DM1 and DM2 when $k_{-B} = 1 \times$ $10^{-1}\text{s}^{-1}$ and $k_{-C} = 1 \times 10^{-3}\text{s}^{-1}$ . . . . .	47

# Chapter 1

## Introduction

### 1.1 Biological Background

#### 1.1.1 Biological roles of nitric oxide

Nitric oxide (NO) is an important molecule in biological systems as it is a signalling molecule in dilute solution and can be a toxic molecule when it is concentrated. For example, NO can act as a retrograde neurotransmitter in synapses [1], may decrease muscle soreness [2], can cause lower blood pressure [3] and may help manage type 2 diabetes [4]. Additionally, the mammalian immune system uses NO to try to kill bacteria [5], and bacteria have defences against it [6]. Also, the immune system makes NO as a general response to bacteria because NO is a signal used by the immune system in order to tell certain components to turn on [7]. Thus, studying NO and its biological roles can be helpful for modern medicine.

Enzymes play an important role in production and removal of NO in microorganisms. Nitric oxide is synthesized by an enzyme called NOS (NO synthase) [8] that catalyzes the conversion of L-arginine to L-citrulline [9]. On the other hand, NORs (nitric oxide reductases) which are bacterial enzymes, catalyze the reaction of NO to N<sub>2</sub>O (nitrous oxide) and H<sub>2</sub>O [10]. In general, four families of reductases catalyze the conversion of NO<sub>3</sub><sup>-</sup> (nitrate) to N<sub>2</sub> (nitrogen) as follows [11, 12]: NO<sub>3</sub><sup>-</sup>  $\xrightarrow{\text{Nar}}$  NO<sub>2</sub><sup>-</sup>  $\xrightarrow{\text{Nir}}$  NO  $\xrightarrow{\text{Nor}}$  N<sub>2</sub>O  $\xrightarrow{\text{N}_2\text{Or}}$  N<sub>2</sub> where Nar is the nitrate reductase enzyme, Nir is the nitrite reductase enzyme, Nor is the nitric oxide reductase enzyme and N<sub>2</sub>Or is the nitrous oxide reductase enzyme.

### 1.1.2 Antibiotics and resistance

The most effective treatment for bacterial infection is applying an antibiotic when the immune system cannot kill them. How can antibiotics help our immune system to kill the bacteria? There are some possibilities here [13]. Most traditional antibiotics attack the bacterial ribosome which stops translation. Some antibiotics interfere with the production of the cell wall. One of the big problems of developing antibiotics right now is that most of them have the same parts of the cell as targets. So, it is fairly easy for bacterial cells to evolve resistance to new antibiotics working in the same way.

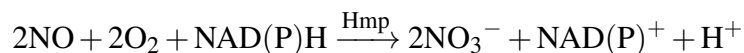
Some bacteria show resistance to antibiotics and are called antibiotic-resistant bacteria. For instance, *Escherichia coli*, *Klebsiella pneumoniae*, *Staphylococcus aureus*, and *Streptococcus pneumoniae* are bacteria that commonly develop antibiotic resistance [14]. Studying antibiotic-resistant bacteria can give us new approaches to the problem of antibiotic resistance by discovering how bacteria can handle antibiotic effects. One possibility is that the bacteria use efflux transporters to pump the antibiotic out of the cell. Bacteria can also evolve to change an antibiotic's target by mutating the target or using post-translational modifications in order to prevent binding of an antibiotic to its target [15].

According to the WHO's 2018 report entitled *Global Antimicrobial Surveillance System* [14], 500,000 patients were placed under bacterial infection surveillance in 22 different countries in a sampling process. The statistical review revealed that the percentage of bacteria showing defences against antibiotics ranged from 0 to 82 percent by country (resistant to at least one antibiotic), 0 to 51 percent resistant against penicillin and 8 to 65 percent of *E. coli* resistant against ciprofloxacin. Thus, studying a bacterial defence system such as the defence against NO could give us new approaches to treat patients with antibiotic-resistant infections, which are sorely needed.

### 1.1.3 Eliminating the toxicity of NO

Bacterial cells need a pathway to eliminate NO as NO damages the proteins and DNA of bacteria if they cannot eliminate it [16]. There are variations between types of bacteria, but typically an NO sensor based on an iron-sulfur cluster controls the expression of genes necessary to detoxify NO. For example, in *Streptomyces*, when NO is penetrating into a bacterial cell, it reacts with the iron-sulfur cluster of a transcription factor called NsrR. It takes several NO to completely react with the cluster, but as each NO reacts, it loosens the binding between NsrR and the promoters to which the former binds. This eventually allows the *hmp* gene to be expressed.

Hmp is the key enzyme that eliminates NO in most bacteria [16]. This detoxifying reaction is catalyzed by the Hmp enzyme [17]:



In this reaction, NAD(P)H binds to the enzyme first, and then O<sub>2</sub> and NO respectively [18]. If NO binds before O<sub>2</sub>, what will happen? NO binding before O<sub>2</sub> prevents O<sub>2</sub> binding to Hmp. Thus, Hmp cannot catalyze this reaction until the inhibitory NO dissociates.

The only difference between NADPH and NADH is that NADPH has one additional phosphate group (Fig. 1.1). Hmp can use both of them interchangeably.

### 1.1.4 Regulation of NO-responsive genes

One of the most important parts of any gene is its promoter which plays an integral role for the control of protein expression [19]. Transcription will be continued or stopped based on the type of regulatory proteins bound to the promoters of a gene [20]. Regulators of transcription can be either repressors or activators. If a repressor is bound to a promoter, transcription is stopped while an activator helps RNA polymerase bind to promoters that the polymerase cannot bind to on its own.

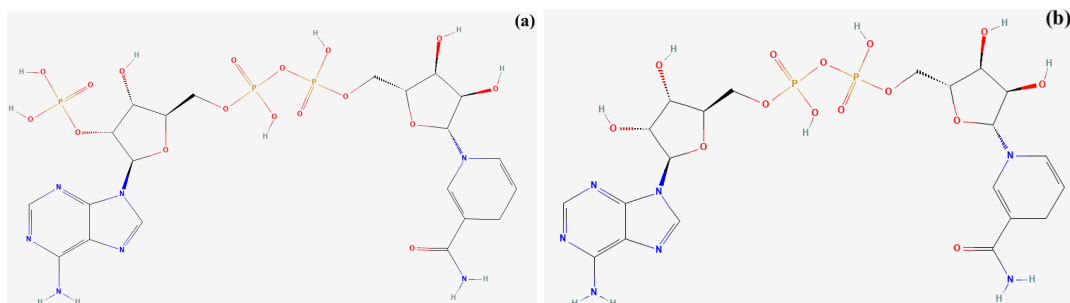


Figure 1.1: Structures of NADPH and NADH.

(a) NADPH structure. PubChem for CID 5884, Dihyronicotinamide-adenine dinucleotide phosphate beta-NADPH. <https://pubchem.ncbi.nlm.nih.gov/compound/5884>, in the public domain. (b) NADH structure. National Center for Biotechnology Information (2022). PubChem Compound Summary for CID 439153, 1,4-Dihyronicotinamide adenine dinucleotide. Retrieved October 29, 2022 from [https://pubchem.ncbi.nlm.nih.gov/compound/1\\_4-Dihyronicotinamide-adenine-dinucleotide](https://pubchem.ncbi.nlm.nih.gov/compound/1_4-Dihyronicotinamide-adenine-dinucleotide), in the public domain

Transcription factors often act as dimers or higher oligomers [21]. Some transcription factors are able to generate a number of distinct dimers with different binding partners. A protein can have different functions depending on its binding partner. A homodimer is a dimer which is formed from identical monomers and heterodimers are dimers consisting of different monomers. Homodimers are the most prevalent type of dimers across all species [22]. The transcription factor NsrR is a good example of a homodimer.

NsrR is a repressor of gene expression which is a member of the Rrf2 transcriptional regulator family [23]. The Rrf2 family belongs to the winged helix-turn-helix superfamily of prokaryotic transcriptional regulators [24]. A majority of its members act primarily as repressors [25]. Some of the other members of this superfamily are RsrR (Redox-sensitive response regulator) and IscR (Iron-sulfur cluster regulator) [25]. In most bacteria, there is at least one gene from the Rrf2 family. In this family, the N-terminus acts for binding to the promoter and the C-terminal is involved in signalling [26].

NsrR is widespread in bacteria. It was previously known to act as a repressor for redox reactions in *Nitrosomonas spp*, and has more recently been discovered to act as a regulator of nitric oxide metabolism in a number of bacterial species including gamma- and beta-proteobacteria, as well as gram-positive *Bacillus* and *Streptomyces*, based on the analysis

of Arkin's group [27].

NsrR requires a [4Fe-4S] cluster to act as a repressor. NO can react with the iron-sulfur cluster of NsrR. Since interfering with NsrR functions could sensitize bacterial cells to NO and make them vulnerable to attack by the mammalian immune system, it might be a new antibiotic target because of this role.

## 1.2 Statement of the problem

NsrR acts as a dimer in its biological functions. As mentioned, the effects of dimerization of transcription factors in gene expression models are not well studied. The reason is that generating and writing down a large number of differential equations for a dimeric system is a complicated and error-prone process. To address this issue, we used rule-based modeling to create models, as computers are good at repetitive tasks.

In a previous study, Roussel ignored the effects of dimerization of FNR in the Hmp control system in *E. coli* [18]. In *E. coli*, *hmp* is regulated by both FNR and NsrR, and FNR senses both nitric oxide and oxygen. Thus, pursuing the Hmp control system in *E. coli* might not be a good idea because of its complexity. On the other hand, in *Streptomyces*, *hmp* is regulated only by NsrR which only responds to nitric oxide.

Since NsrR is a representative of a group of iron-sulfur proteins that respond to NO [28, 29] and, more importantly, the kinetics of the reaction of NO with NsrR has been studied for *Streptomyces* [23], my main focus is on considering the effects of NsrR dimerization in models for the control of Hmp synthesis by NsrR in *Streptomyces* with the use of rule-based modeling.

## 1.3 Previous work

Roussel [18] has developed a delayed mass-action model for the control system for Hmp by another iron-sulfur protein called FNR in *E. coli*. He assembled a detailed biochemical model for the control of the synthesis of Hmp when FNR acts as a repressor of *hmp* tran-

scription. Also, he estimated parameters for the reactions, showed bistability in this model, and carried out the steady-state analysis for this model to show how the system dynamically behaves. In *E. coli*, *hmp* expression is controlled by both FNR and NsrR; however, he didn't consider regulation by NsrR. To my knowledge, there are no other detailed models of an *hmp* control system in any bacteria.

Robinson and Brynildsen described models for nitric oxide metabolism in *E. coli* [30, 31]. They demonstrated that Hmp is not just *an* enzyme that detoxifies NO, but that in fact it provides the main pathway for detoxifying NO. This is really important because it means that I can really focus on Hmp without worrying about other pathways that may consume NO. Their models are comprehensive ones for NO metabolism including empirical expressions for the control of Hmp expression. Although their models answer important questions about nitric oxide metabolism, they didn't take the molecular details of this system into account and they didn't model the control system for the synthesis of Hmp at a mechanistic level. Then, this limits the possibility of using these models to think about possible new antibacterial strategies.

Also, Crack and his colleagues [23] demonstrated that in *Streptomyces*, the NsrR iron-sulfur cluster reacts with NO. They mentioned that *hmpA1* and *hmpA2* are two *hmp* paralogs in *Streptomyces*. The ratios of NO to NsrR required to abolish binding to the three relevant promoters differ among *hmpA1*, *hmpA2* and *nsrR*. They experimentally showed that reaction with 4, 2 and 8 equivalents of NO respectively, will completely abolish the binding of NsrR to those three promoters. Also, they studied the kinetics of the reaction of NO with the iron-sulfur cluster in NsrR.

## 1.4 Justifying a study based on *Streptomyces*

As mentioned before, NO is a toxic molecule at higher concentration. When bacterial cells are exposed to NO, they can remove it and avoid its toxic effects by making Hmp. Currently, NO is not attacking bacteria effectively because many bacteria have an *hmp*

gene.

Since a number of bacteria live in the human digestive system, and probably most of the bacteria that are of medical concern have at least one *hmp* gene, Hmp and its control system are interesting targets for new antibacterial agents [30, 31].

In *E. coli*, NsrR regulates different genes such as *hmp*, *hcp*, *hcr*, *ytfE* and *ygbA* [27]. Similarly, in *Klebsiella pneumoniae*, NsrR regulates different genes including *hcp*, *hcr*, *hmp*, *tehB* and *dnrN* [27]. But in *Streptomyces*, NsrR regulates only three genes: two independent copies of the *hmp* gene, each with its own promoter, and also *nsrR* itself [23].

On one hand, *Streptomyces* is a non-pathogenic bacteria [32]. On the other hand, a small number of genes are controlled by NsrR in *Streptomyces*. Additionally, the kinetics of the reaction of NO with the NsrR iron-sulfur cluster has been studied for the *Streptomyces* protein. Hmp is only controlled by NsrR in *Burkholderia pseudomallei* [27] which is a medically relevant bacteria. Since the Hmp control system in *Burkholderia pseudomallei* is of a similar simplicity to the control system in *Streptomyces*, and since the latter is a well-studied Hmp control system involving only repression by NsrR, *Streptomyces*' Hmp control system can be a good starting point for studying the function of NsrR in detail.

## 1.5 Rule-based modeling

Rule-based modeling generally uses a formal pattern-matching language to describe the rules by which molecules of certain classes interact [33]. A rule-based model is a chemical model including a number of rules from which differential equations are translated. By having differential equations, we can integrate them, compute steady states, study the bifurcation diagram, etc.

BioNetGen is software for rule-based modeling that uses a pattern-matching language called BNGL. Based on the observations of Crack et al [23], there are five kinetically distinguishable reactions of NsrR containing iron-sulfur clusters with NO, so we have six states for an NsrR monomer and then, the total number of states for an NsrR dimer is  $6^2=36$  states.

So, BioNetGen as a rule-based modeling software can generate the differential equations in the dimeric system.

### 1.5.1 Modeling

As mentioned previously, NsrR binds DNA as a dimer in bacterial cells. A similar monomer-based model has been studied by Roussel [18] focusing on the effects of delays in gene expression. Roussel ignored the dimeric nature of FNR, so the dynamical effects of dimerization of this transcription factor were not studied. Therefore, studying these effects for NsrR would be dynamically interesting.

In this work, I built several models for the detoxification of nitric oxide in *Streptomyces* based on the control of the expression of the Hmp enzyme by NO, mediated by NsrR. For the baseline model, the dimeric nature of NsrR has been ignored. Afterwards, the model was exported from BioNetGen in order to study its dynamics in XPPAUT [34]. Meantime, a majority of the parameters were estimated. Then, I carried out simulation studies using both XPPAUT and BioNetGen. Finally, we carried out the numerical bifurcation analysis for the model. After that, we could develop new models by considering the effects of dimerization of NsrR and could compare the results between the models in which NsrR acts as monomer and the models where NsrR is a dimer. The baseline model we have been developing is based on Roussel's model [18]. Roussel created a model for the synthesis of Hmp in *E. coli* under the control of FNR. In three models, we considered the effects of binding of NsrR to two different promoters, *hmpA1* and *hmpA2*. For the *nsrR* promoter, binding of the NsrR complex needs 8 NO's to be entirely abolished [23], so the degree of nitrosylation is eight when binding of NsrR to *nsrR* promoters has been lost. Since *nsrR* expression is much less sensitive to NO than expression of *hmp*, we assumed NsrR is constant in order to focus on the effects of dimerization of NsrR on expression of the *hmpA1* and *hmpA2* genes. Then, two models based on NsrR dimers were developed and studied.

The dynamics of models including dimeric NsrR were studied and we will see that

the dynamics of these systems can be different from those of simpler systems considering only NsrR monomers. These studies will also reveal under which conditions we can use a reduced model not considering dimerization.

## **1.6 Plan of thesis**

Methods and software applied in this thesis are described in chapter 2. Hmp kinetics is studied in chapter 3. Additionally, in chapter 3, a base model is built where the dimerization of the transcription factor NsrR has been ignored and afterwards, two other models are created where NsrR acts as a dimer. The reason for creating two different dimer models is that we do not know how differences in the nitrosylation states of two monomers in a dimer affect binding of NsrR to the promoters. Moreover, rule-based modeling is used to generate the differential equations for the dimer models. Parameter estimates from experimental data are obtained and as a result, a set of baseline parameters used throughout the study is reported in table 3.1. The effects of dimerization of NsrR in the Hmp gene expression models is explored. Then, the three models are compared in order to find the conditions that make the three models behave differently as well as the situations where the three models behave identically. Chapter 4 contains a summary as well as showing that our results are a platform for new studies in the future.

# Chapter 2

## Methods

In nonlinear dynamics, a bifurcation is a qualitative change in the behavior of the solutions of a system of equations as a parameter changes. The parameter-dependent behavior is displayed in a bifurcation diagram. For instance, it shows stable and unstable steady states and limit cycles [35].

There is software available to compute and plot bifurcation diagrams. In this study, BioNetGen [33], Copasi [36], XPPAUT [34] and AUTO were used.

BioNetGen [33] was used for generating the differential equations.

Copasi [36] is software for simulating biochemical systems and analyzing their dynamical behavior. It was used as an intermediate for generating ODE files (XPPAUT input files) from SBML (Copasi input files). The systems biology markup language, SBML, is a file format for description of biological systems [37, 38].

XPPAUT [34] was used for two purposes: we can numerically solve differential equations with it (i.e. simulate our system), and we can use the built-in version of AUTO to carry out bifurcation analysis.

AUTO can calculate branches of steady states (stable or unstable), periodic solutions (stable or unstable) and bifurcation points of different kinds such as saddle-node, Hopf and so on. In a saddle-node bifurcation, an unstable saddle point collides with a stable equilibrium, and the two annihilate. Additionally, by varying a parameter, a stable focus may be converted into an unstable focus creating a limit cycle. This kind of bifurcation is called a Hopf bifurcation [35].

BioNetGen integrates differential equations forward in time, so it provides only stable solutions. Since BioNetGen is able to show only stable steady state branches, which gives us an incomplete picture of dynamics, we exported the models from BioNetGen's .bnfl format to SBML files and imported the SBML files to Copasi. Then, we exported the .ode files to XPPAUT to enable the computation of both stable and unstable steady state branches, limit cycles and bifurcation points.

## **Chapter 3**

# **Dimerization of transcription factors in gene expression models: the control of Hmp synthesis by NsrR as a case study**

### **CRedit authorship contribution statement**

**Mohammad Hamidi:** Investigation, Methodology, Visualization, Writing — original draft. **Marc Roussel:** Conceptualization, Investigation, Funding acquisition, Supervision, Validation, Writing — review & editing.

# Abstract

Many transcription factors are active as dimers or higher oligomers. Moreover, the activity of transcription factors is often controlled by chemical modification of or by ligand binding to the individual monomers. In these cases, a multiplicity of states of the oligomeric transcription factor results. How important is the high-dimensional state space of the oligomer to the behavior of a gene control system? In this paper, we study a model for the control of the transcription of the *hmp* genes by NsrR in *Streptomyces*, a dimeric protein whose active form carries one [4Fe–4S] cluster per monomer. In *Streptomyces*, NsrR represses the transcription of two independent copies of the *hmp* gene whose product, Hmp, is an enzyme that catalyzes the conversion of toxic nitric oxide (NO) to nitrate. Reaction of the iron-sulfur cluster of NsrR with NO eventually alleviates the repression of the *hmp* genes, but little is known about the effect of unequal nitrosylation of the two monomers forming the NsrR dimer. To study the importance of the dimeric nature of NsrR on its control characteristics, we built a model based on a fictitious monomeric NsrR repressor and two models in which we account for the dimeric nature NsrR but making different assumptions about the kinetic characteristics of unevenly nitrosylated monomers within a dimer. For our default parameters, which were largely based on experimental data available from the literature, we found little difference between the three models provided repair of damaged iron-sulfur clusters was fast. However, significant differences were found when repair was slow. Leaving aside experimental parameter estimates, differences could also be observed when the first nitrosylation step tightened binding of the repressor to the *hmp* promoters rather than loosening it.

**Keywords:** Transcription factor; Dimerization; Nitric oxide; Hmp synthesis; NsrR; Rule-

based modeling; BioNetGen

### 3.1 Introduction

Gene expression is almost always controlled at least in part by the binding of regulatory proteins, known as transcription factors, to the gene's promoter [19]. Transcription factors can either be activators or repressors, and some transcription factors can assume different roles on different promoters. The active form of a transcription factor is sometimes a dimer or higher oligomer. Some transcription factors are able to form a number of distinct dimers with different binding partners, each dimer having different biological properties [21].

From a modeling perspective, dimeric transcription factors pose some challenges due to combinatorial complexity. Although every situation is different, it is occasionally tempting to ignore dimerization and to treat the transcription factor as a monomer. What are the effects of ignoring the dimeric nature of a transcription factor in a model of gene expression? This is the question broached in this paper via a case study of a particular sensing and control system, namely the nitric oxide (NO) sensing system mediated by the dimeric iron-sulfur protein NsrR, which controls the expression of the NO detoxifying enzyme Hmp in a number of bacterial species [27].

NsrR is a member of the Rrf2 transcriptional regulator family, generally acting as a repressor in a wide variety of bacterial species [39]. NsrR was originally discovered as a repressor controlling the expression of nitrite reductase in *Nitrosomonas europaea* [40]—hence its name, which stands for nitrite-sensitive repressor—and was later found to act as a global regulator of nitric oxide metabolism in a number of bacterial species including gamma- and beta-proteobacteria, and the more evolutionarily distant *Bacillus* and *Streptomyces* [27]. The holo form of NsrR contains a [4Fe–4S] cluster [39]. This iron-sulfur cluster reacts with NO. After several equivalents of NO have reacted, NsrR becomes unable to bind DNA, and the genes under its control can therefore be transcribed [23].

One of the genes frequently controlled by NsrR in this manner is *hmp*. Hmp is an NO-

detoxifying enzyme that catalyzes the conversion of NO to nitrate [17]. Because it allows bacteria to survive NO generated by the immune system, Hmp is a virulence factor [31, 41]. Thus, Hmp and its NsrR-mediated control system could be interesting targets for the design of new antibiotics.

To better understand this system, we built a mathematical model of Hmp and its control system. We specifically chose to model this control system in the soil bacterium *Streptomyces* because of its relative simplicity: in *Streptomyces*, NsrR regulates only three genes; two independent copies of the *hmp* gene, and also *nsrR* itself [23]. As we were building this model, we realized that the dimeric nature of the NsrR repressor posed a problem: NO will necessarily react at each of the two iron-sulfur clusters contained in a dimer. What is the effect of considering the effect of the pair of iron-sulfur clusters on the behavior of a model for the control of the expression of Hmp by dimeric NsrR? A previous model for the similar FNR-mediated control system in *Escherichia coli* had swept this issue under the carpet [18], treating the *hmp* gene as if it was controlled by a monomeric FNR repressor. We therefore decided to focus on the role of dimers in this control system. We set aside the regulation of *nsrR* by NsrR for now, on the basis that the latter regulatory interaction presumably exists to maintain homeostasis in the NsrR concentration.

The family of *hmp* control systems presents an interesting advantage from the perspective of these studies: the *E. coli* FNR-mediated control system displays bistability [18], i.e. a pair of saddle-node bifurcations, when NO is supplied to the cells at constant rate. Because the two control systems are in many ways similar, a *Streptomyces* model for the expression of Hmp under the control of NsrR would be expected to also display bistability, which is exactly what we found, as outlined below. Bifurcation points can be sensitive to the details of a model, so it seemed to us that a study of this system would illuminate the conditions under which dimerization of transcription factors might be quantitatively or qualitatively important.

In order to study this question, we devised three variations of a model for the control

of Hmp expression by NsrR. All three models share a submodel for the detoxification of NO by Hmp described in section 3.2.1. The remainder of section 3.2 describes three treatments of NsrR and of its interaction with the two *hmp* promoters in *Streptomyces*: a simple monomer model (section 3.2.2), and two slightly different models for the interaction of the dimer with the promoters (sections 3.2.3 and 3.2.4). A full set of parameter estimates is provided in section 3.2.5. Because of their complexity, the differential equations for the dimer models were generated using the rule-based modeling software BioNetGen [33]. Section 3.4 presents the results of this study. Specifically, in section 3.4.1, we study the three models with our best estimates of the parameters. Under these conditions, the three models behave essentially identically. Then in section 3.4.2, we deliberately study parameter sets for which differences are observed between the monomer and dimer models in order to illuminate the conditions that will make it necessary to consider dimerization in models with similar features to ours. Finally, in section 3.5, we offer some concluding thoughts.

## 3.2 Description of the models

### 3.2.1 Hmp kinetics

We begin with a description of Hmp kinetics, which is common to all the models studied in this contribution. The core of this submodel is based on one previously described for the synthesis of Hmp in *E. coli* under the control of FNR [18].

We consider a cell bathed in an external pool of NO, whose concentration is assumed constant. The following model reaction represents the permeation of NO through the cell membrane:



where NO without any subscripts indicates nitric oxide inside the cell, while  $\text{NO}_{[\text{ext}]}$  represents the constant, external pool of NO.

In *Streptomyces*, NO can be produced internally through a series of conversions from

nitrate [42]:

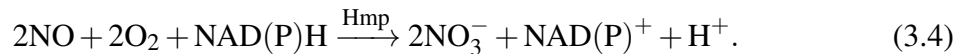


Thus, we should also consider endogenous generation of NO. For simplicity, we assume this occurs at constant rate:



This is equivalent to assuming that the internal pools of nitrate and nitrite are roughly constant.

Nitric oxide can be converted back to nitrate by the action of Hmp [17]. The reaction catalyzed by Hmp is



The catalyzed reaction proceeds by an ordered mechanism where, for catalysis to occur, NAD(P)H binds in the active site of the enzyme first, then O<sub>2</sub>, and then NO [43]. If NO binds to the enzyme before oxygen, the result is a non-productive complex which is not able to carry out catalysis. Before writing down our model, we consider the cellular concentrations of NADH and NADPH.

According to Kumar and Bruheim [44], metabolite concentrations ranges for NADH and NADPH are 0.004–0.356 nmol/mg DCW (dry cell weight) and 0.016–0.203 nmol/mg DCW respectively. The Michaelis constants of Hmp for NADH and NADPH are 3.2 μM and 180 μM respectively [43]. Owing to the discrepancy in units, for comparing the cellular concentrations of NADH and NADPH with their Michaelis constants, a relationship between dry cell weight and volume for *Streptomyces* is needed.

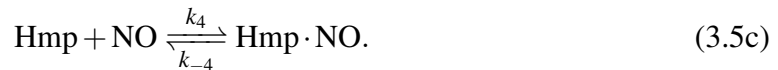
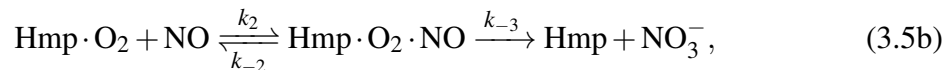
*Streptomyces* grows by developing hyphae which are subdivided into compartments that contain many copies of its single linear chromosome [45, 46, 47]. For simplicity, we assume that the volume occupied per chromosome is roughly equivalent to the volume of a sphere of the same diameter as a hypha. We treat this volume as that of a ‘cell’ in the calculations

below. *Streptomyces* have typical diameters in the range of 0.5–1  $\mu\text{m}$  [48]. The median radius is therefore approximately 0.4  $\mu\text{m}$ , from which we calculate a volume of 0.27  $\mu\text{m}^3$ .

Loferer-Krössbacher et al determined a general relationship between dry cell weight and volume for bacteria, namely  $\text{DCW} = 435V^{0.86}$ , where DCW is in fg, and  $V$  is in  $\mu\text{m}^3$  [49]. The dry weight of a typical cell is then, from Loferer-Krössbacher’s formula, 140 fg, from which we calculate a dry weight to volume ratio of 523  $\text{fg}/\mu\text{m}^3$  or 0.523  $\text{g}/\text{cm}^3$ . Thus, the range of cellular concentrations of NADH and NADPH are estimated to be 2–186  $\mu\text{M}$  and 8–106  $\mu\text{M}$ . The smallest values for NADH are only observed when the cells are grown in phosphate-limited batch culture for a lengthy period. Otherwise, NADH is found in *Streptomyces* cells in concentrations above 46  $\mu\text{M}$ .

Since Hmp can use NADH and NADPH interchangeably and by comparing the Michaelis constants with the estimated range of cellular concentrations of NADH and NADPH, we would conclude that the enzyme will be saturated with one of these two substrates at all times provided they are not starved of phosphate. Assuming that phosphate levels are sufficient to sustain NADH levels much greater than the Michaelis constant of Hmp for this cofactor, and given that the rate constant for NADH binding to Hmp is substantial [43], the saturating concentration of NADH implies that an NAD(P)H molecule should bind to the enzyme roughly as fast as the active site is cleared. We therefore do not include the NAD(P)H binding step in the model below.

The key reactions of the catalytic mechanism are then

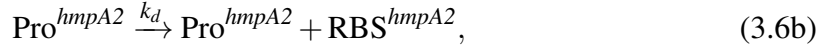
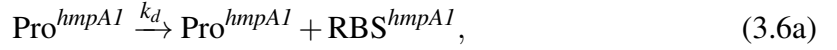


Compare reactions (3.5a) and (3.5c), and note that the latter reaction represents an example of competitive substrate inhibition by NO. Substrate inhibition often generates bista-

bility [50, 51, 52, 53].

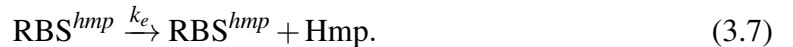
Because we want to focus on the effects of dimerization of NsrR, for simplicity, we ignore transcriptional and translational delays, as well as clearance delays [54], although delays can have significant effects on the behavior of a model. An ordinary differential equation model with NsrR monomers will act as the control to which dimer models will be compared.

Since *Streptomyces* has two *hmp* genes, *hmpA1* and *hmpA2*, we need transcription reactions for both. In principle, each transcription process could have different rate constants since their promoters are different [23]. However, since there are no measurements available of the rates of transcription at these two promoters, we assume that the rate constants are identical. Thus we write



where  $\text{RBS}^{hmpA1}$  and  $\text{RBS}^{hmpA2}$  represent the ribosome binding sites of the respective mRNAs. We focus on the RBS rather than on the full mRNA transcript because, in prokaryotic cells, translation can be initiated as soon as the RBS becomes available. We treat transcription as a pseudo-first-order process assuming that bacterial cells have a constant level of free RNA polymerase.

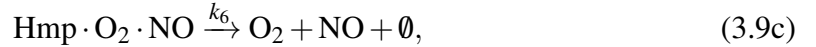
In theory, the two *hmp* genes generate two distinct mRNAs, which could also have distinct transcription kinetics. However, for lack of data on the transcription rates of these mRNAs, we assume in fact that the two mRNAs are identical, and henceforth simply write  $\text{RBS}^{hmp}$ . Again, assuming a constant concentration of free ribosomes, mRNA translation can be modeled by the following reaction:



We also need to consider the decay of Hmp and of its mRNA. For the mRNA:



In the case of Hmp, given that the function of this enzyme requires it to be in intimate contact with highly reactive substances, we would expect it to have some rate of breakdown. Indeed, in *Salmonella*, Hmp has a half-life of 66 minutes [55]. We assume that when Hmp breaks down, any substrates to which it was bound are released. Of course, if one of these substrates has reacted with the protein, that may not be correct. However, the behavior of the model is insensitive to this detail. Moreover, lacking data to the contrary, we also assume that binding substrates does not affect the rate of degradation.



### 3.2.2 Monomeric model of NsrR dynamics (MM model)

Both the FNR [56] and NsrR [39] holo-protein monomers contain an iron-sulfur cluster, specifically a [4Fe—4S] cluster. This iron-sulfur cluster is essential for binding of these transcription factors to specific sequences in the promoter regions of the genes they regulate. These proteins sense nitric oxide due to the reactions of NO with their iron-sulfur clusters. The accumulation of these reactions eventually results in the loss of ability of these proteins to bind their respective promoter sequences.

In a previous model of the control of Hmp synthesis by FNR in *E. coli*, the dimeric nature of the FNR transcription factor was neglected [18]. Two reasons were given for treating FNR as a monomer: First, reaction of the iron-sulfur clusters in the two monomers

appears to be independent [57], i.e. there is no detectable cooperativity or anti-cooperativity. Secondly, the formation of dimers under cellular conditions is rapid and nearly quantitative [56]. An additional kinetic factor in favor of a monomer model not discussed in this earlier contribution is that there is a reasonable time-scale separation between the nitrosylation steps, with early nitrosylation steps being substantially faster than later ones [57]. NsrR similarly forms dimers that are likely the dominant species *in vivo* [58], and the nitrosylation of its iron-sulfur cluster displays significant time-scale separation [23]. It may be hoped that a monomer model, which will be the baseline model in this study, can capture the key dynamics of this system, perhaps even quantitatively.

NsrR almost universally acts as a repressor [39]. In *Streptomyces*, NsrR controls just three genes, the two copies of the *hmp* gene and *nsrR* itself. The latter is almost certainly a homeostatic mechanism, which we set aside in this study in order to focus on the main feedback loop between iron-sulfur cluster damage by NO, expression of Hmp, and removal of NO by Hmp. The two *hmp* promoters do not respond identically to nitrosylation of NsrR's iron-sulfur cluster. Crack and coworkers found that, for the *hmpA2* promoter, binding was abolished after reaction of two molecules of NO per cluster, while four molecules of NO were required to abolish binding at the *hmpA1* promoter [23]. Interestingly, NsrR continues to bind to the *nsrR* promoter until eight equivalents of NO have reacted with the repressor's iron-sulfur cluster. This lesser sensitivity to NO at the *nsrR* promoter presumably curbs the synthesis of a repressor that would inhibit the synthesis of Hmp while the cell is coping with elevated levels of NO. This regulatory arrangement further supports treating the total cellular concentration of NsrR as a constant in this model.

The iron-sulfur cluster of NsrR reacts with up to eight NO molecules [23]. Only five of the nitrosylation steps are kinetically distinguishable, but each of these steps displays first-order kinetics with respect to NO. The latter piece of data suggests that there are in fact eight distinct nitrosylation steps. Our model includes only the five kinetically distinguishable steps. We have experimented with variations in which we insert the “missing”

NO molecules into the stoichiometries of some of the reactions, but this had a completely negligible effect on our results. Moreover, there was no easy way to implement a similar “fix” in the dimer models described in sections 3.2.3 and 3.2.4. In the interests of maximizing the consistency between models, we therefore left out these rapidly-added nitric oxide molecules. The only remaining puzzle was then the assignment of the remaining states to the two- and four-NO reaction products, which we return to shortly. The modeled reactions are thus

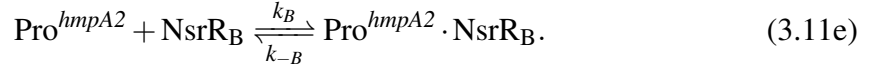
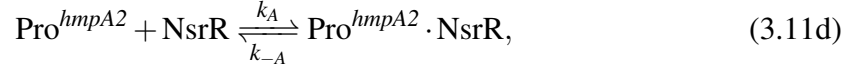
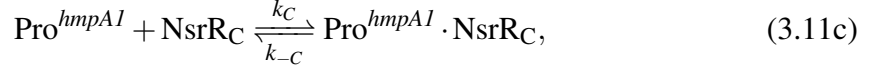
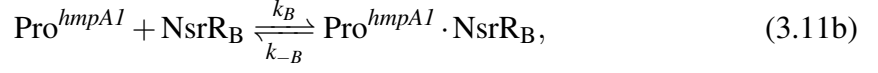
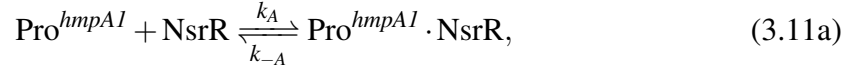


In these equations, NsrR is the holo-protein with an intact iron-sulfur cluster, while Nsr<sub>B,C,D,E,F</sub> represent nitrosylation products of NsrR.

Because of the kinetically invisible steps, we have no way of knowing which of the NsrR nitrosylation products explicitly represented corresponds to which nitrosylation state of NsrR. Time-scale separation between these steps is least distinct between steps (3.10c) and (3.10d), and between steps (3.10b) and (3.10c) [23]. It is tempting to speculate that this made the identification of other kinetic steps with similar kinetics impossible, i.e. that the kinetically invisible steps are, for lack of a better term “hiding” in a part of the mechanism where time-scale separation is less clear. Step (3.10a) would then represent a single nitrosylation step. NsrR<sub>C</sub> could then be the 2-NO intermediate and NsrR<sub>D</sub> the 4-NO intermediate. We did test other possibilities, but again, they made no difference to the modeling results presented below.

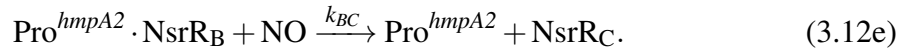
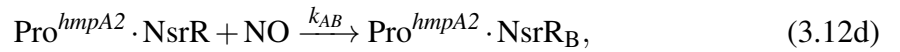
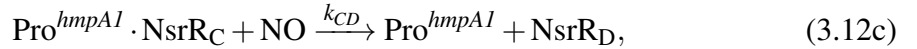
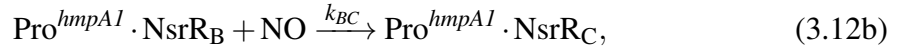
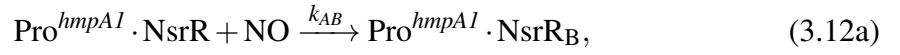
Binding of NsrR to the *hmpA1* and *hmpA2* promoters is modeled by the following reac-

tions:



In accordance with the foregoing discussion, these reactions allow binding of NsrR to the *hmpA1* promoter until four equivalents of NO have reacted with NsrR's iron-sulfur cluster (the NsrR<sub>D</sub> state), and to the *hmpA2* promoter until two equivalents of NO have been added (the NsrR<sub>C</sub> state).

NO can react with NsrR even when it is complexed with promoter [23]. We assume similar kinetics as for reactions of NO with free NsrR.



Note the dissociation of NsrR from the promoters in reactions (3.12c) and (3.12e).

Overton et al showed that many bacteria have enzymes that restore the iron-sulfur clusters in NsrR, among other iron-sulfur proteins [59]. Also, they showed that *Streptomyces* has such an enzyme. We therefore include a recycling reaction for NsrR species with damaged iron-sulfur clusters. Since little is known about the kinetics of these recycling pro-

cesses, we treat these reactions as simple first-order processes with a common rate constant:



with  $\gamma \in \{\text{B}, \text{C}, \text{D}, \text{E}, \text{F}\}$ . Including a recycling pathway will allow us to treat the total concentration of NsrR as a constant.

The monomer model (MM) consists of reactions (3.1), (3.3) and (3.5)–(3.13). Under the assumptions already presented, this model admits three conservation relations:

$$\begin{aligned} [\text{NsrR}]_0 &= [\text{NsrR}] + [\text{NsrR}_\text{B}] + [\text{NsrR}_\text{C}] + [\text{NsrR}_\text{D}] \\ &\quad + [\text{NsrR}_\text{E}] + [\text{NsrR}_\text{F}] + [\text{Pro}^{\text{hmpA1}} \cdot \text{NsrR}] \\ &\quad + [\text{Pro}^{\text{hmpA1}} \cdot \text{NsrR}_\text{B}] + [\text{Pro}^{\text{hmpA1}} \cdot \text{NsrR}_\text{C}] \\ &\quad + [\text{Pro}^{\text{hmpA2}} \cdot \text{NsrR}] + [\text{Pro}^{\text{hmpA2}} \cdot \text{NsrR}_\text{B}], \end{aligned} \quad (3.14a)$$

$$\begin{aligned} [\text{Pro}^{\text{hmpA1}}]_0 &= [\text{Pro}^{\text{hmpA1}}] + [\text{Pro}^{\text{hmpA1}} \cdot \text{NsrR}] \\ &\quad + [\text{Pro}^{\text{hmpA1}} \cdot \text{NsrR}_\text{B}] \\ &\quad + [\text{Pro}^{\text{hmpA1}} \cdot \text{NsrR}_\text{C}], \end{aligned} \quad (3.14b)$$

$$\begin{aligned} [\text{Pro}^{\text{hmpA2}}]_0 &= [\text{Pro}^{\text{hmpA2}}] + [\text{Pro}^{\text{hmpA2}} \cdot \text{NsrR}] \\ &\quad + [\text{Pro}^{\text{hmpA2}} \cdot \text{NsrR}_\text{B}]. \end{aligned} \quad (3.14c)$$

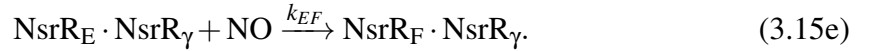
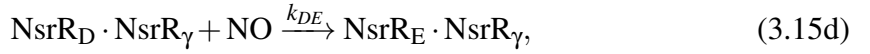
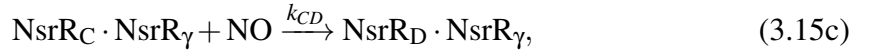
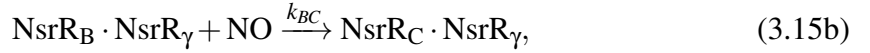
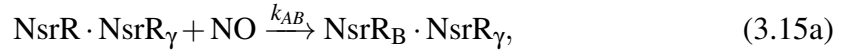
These conservation relations can be used to eliminate, respectively,  $[\text{NsrR}]$ ,  $[\text{Pro}^{\text{hmpA1}}]$  and  $[\text{Pro}^{\text{hmpA2}}]$ .

### 3.2.3 Dimer model 1 (DM1)

As mentioned previously, NsrR exists as a dimer *in vivo*. Since the ability of NsrR to bind to promoters depends on the nitrosylation of NsrR, we need to consider the nitrosylation states of both monomers within a dimer. This leads to a combinatorial problem: with six possible nitrosylation states (NsrR, NsrR<sub>B</sub>, . . . NsrR<sub>F</sub>), there are 36 possible dimer

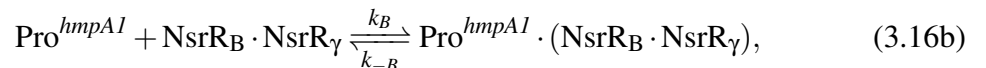
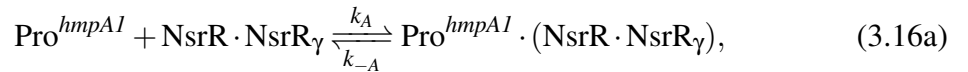
states. Trying to write down reactions or differential equations for all of these states as well as the possible complexes of the various NsrR dimers with the two promoters considered in this study would be extremely error-prone. To solve this problem, we turn to rule-based modeling [60]. Rule-based modeling generally uses a formal pattern-matching language to describe the rules by which molecules of certain classes interact. In this work, we used BioNetGen and its rule-based language BNGL [33]. In this section, we build dimer counterparts to the reactions described in section 3.2.2.

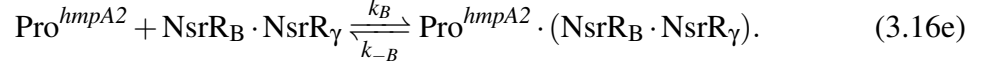
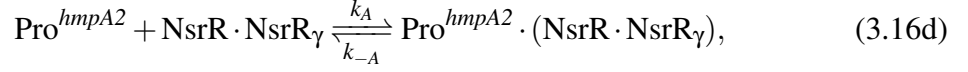
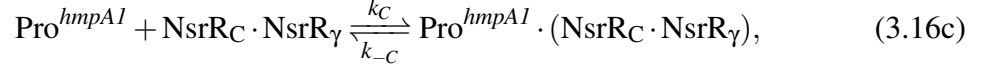
In FNR, nitrosylation reactions at the two iron-sulfur clusters proceed independently [57]. We assume the same to be true for NsrR. Then the reactions of NsrR dimers with NO can be represented as follows:



where  $\text{NsrR}_\gamma$  can be any possible state of an NsrR monomer including  $\text{NsrR}$ ,  $\text{NsrR}_B$ ,  $\text{NsrR}_C$ ,  $\text{NsrR}_D$ ,  $\text{NsrR}_E$  and  $\text{NsrR}_F$ .

Modeling the binding of NsrR dimers to the promoters requires a decision about the rule obeyed by the dimers. Available experimental data tells us at what nitrosylation states binding is lost to different promoters, but it does not tell us how mixed states behave. We implemented promoter binding rules in the simplest possible way in BioNetGen as follows:





where, again,  $\text{NsrR}_\gamma$  represents an arbitrary monomer state.

Because of the pattern-matching syntax of BNGL,  $\text{NsrR}_B \cdot \text{NsrR}_C$ , for example, will match the rules corresponding to both of the reactions (3.16b) and (3.16c), as well as reaction (3.16e). This has several important implications. First, binding of  $\text{NsrR}_B \cdot \text{NsrR}_C$  to the *hmpA1* promoter will have an effective dissociation constant

$$K_d \left( \text{Pro}^{hmpA1} \cdot (\text{NsrR}_B \cdot \text{NsrR}_C) \right) = \frac{k_{-B} + k_{-C}}{k_B + k_C}.$$

This can be seen by writing down the mass-action terms corresponding to the two matching binding processes, and then considering the implied equilibrium relationship. In other words, the dissociation constant for  $\text{NsrR}_B \cdot \text{NsrR}_C$  at the *hmpA1* promoter will be a compromise between the monomeric dissociation constants. In fact, it is easy to show that

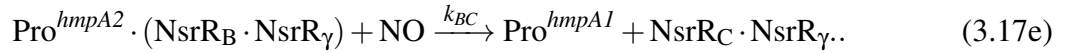
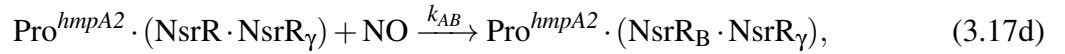
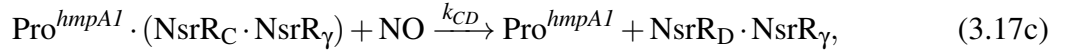
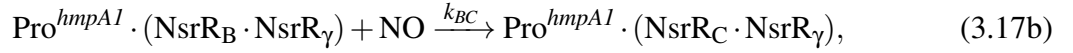
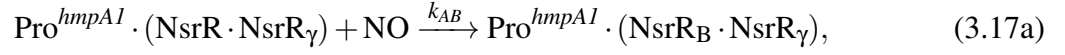
$$\frac{k_{-B}}{k_B} < K_d \left( \text{Pro}^{hmpA1} \cdot (\text{NsrR}_B \cdot \text{NsrR}_C) \right) < \frac{k_{-C}}{k_C}.$$

This is perhaps not an unreasonable assumption given our lack of knowledge of the effects of mixed nitrosylation states on the binding. However, kinetically, the binding and dissociation reactions will be faster than in the monomer model because they will proceed with effective rate constants that are sums of microscopic rate constants for the two matching reactions. This is unrealistic, although irrelevant in this study since we focus on the steady-state structure of the model.

A slightly more serious consequence is that any dimer  $\text{NsrR}_B \cdot \text{NsrR}_\gamma$  with  $\gamma \geq B$  will bind to the *hmpA2* promoter with the same affinity. While this is not impossible, a plausible

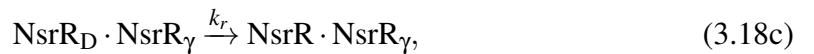
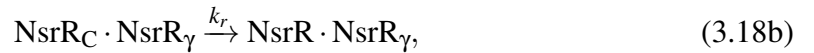
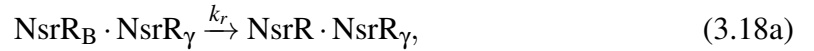
guess would be that higher nitrosylation states  $\gamma$  weaken the  $\text{Pro}^{hmpA2} \cdot (\text{NsrR}_B \cdot \text{NsrR}_\gamma)$  complex. Still, lacking data on the binding of dimers in mixed nitrosylation states, the simple BNGL rule used in this study is as good a hypothesis as any.

As in the monomer model, we consider reaction of NO with NsrR complexed to DNA:



Again, the pattern-matching BNGL language has some interesting consequences. For example, reaction (3.17c) causes the immediate dissociation from the *hmpA1* promoter of an  $\text{NsrR}_D \cdot \text{NsrR}_\gamma$  dimer formed on that promoter. However, if  $\gamma \leq C$ , then this dissociative process will be counteracted to some extent by binding via reactions (3.16a) to (3.16c).

Finally, the NsrR recycling pathway is described as follows, assuming that the iron-sulfur cluster repair enzyme operates on one monomer at a time:



with  $\gamma \geq B$ .

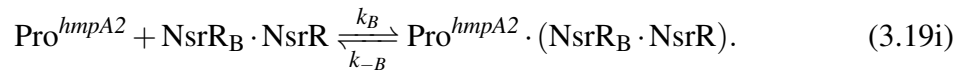
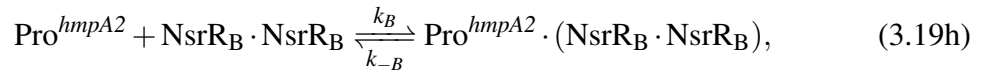
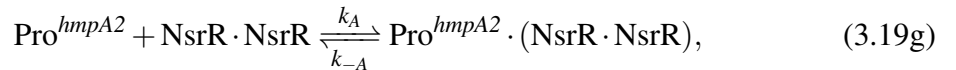
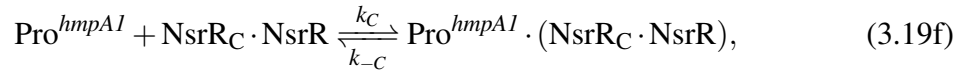
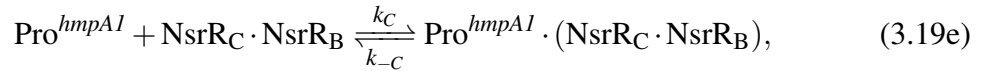
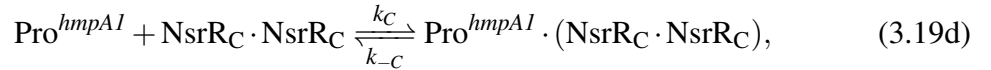
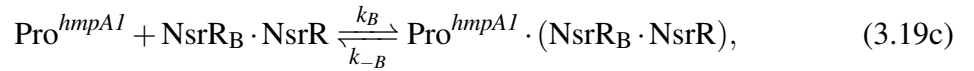
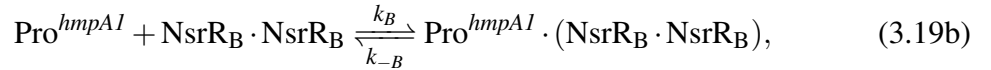
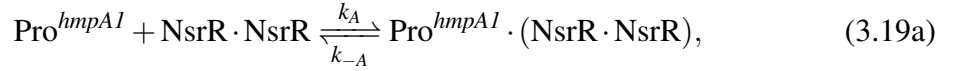
Model DM1 includes reactions (3.1), (3.3), (3.5)–(3.9) and (3.15)–(3.18). The final model consists of 168 reactions linking 57 species (not counting the sink species  $\text{NO}_3^-$ ).

Like model MM, DM1 is subject to conservation relations for the total concentrations of NsrR and of the two promoters. These conservation relations are automatically detected by BioNetGen and used to eliminate three differential equations.

### 3.2.4 Dimer model 2 (DM2)

As discussed above, DM1 has some odd and, arguably, unphysical characteristics in terms of allowing binding of complexes in which one NsrR monomer is in a high nitrosylation state. Because of the limited programmability of the BNGL pattern-matching language, one alternative is to explicitly list cases. This is tedious and loses some of the advantages of rule-based modeling, but it does allow us to implement a different logic for binding of NsrR dimers to the promoters.

One of many possible alternatives is to have the binding strength of an NsrR dimer to the promoters be determined by the ‘most damaged’ cluster. Fortunately in this particular instance, only a limited number of dimers are able to bind to the promoters under this rule. The relevant reactions are



Model DM2 consists of reactions (3.1), (3.3), (3.5)–(3.9), (3.15) and (3.17)–(3.19) representing 109 distinct reactions linking 40 chemical species ( $\text{NO}_3^-$  excepted).

### 3.2.5 Parameter estimates

We now turn to the problem of estimating the parameters of the model.

To calculate  $[\text{Pro}^{\text{hmpA1}}]_0$  or  $[\text{Pro}^{\text{hmpA2}}]_0$ , we consider that the compartments from the subdivision of *Streptomyces* during growth will typically contain many copies of its single linear chromosome per cell. We assume that the volume occupied per chromosome is roughly equivalent to the volume of a sphere with the same diameter as a hypha in the calculation below, as in section 3.2.1. Assuming once again a typical radius of  $0.4\mu\text{m}$ , a straightforward calculation then gives a promoter concentration of  $6 \times 10^{-9}$  mol/L. Some simulations not reported here show that the results are not very sensitive to this parameter, presumably because of the control of the Hmp concentration by NO.

We note in passing that the small population of any given gene in a cell means that the model will only describe the behavior averaged over a large population [61]. Given the objective of this study, this should not be a significant limitation.

To our knowledge, there have been no measurements of the concentration of NsrR *in vivo*. We assume, arbitrarily, that the concentration of NsrR in *Streptomyces* is similar to the concentration of FNR in *E. coli* [18].

The rate constant  $k_m$  represents permeation of NO through the cell membrane. We assume that the cell is surrounded by an aqueous medium. This may not represent the situation for a *Streptomyces* cell in its natural environment, soil, but it would describe laboratory experiments in which, for example, *Streptomyces* is grown in a chemostat. (*Streptomyces* grows well in chemostat culture, although some precautions must be taken to avoid the formation of pellets and biofilms [62].)

The rate of change of the concentration of NO inside the cell due to permeation is [63]

$$v_{\text{perm}} = \frac{AP}{V} ([\text{NO}]_{\text{ext}} - [\text{NO}]), \quad (3.20)$$

where  $P$  is the permeability coefficient of the cell for NO,  $A$  is the surface area of the cell and  $V$  is its volume. By comparing this equation with the permeation process (3.1), we see that

$$k_m = AP/V. \quad (3.21)$$

It is difficult to find permeability coefficients for NO through biological membranes or artificial analogs thereof. The octanol-water partition coefficient of NO suggests poor permeation of membranes given NO's small size and low polarity [64]. On this basis, one could reasonably guess that the permeability coefficient of NO might be somewhere between those of water and carbon dioxide, i.e. in the range  $3.4 \times 10^{-3}$ – $3.5 \times 10^{-1} \text{ cm s}^{-1}$  [65]. As a convenience, because our immediate objective is to study the behavior of models and not to draw conclusions about the detoxification properties of the system, we adopt a value towards the bottom of this range of  $10^{-2} \text{ cm s}^{-1}$ . Values of  $P$  in this range place the system in a regime where bistability is observed over a substantial range of  $k_p$  and  $[\text{NO}]_{\text{ext}}$  values, as we will see later. Again using a typical cell radius of  $0.4 \mu\text{m}$ ,  $k_m$  then works out to  $750 \text{ s}^{-1}$ .

External NO concentrations encountered by bacteria in various environments can occasionally be as high as  $10^{-6} \text{ M}$  [66], setting an upper bound for values of  $[\text{NO}]_{\text{ext}}$ . Similarly, maximum intracellular NO concentrations of  $10^{-7} \text{ M}$  will provide a basis for interpreting some of the results as well as constraining possible values of  $k_p$ .

For *Streptomyces* in the wild, the maximum oxygen pressure the cells are likely to experience is sea-level air, with  $p_{\text{O}_2} = 0.21 \text{ atm}$ . The Henry's law constant of oxygen in water at  $25^\circ\text{C}$  is  $1.3 \times 10^{-8} \text{ mol L}^{-1} \text{ Pa}^{-1}$  [67]. Assuming a laboratory experiment at a controlled temperature of  $25^\circ\text{C}$ , the maximum possible intracellular oxygen concentration is therefore approximately  $277 \mu\text{M}$ . *Streptomyces*' aerobic metabolism will decrease the intracellular concentration of  $\text{O}_2$ , and in its natural habitat, there is a further decrease in the availability of oxygen with depth in the soil [68]. Accordingly, we use a somewhat lower  $\text{O}_2$  concentration of  $200 \mu\text{M}$  for most of our calculations.

We assume that the half-life of Hmp sets the rate constant  $k_6$ . This will be roughly correct provided cells grow slowly, which they might if they are subjected to prolonged nitrosylation stress. The half-life of Hmp in *Salmonella* is 66 minutes [55]. Lacking data specific to *Streptomyces*, we calculate  $k_6$  using this value.

Isabella et al have measured dissociation constants for NsrR with several promoters, obtaining values in the low-nM range [69]. If we assume  $K_d \approx 35$  nM (the NsrR-*nsrR* dissociation constant measured by Isabella) and a moderate binding constant  $k_A = 10^7 \text{M}^{-1}\text{s}^{-1}$ , then from  $K_d^{(A)} = k_{-A}/k_A$ , we get  $k_{-A} = 0.35$  s. A progressive loosening of the NsrR-promoter complexes as NO reacts with NsrR’s iron-sulfur cluster would lead to increasing values of  $K_d$ . However, the results reported by Crack et al do not suggest a large drop in binding affinity prior to each promoter passing the threshold where it completely loses its ability to bind NsrR. We therefore assume a modest drop in affinity prior to the sharp cutoff indicated by [23]. Table 3.1 summarizes the baseline set of parameters used in this study. For lack of appropriate data for NsrR in *Streptomyces*, parameters relating to transcription and translation rates were reused from the study of Roussel on the FNR control system in *E. coli* [18].

### 3.3 Methods and software

As previously mentioned, we built the dimer models in BioNetGen 2.5.1 [33]. These models were converted to SBML, imported into Copasi 4.37 [36], and then exported to XPPAUT input files. While BioNetGen has a primitive “bifurcate” command that finds attractors based on forward time integration, the version of AUTO built into XPPAUT 8.0 is able to generate true bifurcation diagrams based on standard continuation methods [34]. The XPPAUT input files generated by this process require minimal editing, namely the removal of the differential equation for  $[\text{NO}_3^-]$  which accumulates without bound since we have not provided a sink for this species. As there is no dynamical role for this species, removing it does not change the dynamics of the model.

Table 3.1: Default model parameters. Notes: [c] value calculated in the text; [a] assumed value; [s] value from a different species used for lack of *Streptomyces* data.

Parameter	Value	Notes	Parameter	Value	Notes
Hmp dynamics			NsrR dynamics		
$k_1$	$3.5 \mu\text{M}^{-1}\text{s}^{-1}$	[43][s]	$k_{AB}$	$4.52 \mu\text{M}^{-1}\text{s}^{-1}$	[23]
$k_{-1}$	$0.44 \text{s}^{-1}$	[43][s]	$k_{BC}$	$0.113 \mu\text{M}^{-1}\text{s}^{-1}$	[23]
$k_2$	$850 \mu\text{M}^{-1}\text{s}^{-1}$	[43][s]	$k_{CD}$	$1.34 \times 10^{-2} \mu\text{M}^{-1}\text{s}^{-1}$	[23]
$k_{-2}$	$2 \times 10^{-4} \text{s}^{-1}$	[43][s]	$k_{DE}$	$7.48 \times 10^{-3} \mu\text{M}^{-1}\text{s}^{-1}$	[23]
$k_{-3}$	$200 \text{s}^{-1}$	[43][s]	$k_{EF}$	$0.43 \times 10^{-3} \mu\text{M}^{-1}\text{s}^{-1}$	[23]
$k_4$	$26 \mu\text{M}^{-1}\text{s}^{-1}$	[43][s]	$k_A$	$10 \mu\text{M}^{-1}\text{s}^{-1}$	[a]
$k_{-4}$	$2 \times 10^{-4} \text{s}^{-1}$	[43][s]	$k_B$	$10 \mu\text{M}^{-1}\text{s}^{-1}$	[a]
$k_5$	$0.014 \text{s}^{-1}$	[70][s]	$k_C$	$10 \mu\text{M}^{-1}\text{s}^{-1}$	[a]
$k_6$	$1.8 \times 10^{-4} \text{s}^{-1}$	[55][s]	$k_{-A}$	$0.35 \text{s}^{-1}$	[c]
$[\text{Pro}^{hmpA1}]_0$	$6 \times 10^{-3} \mu\text{M}$	[c]	$k_{-B}$	$0.4 \text{s}^{-1}$	[c]
$[\text{Pro}^{hmpA2}]_0$	$6 \times 10^{-3} \mu\text{M}$	[c]	$k_{-C}$	$0.45 \text{s}^{-1}$	[c]
$[\text{NsrR}]_0$	$2.5 \mu\text{M}$	[a]	$k_r$	$0.1 \text{s}^{-1}$	[a]
$[\text{O}_2]$	$200 \mu\text{M}$	[a]	NO transport		
$k_d$	$0.71 \text{s}^{-1}$	[18][s]	$k_m$	$750 \text{s}^{-1}$	[c]
$k_e$	$0.83 \text{s}^{-1}$	[18][s]			

Because of its relative simplicity, we originally created an XPPAUT input file directly for the monomer model. To verify our BioNetGen modeling, we also generated a BNGL file describing the monomer model, and verified that identical results were obtained after translating it into an XPPAUT input file as were obtained with our hand-written input file.

BioNetGen has a useful  $\$$  syntax to fix the concentrations of desired variables. This allowed us to study the effect of intracellular [NO] on the concentrations of the various species (Figs. 3.4 and 3.9). In these calculations, we scan [NO] (via its initial concentration, which appears as a parameter in the BNGL script) and BioNetGen computes (by forward integration) the steady-state concentrations of dimers at a set of fixed NO concentrations.

### 3.4 Results

In this paper, we investigate the dynamical behavior of MM, DM1 and DM2, which differ mainly in their treatment of the rules by which NsrR binds to the *hmp* promoters.

Bifurcation diagrams are sensitive probes of dynamics, and since models of this type frequently have saddle-node bifurcations [18], we carried out a set of bifurcation studies for these models, reported below. Since  $k_p$  represents endogenous production of NO, it acts as a natural control parameter reflecting changing conditions within a cell. Alternatively,  $[\text{NO}]_{\text{ext}}$  could be varied.

### 3.4.1 Dynamical behavior of the models at the default parameters

We started by computing a bifurcation diagram of the monomer model (MM) at the default parameters. This bifurcation diagram is shown in Fig. 3.1(a). We found a range of  $k_p$  values where we observe bistability, i.e. two stable states, delimited by a pair of saddle-node bifurcations (the turning points where a branch of stable steady states meets a branch of unstable steady states) [18, 71].

We note in passing that varying either  $k_p$  or  $[\text{NO}]_{\text{ext}}$  is equivalent due to the appearance of these two parameters in the combination  $p_{\text{total}} = k_p + k_m[\text{NO}]_{\text{ext}}$  in the equation for  $d[\text{NO}]/dt$ . Thus, witness the straight-line boundaries of the bistable region shown in the phase diagram of Fig. 3.1(b), which are lines of constant  $p_{\text{total}}$ . While we focus on  $k_p$  as a control parameter in our bifurcation diagrams, similar results would therefore be obtained using  $[\text{NO}]_{\text{ext}}$  as the control parameter, give or take a transformation of the scale of the parameter axis. In other words, either internal NO production ( $k_p$ ) or external nitric oxide can drive this system into or out of the bistable region.

There is substantial uncertainty in the permeability rate constant,  $k_m$ . We therefore generated a phase diagram in the  $(k_p, k_m)$  parameter plane, shown in Fig. 3.2. This shows a relatively broad range of  $k_m$  values at which bistability could be observed. However, based on the discussion of section 3.2.5,  $k_m$  might be as high as  $2.6 \times 10^4 \text{ s}^{-1}$ . Thus, at the higher end of the plausible range of values for this parameter, there is a single steady state.

We followed up this brief study of the bifurcation structure of model MM with a similar study of the bifurcations of models DM1 and DM2. Figure 3.3 shows that the two dimer

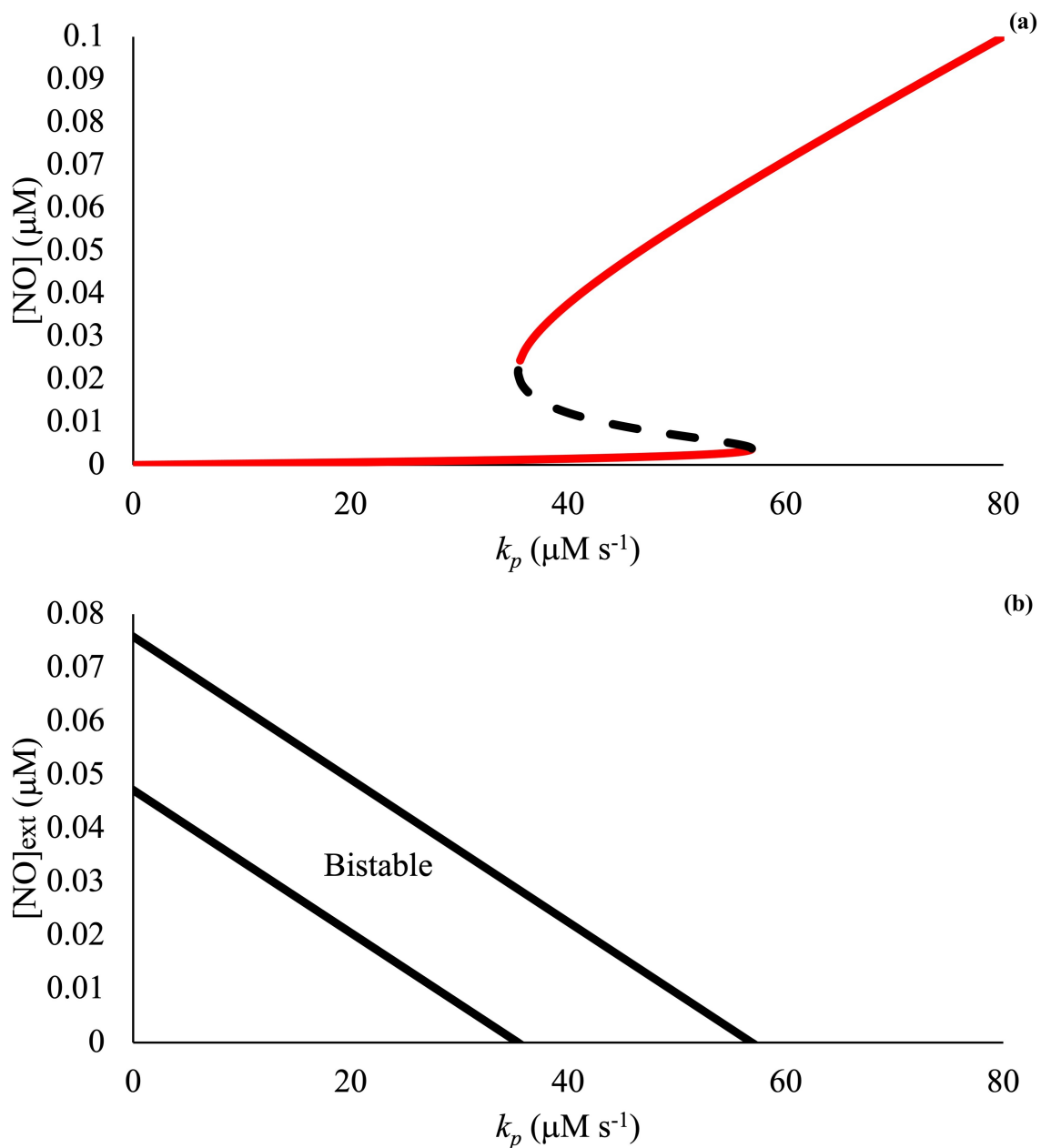


Figure 3.1: Bifurcation diagram for model MM at the default parameters values. (a) Bifurcation diagram, showing a bistable region between two saddle-node bifurcations at  $[\text{NO}]_{\text{ext}} = 0$ . In this and all subsequent bifurcation diagrams, solid red lines represent stable steady states and dashed black lines represent unstable steady states. (b) Phase diagram showing the bistable region in the  $(k_p, [\text{NO}]_{\text{ext}})$  parameter plane. Outside of the bistable region, the system has one stable steady state. The boundaries of the bistable region have common slope  $k_m^{-1}$ .

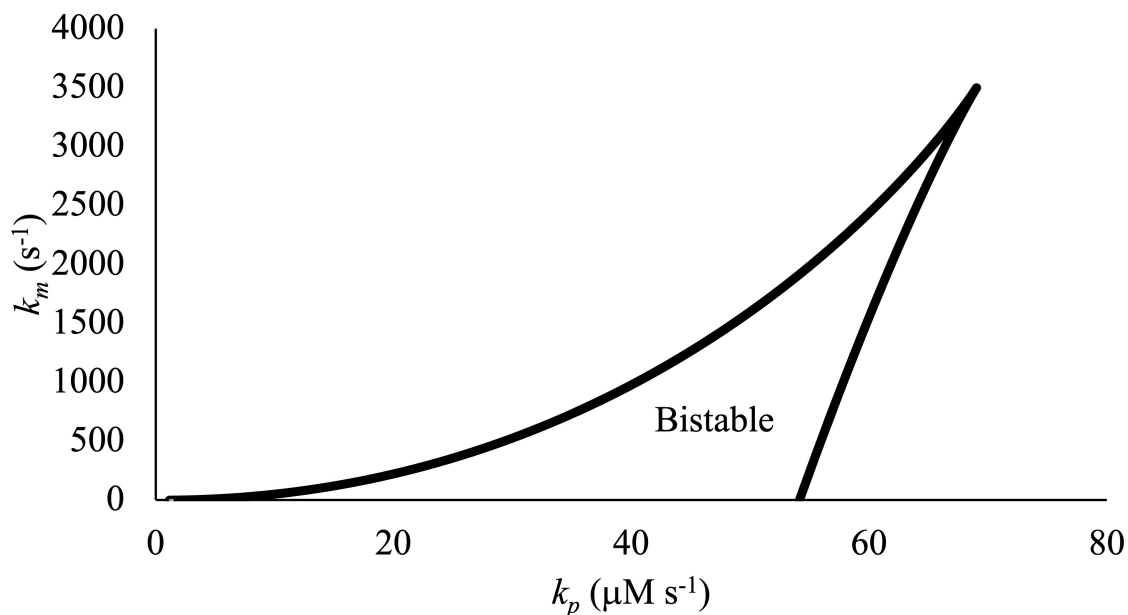


Figure 3.2: Two-parameter phase diagram showing a cusp bifurcation. All parameters are at the default values for the MM model.

models behave essentially identically to the MM model. Thus, given our best estimates of the parameters, the simpler monomer model is a perfectly adequate predictive model for the behavior of this entire class of models. But why would that be?

Thinking of the possible dimer states as analogous to elements of a matrix, we define diagonal dimer states, which are the complexes including the same monomer states, i.e.  $\text{NsrR}_X \cdot \text{NsrR}_X$  complexes. Pursuing the matrix analogy, we define sub-diagonal states as those that lie just below the diagonal states and super-diagonal states as those just above the diagonal. To put it another way, the sub- and super-diagonal states consist of monomers that differ from the diagonal states by a single nitrosylation event, e.g. states such as  $\text{NsrR}_C \cdot \text{NsrR}_B$  and  $\text{NsrR}_B \cdot \text{NsrR}_C$ . Sub- and super-diagonal complexes that differ by a permutation of the states such as the latter two represent the same chemical species since the two NsrR dimers are indistinguishable. We thus refer to sub- and super-diagonal states collectively as near-diagonal states. We also define the central band to consist of states that are either diagonal or near-diagonal.

Our dimer models were built on the assumption, supported by experimental evidence

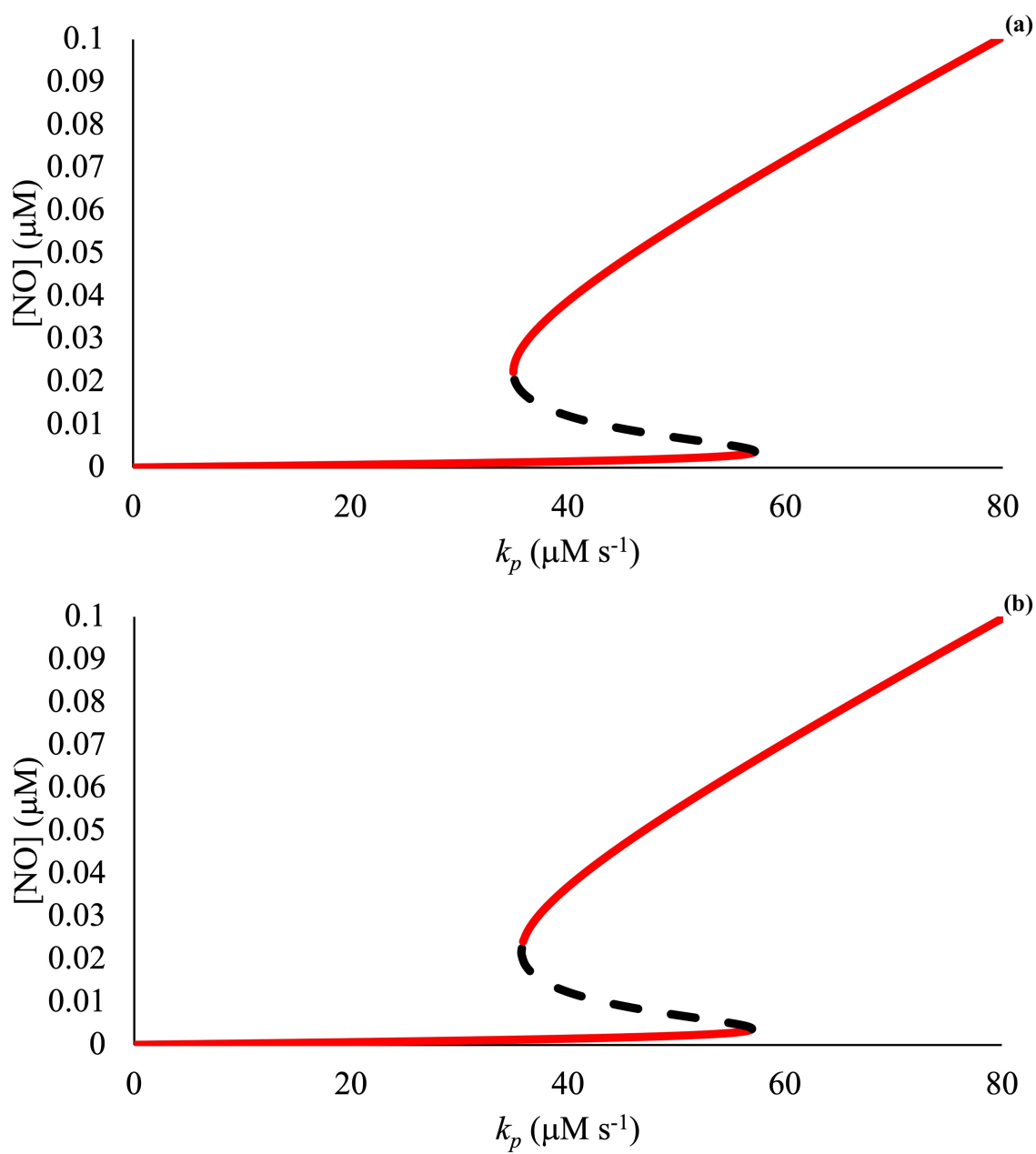


Figure 3.3: Bifurcation diagrams for models DM1 and DM2. (a) Bifurcation diagram for model DM1. (b) Bifurcation diagram for model DM2. All parameters are as shown in table 3.1.

[57], that nitrosylation reactions at the two iron-sulfur clusters in a dimer are independent events. Examining the values of  $k_{AB}$  to  $k_{EF}$  in Table 3.1, we see that there is a rapid decrease in the nitrosylation rate constants with increasing nitrosylation. Thus, despite the assumption of independence, the consequent separation of time scales implies that we should mostly see an orderly ‘walk’ of individual dimers from the diagonal to the next near-diagonal state, then to the next diagonal state, with states farther from the diagonal rarely visited.

Figure 3.4(a) shows the concentrations of a ‘family’ of NsrR dimers in model DM1, in this case the  $\text{NsrR}_C \cdot \text{NsrR}_X$  family, as we vary the intracellular NO concentration as described in the Methods section. As expected, the highest dimer concentrations are seen in the diagonal and near-diagonal states,  $\text{NsrR}_C \cdot \text{NsrR}_B$ ,  $\text{NsrR}_C \cdot \text{NsrR}_C$  and  $\text{NsrR}_C \cdot \text{NsrR}_D$ .  $\text{NsrR}_C \cdot \text{NsrR}_E$ , which is not in the central band, grows to be almost as large as  $\text{NsrR}_C \cdot \text{NsrR}_D$  because of the relatively small ratio of  $k_{CD}$  to  $k_{DE}$  (less than 2) than for any other adjacent pair of nitrosylation rate constants in Table 3.1, the next smallest ratio being greater than 8. Thus, for families that include  $\text{NsrR}_X \cdot \text{NsrR}_D$  among the near-diagonal states, the  $\text{NsrR}_X \cdot \text{NsrR}_E$  complex may reach relatively high concentrations even when it is not in the central band, but otherwise the diagonal and near-diagonal complexes dominate the dynamics. Moreover, in DM1,  $\text{NsrR}_X \cdot \text{NsrR}_E$  dimers with  $X > C$  do not bind any promoter, and in DM2, no  $\text{NsrR}_X \cdot \text{NsrR}_E$  dimer is able to bind a promoter, so the concentrations of these dimers are less significant to the overall dynamics of the model than would be the case for dimers that are directly involved in the control of *hmp* expression.

Other NsrR dimer families behave similarly to the  $\text{NsrR}_C$  family, with the caveat noted above about the D and E states.

Figure 3.4(b) shows the concentrations of the diagonal dimers as a function of the NO concentration. Because of the separation of time scales implied by the nitrosylation rate constants, at most concentrations, a single dimer form will dominate and there are never high concentrations of three diagonal dimers simultaneously. Thus, there is generally a

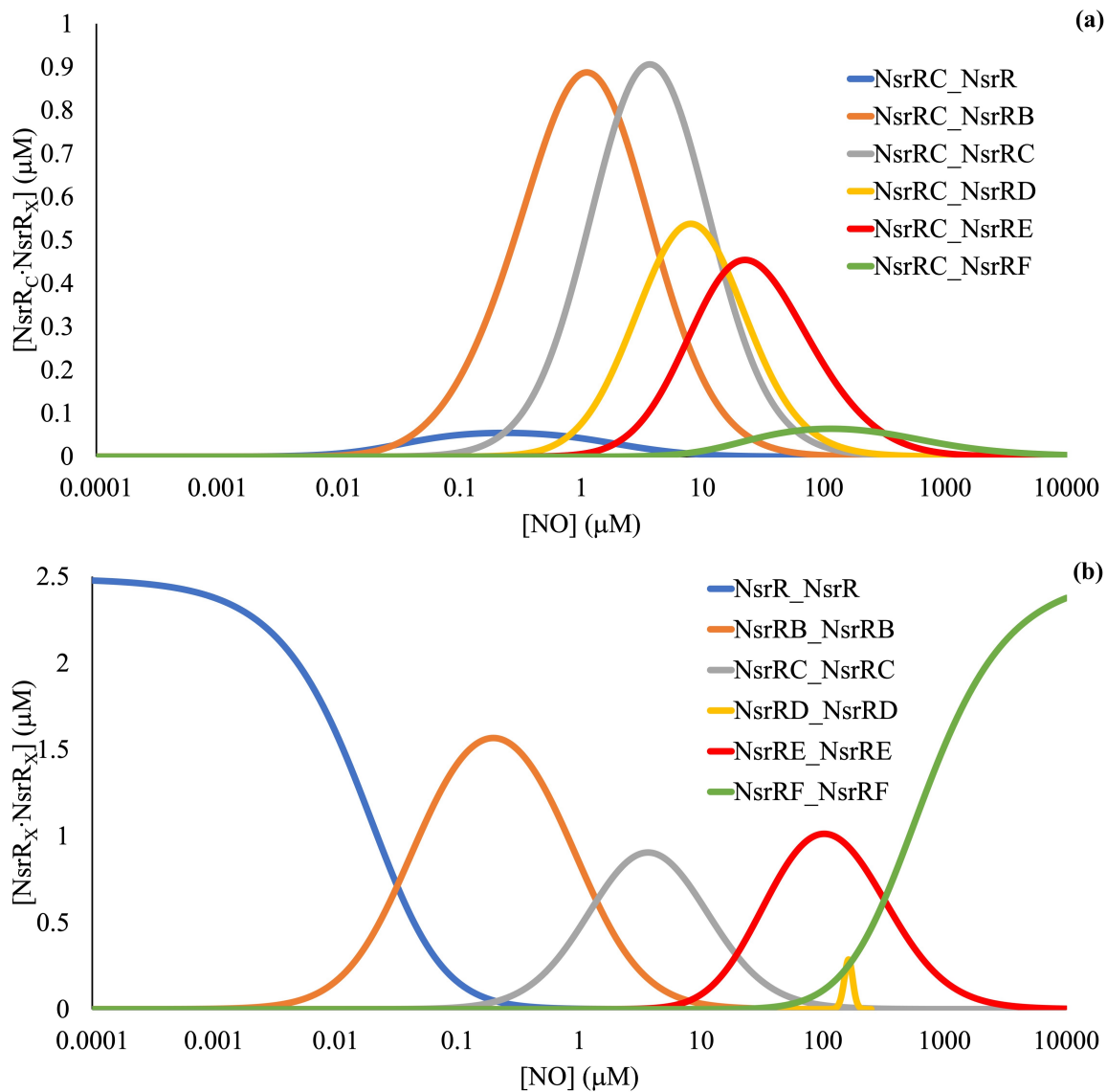


Figure 3.4: NsrR family dimer concentrations vs [NO] at the default parameters for DM1. (a) NsrR<sub>C</sub> family dimer concentrations vs [NO] at the default parameters. The concentration of NsrR<sub>C</sub> · NsrR<sub>F</sub> reaches a maximum of  $0.064 \mu\text{M}$  near  $[\text{NO}] = 10^2 \mu\text{M}$  (not shown). (b) Concentrations of diagonal dimers as a function of [NO] plotted on a logarithmic scale.

simple ordered transition from one state to the next of the dimers.  $\text{NsrR}_D \cdot \text{NsrR}_D$  is an exception due to the small ratio of  $k_{CD}$  to  $k_{DE}$  noted above. This allows the formation of  $\text{NsrR}_E \cdot \text{NsrR}_E$  via the pathway  $\text{NsrR}_C \cdot \text{NsrR}_D \rightarrow \text{NsrR}_C \cdot \text{NsrR}_E \rightarrow \text{NsrR}_D \cdot \text{NsrR}_E \rightarrow \text{NsrR}_E \cdot \text{NsrR}_E$ , bypassing  $\text{NsrR}_D \cdot \text{NsrR}_D$ .

DM2 behaves identically both with respect to the dominance of the central band states and to the orderly succession of dimer states as  $[\text{NO}]$  increases. The orderly walk of dimer states up the central band explains the sharp results obtained experimentally with respect to the number of NO molecules required to lose binding at the *hmpA1*, *hmpA2* and *nsrR* promoters in *Streptomyces* [23]. Had all of  $k_{AB}$  to  $k_{EF}$  been similar in size, for instance, we would not obtain the clean separation between dimer states as  $[\text{NO}]$  increased. Instead, at any given NO concentration, a complex mixture of NsrR states would result (Fig. 3.5), which would weaken the straightforward stoichiometric relationship between administered NO and the population of bound promoters observed in the experiments. Interestingly however, the bifurcation diagrams of the three models (not shown) continue to agree nearly perfectly despite the disordered nitrosylation sequence in the dimer models. In fact, we have tried changing the nitrosylation rate constants  $k_{AB}$  to  $k_{EF}$  in various ways, including reversing their order and randomly shuffling their values, and the bifurcation diagrams of the three models always agree closely holding the other rate constants at their default values. The selection of a monomer model vs a dimer model is therefore indifferent to the nitrosylation kinetics.

*Streptomyces* are soil-dwelling bacteria, and the oxygen concentration decreases with depth in the soil. The dependence of  $[\text{O}_2]$  on soil depth depends on a number of factors, but for reference we consider the measurements of Sheppard et al, which were obtained in a grassland environment [68]. At an 11 cm depth, these measurements give an  $\text{O}_2$  concentration of roughly  $16\mu\text{M}$ . Figure 3.6 shows a bifurcation diagram obtained at this concentration for model MM. There is a shift of the bistable region to lower concentrations, but otherwise the behavior of the model is unaffected.

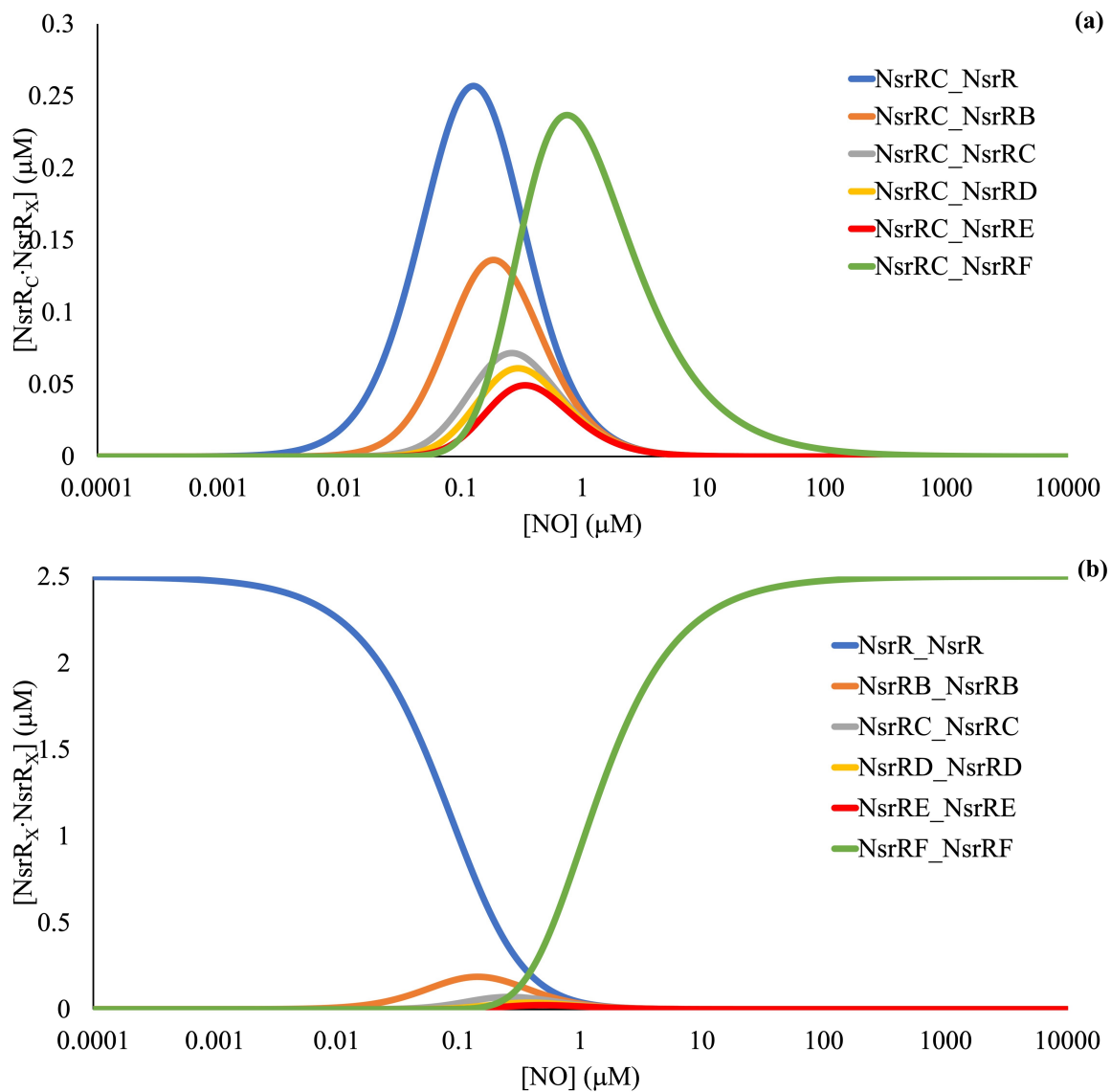


Figure 3.5: NsrR family dimer concentrations vs [NO] for model DM1 when  $k_{AB} = k_{BC} = k_{CD} = k_{DE} = k_{EF} = 1 \mu\text{M}^{-1}\text{s}^{-1}$ , other parameters being at their default values. (a) NsrRC family dimer concentrations vs [NO]. (b) Concentrations of diagonal dimers as a function of [NO].

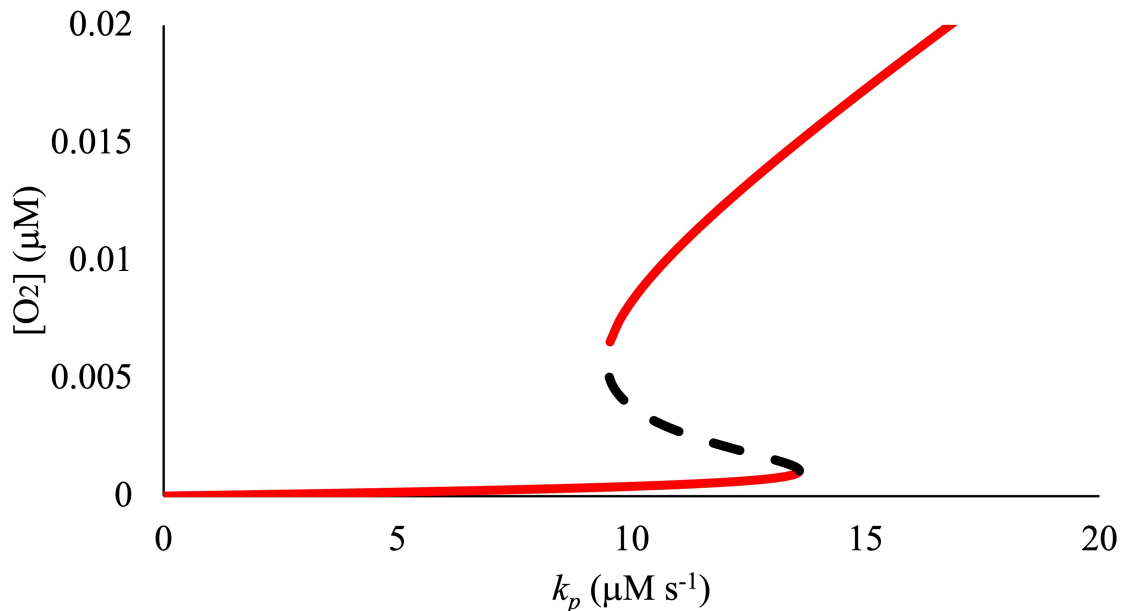


Figure 3.6: Bifurcation diagram for model MM with all parameters as in Table 3.1 except  $[O_2] = 16\mu\text{M}$ .

### 3.4.2 Conditions making the models behave differently

In the previous section, we found that the three models agree in almost perfect quantitative detail for our best-estimate, default parameters, as well as for a variety of different arrangements of the nitrosylation rate constants, and for different oxygen concentrations. But is this necessarily the case? In this section, we explore this question in order to obtain insights that will hopefully extend to other models.

Since the differences between the models are all related to the treatment of the NsrR dimers, and since changing the nitrosylation rate constants (holding other parameters constant) maintains the equivalence between the models, the only rate constants that are directly implicated in the dimer dynamics that remain to be investigated are the recycling rate constant  $k_r$  and the rate constants associated with binding of NsrR (monomers or dimers) to the *hmp* promoters.

The steady states do not depend strongly on  $k_r$  for values of this rate constant similar to or larger than the default value of  $0.1\text{ s}^{-1}$  we have assumed. However, if recycling is slow, the three models make distinctly different predictions, as seen in Fig. 3.7. In the case of

models MM and DM1 [panels (a) and (b)], the differences are only quantitative, with the bifurcation points being shifted to slightly lower values of  $k_p$  in DM1 relative to MM. Unlike the situation with the default parameters, the MM model displays a supercritical Andronov-Hopf bifurcation [18, 71] on the upper branch of steady states, the limit-cycle (oscillatory) regime being observed over an extremely narrow range of parameters and ending in a homoclinic bifurcation [71]. An Andronov-Hopf bifurcation also occurs in the DM1 model, but much closer to the saddle-node point. The type of Andronov-Hopf bifurcation and the ultimate fate of the limit cycle created are difficult to ascertain due to numerical difficulties in the vicinity of the Andronov-Hopf bifurcation. Nevertheless, it is clear that the two bifurcation diagrams make similar predictions and that, if we did not already know that NsrR binds to DNA as a dimer, an experimental bifurcation diagram varying  $k_p$  (or  $[\text{NO}]_{\text{ext}}$ ) would not be sufficient to distinguish between these models.

DM2 on the other hand behaves very differently than the other two models at  $k_r = 0.001 \text{ s}^{-1}$  [Fig. 3.7(c)]. The classic S-shaped steady-state curve leading to regions of bistability has been lost. Instead, the model displays large-amplitude oscillations over a wide range of parameters. Again, the AUTO continuation computations are difficult near the Andronov-Hopf bifurcations, so the maxima and minima of the limit cycles were calculated using the ‘Poincaré map’ feature of XPPAUT. The emergence of large-amplitude oscillations very near the Andronov-Hopf points, as well as the shapes of the limit cycles near these points [Fig. 3.8(a) and (d)] are suggestive of a canard explosion [72]. Moreover, the complex shapes of the limit cycles at some values of  $k_p$  are suggestive of mixed-mode oscillations [Fig. 3.8(c) and (d)]. We leave a deeper investigation of these dynamics for the future.

Our immediate concern is the reason for the significant difference between DM2 and the other two models at smaller values of  $k_r$ . As  $[\text{NO}]$  increases, the *hmpA2* gene is the first to be transcribed (Fig. 3.9), as expected given that fewer equivalents of NO are required to abolish binding of NsrR at this gene’s promoter [23]. Lowering the value of  $k_r$  generally

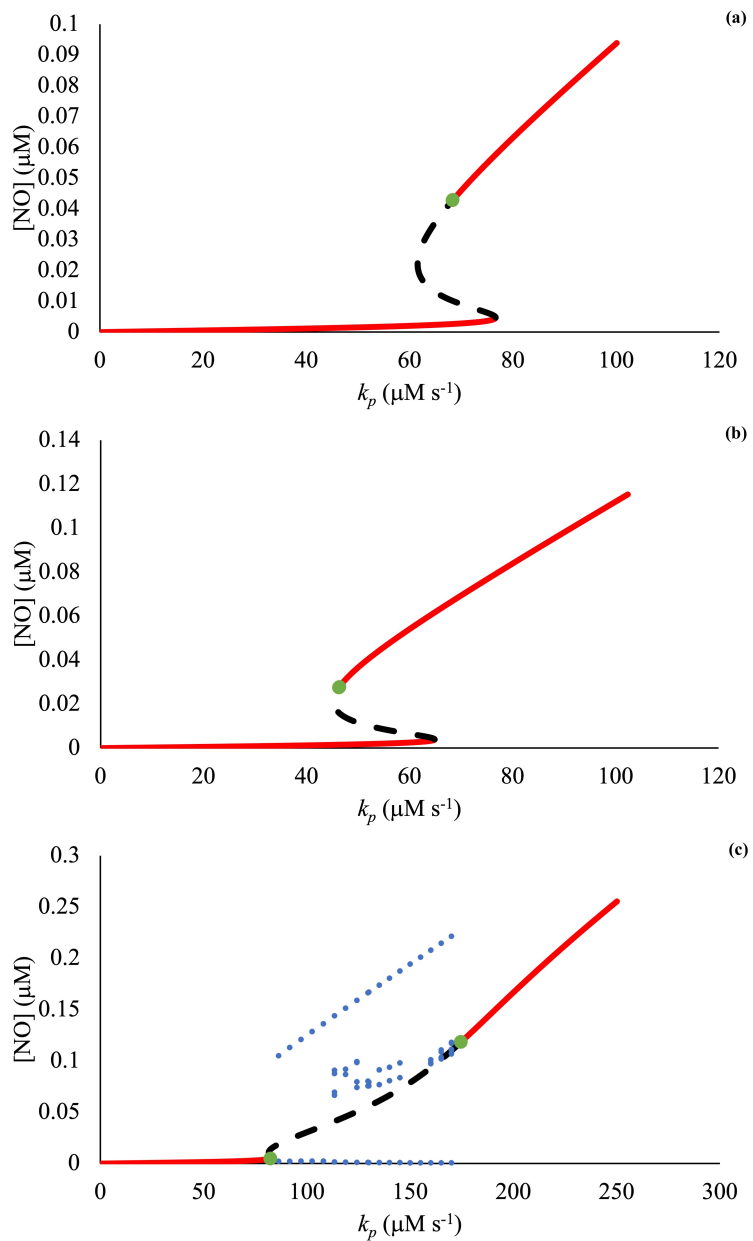


Figure 3.7: Bifurcation diagrams for the three models at  $k_r = 0.001 \text{ s}^{-1}$ . All other parameters are as shown in table 3.1. Green dots show Andronov-Hopf bifurcation points and blue dots depict maxima and minima of periodic trajectories. (a) MM. (b) DM1. (c) DM2.

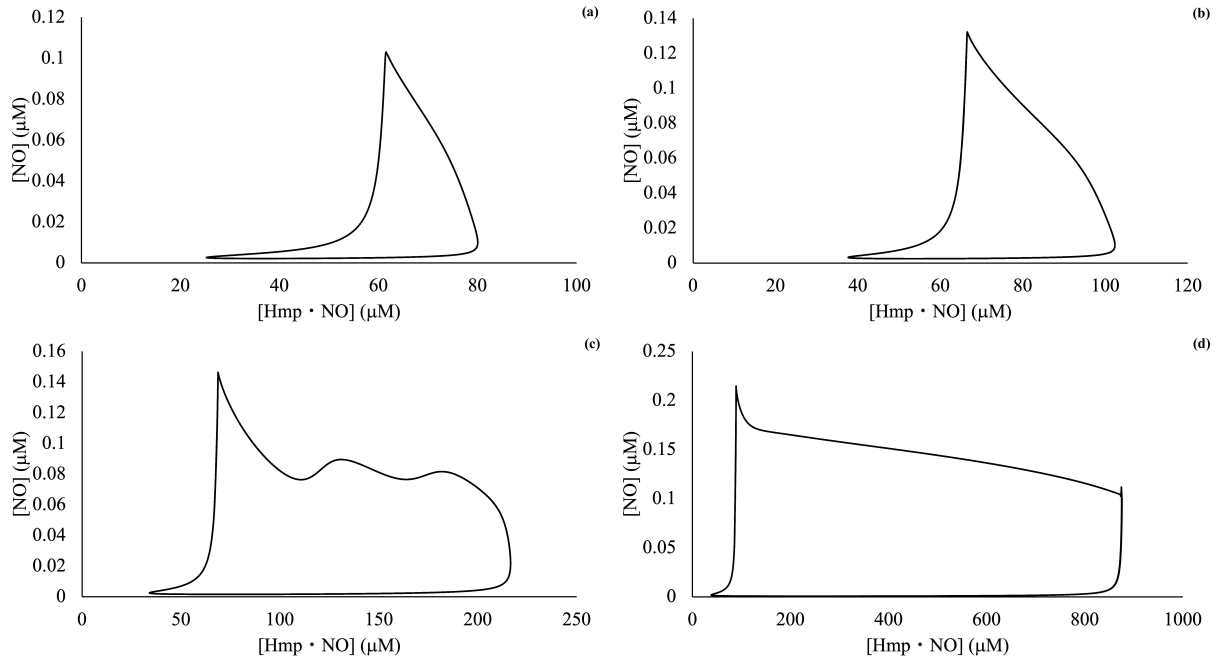


Figure 3.8: Limit cycles for model DM2 at  $k_r = 0.001 \text{ s}^{-1}$ . (a)  $k_p = 85 \mu\text{Ms}^{-1}$ . (b)  $k_p = 105$ . (c)  $k_p = 115$ . (d)  $k_p = 165$ . All other parameters are at default values as shown in table 3.1.

makes the control system more sensitive to [NO] in two ways: First, the dose-response curves shift towards the left, i.e. a smaller concentration of NO is required to activate the transcription of each *hmp* gene. Second, the dose-response curves become steeper as measured by, e.g., the slope of a graph of  $[\text{Pro}^{hmp}]$  vs [NO] at half-maximal activation. (Note that this increase in steepness is not visually evident from Fig. 3.9 due to the logarithmic scale of the abscissa.) The increased sensitivity to [NO] at smaller values of  $k_r$  arises because slower recycling tends to result in the accumulation of higher nitrosylation states of NsrR, which are incompetent to bind the *hmp* promoters (data not shown). While all three models have the same qualitative behavior with respect to decreasing  $k_r$ , the effect is much stronger in DM2. The slopes at half-max of the dose-response curves increase by factors of less than 20 when  $k_r$  decreases from  $0.1 \text{ s}^{-1}$  to  $0.001 \text{ s}^{-1}$  in models MM and DM1, but by more than 50 in DM2. In other words, the response to NO becomes much more switch-like in DM2 with falling  $k_r$  than in the other two models. The increased sensitivity to [NO], by both measures, means that threshold-crossing events that switch the genes on and off are

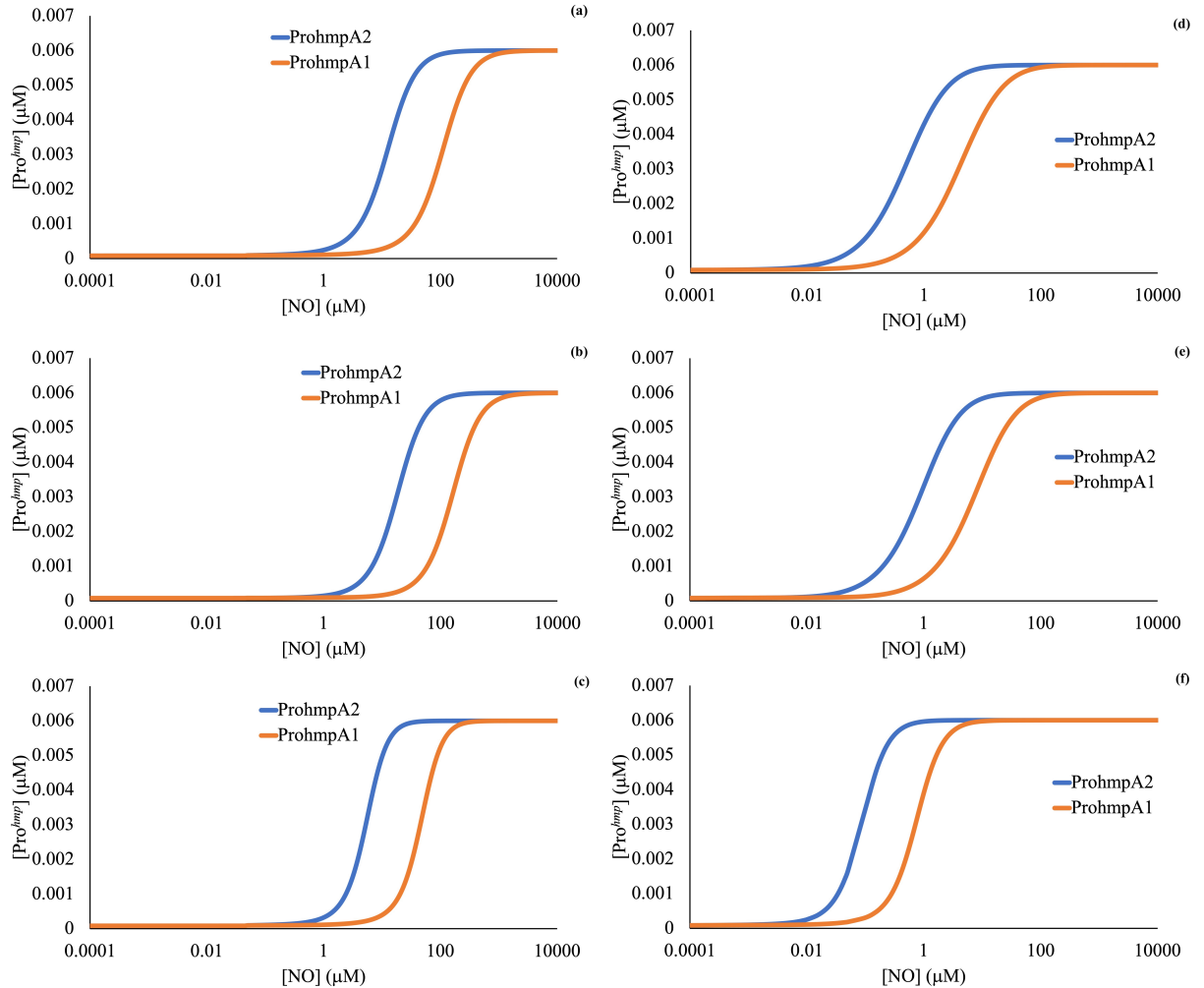


Figure 3.9: Active promoter concentrations vs  $[\text{NO}]$  at  $k_r = 0.1 \text{ s}^{-1}$  [panels (a) to (c)] and  $k_r = 0.001 \text{ s}^{-1}$  [panels (d) to (f)] for the three models. (a), (d) MM; (b), (e) DM1; and (c), (f) DM2. All other parameters are at the default values of table 3.1.

more likely to occur with relatively small changes in  $[\text{NO}]$ . Delays in the response due to the biochemical reactions intervening between a change in  $[\text{NO}]$  and a change in the transcriptional states of the two promoters then result in overcompensation, leading to oscillations.

Altering the rate constants for binding of the NsrR monomers or dimers at the *hmp* promoters— $k_{\pm A}$ ,  $k_{\pm B}$ ,  $k_{\pm C}$ —could reasonably be expected to differentiate the models since the main differences between them are in these binding steps. In order to answer the larger question about conditions that might lead to monomer and dimer models giving different

results, we tried different values of these rate constants, setting aside the experimental data [69] on which we based our original parameter estimates. We explored a number of different combinations of rate constants, most of which resulted in bifurcation diagrams that were negligibly different between the three models. Available experimental data suggest a progressive weakening of the binding as additional equivalents of NO react with NsrR's iron-sulfur cluster [23, 73], i.e. an increasing dissociation constant  $K_d$ , and we generated the rate constants presented in Table 3.1 on this assumption. It was only when we tried to reverse this trend completely, i.e. to assume that the dissociation constants decrease with increasing nitrosylation, that we started to see differences between the models. Figure 3.10 shows one example with  $k_{-A} \gg k_{-B} \gg k_{-C}$ , keeping the other parameters at their default values. Under these conditions, models MM and DM2 behave essentially identically, but DM1 displays bistability over a much wider range of  $k_p$  values. Similar results can be obtained with  $k_{-A} = k_{-B} = k_{-C}$  and  $k_A \ll k_B \ll k_C$ . It is also not strictly necessary to change all of these rate constants in order for DM1 to behave differently from MM and DM2. For example, keeping all other parameters at their default values, reducing  $k_{-B}$  to  $0.01 \text{ s}^{-1}$  results in MM and DM2 having a very narrow range of  $k_p$  values over which bistability is observed ( $k_p \approx 9\text{--}12 \mu\text{M s}^{-1}$ ), whereas bistability is observed over a much wider range for DM1 ( $k_p \in (13.6, 35.9) \mu\text{M s}^{-1}$ ). The key factor seems to be to have a large decrease in the dissociation constant from binding step A to binding step B.

### 3.5 Discussion and conclusion

In previous work, Roussel had argued that an adequate model for the control of Hmp synthesis by an iron-sulfur protein could be obtained by treating the dimeric transcription factor as a monomer [18]. In this paper, we tested this proposition by comparing models for the control of Hmp synthesis in *Streptomyces* based on monomeric and dimeric NsrR repressors. Using, insofar as it was possible, parameters obtained from the literature, we found that at our default set of parameters, the monomer model and both dimer models give

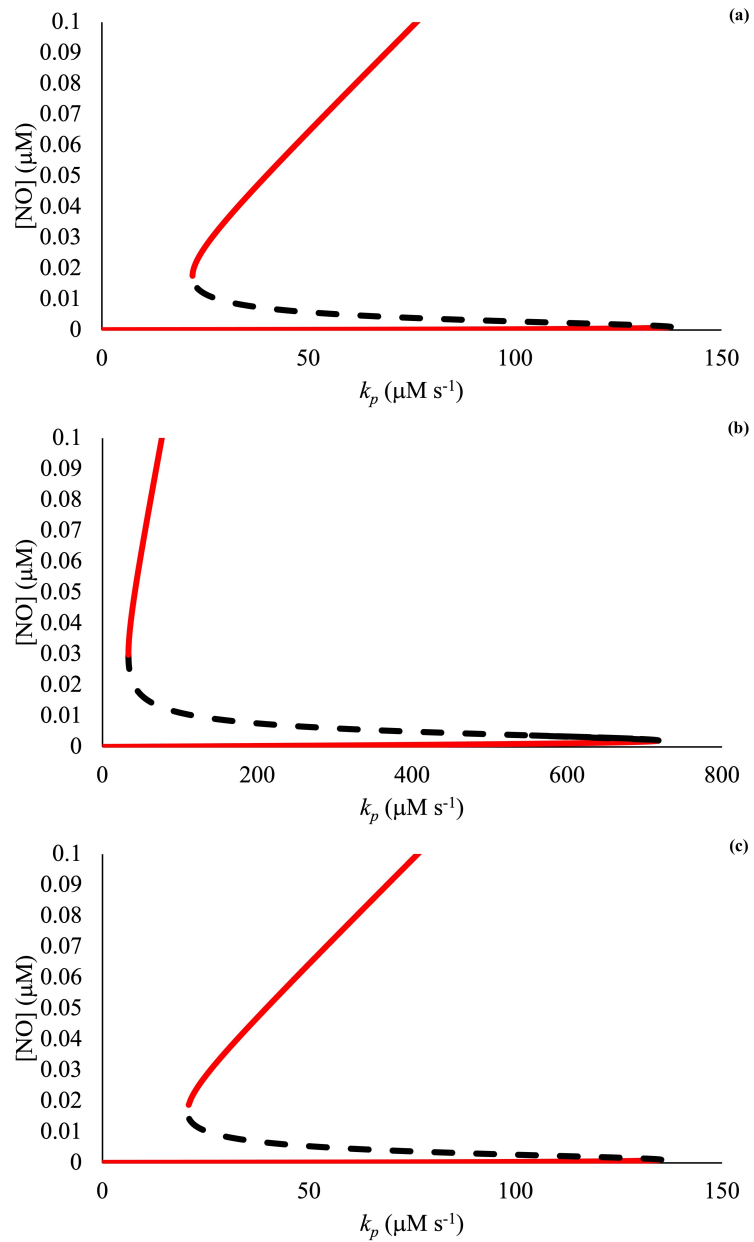


Figure 3.10: Bifurcation diagram for models MM, DM1 and DM2 when  $k_{-B} = 1 \times 10^{-1} \text{s}^{-1}$  and  $k_{-C} = 1 \times 10^{-3} \text{s}^{-1}$ . (a) Bifurcation diagram for MM. (b) Bifurcation diagram for DM1. (c) Bifurcation diagram for DM2. All parameters are as shown in table 3.1 except  $k_{-B}$  and  $k_{-C}$ .

essentially identical results provided recycling of the nitrosylated NsrR proteins to their undamaged state is rapid. Slow recycling can produce very significant differences in the behavior of the models, not only quantitatively, but qualitatively (Fig. 3.7).

Since we had not anticipated the importance of the repair pathway, we modeled recovery of holo-NsrR as a simple first-order reaction. This assumption and its implications for the adequacy of a monomer-based transcription factor model clearly needs deeper examination. The uncertainty surrounding the actors in this pathway [74, 75] makes detailed modeling awkward. Nevertheless, the attempt to build a more refined model of recycling would be worthwhile given its importance in determining the behavior of this class of models.

Recycling of a transcription factor, as in the models presented here, is a conservative process. (See, e.g., Eq. (3.14a).) A production-destruction system in which transcription factors that have reached a certain modification state are degraded and replaced by freshly synthesized proteins lacks a conservation relation and may behave quite differently. However, it is possible that homeostatic control of the protein level would have a somewhat similar effect to a conservation relation so that some of the observations made in this study could find counterparts in a production-destruction system. It would therefore be of considerable interest to study the effects of dimerization or oligomerization of transcription factors in production-destruction systems.

In addition to recycling, we found that assumptions made about the effect of differential nitrosylation between monomers in a dimer on the binding of the transcription factor to a promoter can have important effects on model behavior. DM1 and DM2 can be thought of as two extremes along a continuum of possibilities. In DM1, it is sufficient for one monomer to be in a sufficiently low nitrosylation state for an NsrR dimer to bind to a promoter. In DM2, the highest nitrosylation state in a pair determines the binding properties. Of course, there are many possibilities between these two extremes, and we await experimental data that would allow us to determine how unequal nitrosylation affects binding.

Homodimeric transcription factors that are activated either by covalent modification or

by binding a ligand are not at all unusual, so some of the lessons learned in this study may be applicable to other situations. For example, Smad2 dimers, which are key players in the transduction of TGF- $\beta$  signals, only form when the individual units are phosphorylated. Dephosphorylation results in dissociation of the dimer into its components, and recycling of the Smad2 monomers to the cytosol [76]. Basic helix-loop-helix proteins also frequently form homodimers whose activity is controlled by phosphorylation [77]. In these models, we would expect that both the rate of recycling of the transcription factors and assumptions about the effect of modifying just one monomer would be key parameters in determining model behavior.

In every version of the model and for a wide range of rate constants, we found that bistability was observed. This was useful in this study because it allowed us to visualize the effects of various assumptions about NsrR and its binding properties to the *hmp* promoters on the dynamics of the overall control system. Experimentally, bistability would manifest itself as a hysteresis loop, i.e. different states of the cell observed depending on whether the control parameter was being swept in an increasing or decreasing direction. The simplest way to observe this effect, if indeed it occurs in cells, would be to use the external NO concentration as a control parameter [Fig. 3.1(b)]. However, there is an upper limit in the membrane permeability to NO above which bistability would not be observed [Fig 3.2]. It is therefore an open question whether bistability could be observed in real cells. The *Streptomyces* system is particularly appealing for experimental study of this and many other questions about feedback between NO, the state of NsrR and the Hmp concentration because of its relative simplicity and of the small number of directly interacting components.

We did not take into account the expression of NsrR, which is itself under the control of the NsrR transcription factor, nor did we consider the kinetics of synthesis of NsrR monomers, which includes loading the apo-enzyme with an iron-sulfur cluster, and of the assembly of the monomers into dimers. Instead, we assumed that NsrR dimers (or

monomers in model MM) are present at constant concentration in the cell. In some cases, the expression of the transcription factor, its post-translational modification and its oligomerization kinetics will be critical to the dynamics of the control system. In such cases, it would not be possible to ignore the oligomers, and rule-based modeling would become a critical tool for the study of such systems. The ongoing development of rule-based systems with the ability to describe a larger range of relationships will therefore greatly facilitate research involving the construction and study of models of gene expression.

We created DM2 by explicitly enumerating the states that are able to bind the promoter and manually assigning their rate constants. We were forced to do this because BNGL lacks a comparison operator that would allow us to express rules in terms of “the less nitrosylated monomer”, or other equivalent formulations. Were we to add the *nsrR* gene to our model, this would become a real chore given that NsrR binds to its promoter until 8 NO molecules have reacted per monomer [23]. At that point, it would likely make sense for us to write a program to instantiate any given set of rules rather than use BioNetGen for the purpose. This observation highlights one important limitation of the BNGL language, which we hope future releases will address.

# Chapter 4

## Conclusion

### 4.1 Summary

Holo-NsrR, containing an iron-sulfur cluster, generally acts as a repressor in a number of genes associated with nitrogen oxide metabolism in bacteria and binds to promoters as a dimer. Since Roussel ignored the effects of dimerization of FNR [18], studying these effects for NsrR is dynamically interesting. We therefore built a base model where NsrR acts as a monomer and two dimer models, DM1 and DM2, to study the effect of dimerization of NsrR on Hmp gene expression. Afterwards, we compared the dynamics of the dimer models with the monomer model. Based on the experimental data, binding of NsrR to *hmpA1* and *hmpA2* is entirely abolished at 4 and 2 NO's per cluster, respectively. According to these data, the kinetically distinguishable nitrosylated states of NsrR are NsrR<sub>B</sub>, NsrR<sub>C</sub>, NsrR<sub>D</sub>, NsrR<sub>E</sub> and NsrR<sub>F</sub>. We showed that the behaviors of the monomer and dimer models are similar at the default values of the parameters shown in table 3.1. We also made many changes in the parameters, and generally the monomer and dimer models behaved similarly. Thus, for a wide range of parameters, binding only depends on the properties of the monomers and not on the dimer states. Then, we found that by changing the binding parameters of NsrR to the promoter, DM1 behaves differently than MM and DM2. Additionally, we showed that small values of the recycling rate of NsrR results in different behavior of DM2. In summary, changing the binding parameters or altering the recycling rate of NsrR to the intact holo-protein makes a difference to the results, however the recycling rate is more salient.

Depending on the depth where *Streptomyces* lives in the soil, the oxygen concentration is different [68]. We showed that if *Streptomyces* lives near the soil surface (higher O<sub>2</sub> concentration), the bistable region will be bigger and there is a shift of the bistable region to higher amount of NO and conversely, if *Streptomyces* lives in the deeper layers of the soil (lower O<sub>2</sub> concentration), the bistable region gets smaller and there is a shift of the bistable region to lower concentrations of NO. Therefore, the O<sub>2</sub> concentration affects the dynamical behavior of the system.

## 4.2 Future directions

The aim of this thesis was to study the effects of dimerization of transcription factors in gene expression models. Through a quantitative analysis of mathematical models, several results were obtained that can help direct future research in the field. This section provides some key points for further research such as additional work on the Hmp control system for pathogenic bacteria, the effects of oligomerization of transcription factors in gene expression, and considering the delays in gene transcription and translation.

We did not take into account the expression of NsrR, which is itself under the control of the dimeric NsrR transcription factor, nor we did not consider the kinetics of association of NsrR monomers into dimers. Instead, we assumed that NsrR dimers are present at constant concentration in the cell. In some cases, the expression of the transcription factor and its oligomerization kinetics will be critical to the dynamics of the control system. In such cases, it would not be possible to ignore the oligomers, and rule-based modeling would become a critical tool for the study of such systems. The ongoing development of rule-based systems with the ability to describe a larger range of relationships will therefore greatly facilitate research involving the construction and study of models of gene expression.

A consistent theme throughout the thesis work was studying the control system of Hmp. As mentioned in the first chapter, *nsrR* is much less sensitive to NO, so we assumed NsrR is constant. Allowing NsrR to be variable could be explored in future studies.

In the models presented here, the NsrR recycling pathway is described as a simple first-order process. We found that the recycling pathway is a salient factor in determining whether or not the models behave differently. Thus, studying the enzymic nature of the repair pathway and modeling the repair process of damaged iron-sulfur clusters by an enzyme should be of high priority for future studies.

In chapter three, the dynamical behavior of three different models were investigated. The DM2 model behaved differently at lower  $k_r$ . In DM2, the complex shapes of the limit cycles in Fig.3.7(c) at some values of  $k_p$  are suggestive of mixed-mode oscillations. Future studies should probe the dynamical behavior around the bifurcation points in this model in detail.

Furthermore, we ignored the transcriptional and translational delays, as well as clearance delays in our study, although delays can have significant effects on the behavior of a model [78]. Thus, new studies could examine the use of delayed mass-action kinetics for modeling of the transcription of genes [79]. The existing computational methods and software we applied do not handle delays, so new tools need to be developed to combine rule-based modeling with delays for studying complex transcription factor systems with delays.

Building on this theoretical study of the control system for Hmp in *Streptomyces*, the Hmp control system in organisms of biomedical interest could be studied. *Streptomyces* is rarely pathogenic [32]. Although the Hmp control system in *Streptomyces* differs from those in pathogenic bacteria [27], future study would be expanded to pathogenic bacteria such as *Burkholderia pseudomallei* by modifying the Hmp control system in our models. In *B. pseudomallei*, NsrR regulates different genes including *hmp*, *nnrS2*, *norB* and *nnrS1* [27] but, as in *Streptomyces*, *hmp* is only controlled by NsrR. In other words, studying a simple control system can be a stepping stone to studying more complex systems. So, my work on *Streptomyces* will be directly relevant to those bacteria which are of medical concern and my studies are a platform for thinking about the development of new antibiotics as Hmp is

a virulence factor [80].

Additionally, rule-based modeling can be applied for other transcription factors that act as dimers or higher oligomers. For example, the *EhPgp5* protein confers multi-drug resistance in *Entamoeba histolytica* by altering ion conductance [81], and EhHSTF7 controls the *EhPgp5* gene. Studying EhHSTF7, which acts as an oligomer in *Entamoeba* [82], could be a starting point for future studies.

# Bibliography

- [1] Pol Picón-Pagès, Joan Garcia-Buendia, and Francisco J. Muñoz. Functions and dysfunctions of nitric oxide in brain. *Biochimica et Biophysica Acta (BBA) - Molecular Basis of Disease*, 1865(8):1949–1967, 2019.
- [2] Paul B. Lewis, Deana Ruby, and Charles A. Bush-Joseph. Muscle soreness and delayed-onset muscle soreness. *Clinics in Sports Medicine*, 31(2):255–262, 2012.
- [3] Matthias Hermann, Andreas Flammer, and Thomas F. Lüscher. Nitric oxide in hypertension. *The Journal of Clinical Hypertension*, 8:17–29, 2006.
- [4] Paolo Tessari, Diego Cecchet, Alessandra Cosma, Monica Vettore, Anna Coracina, Renato Millionini, Elisabetta Iori, Lucia Puricelli, Angelo Avogaro, and Monica Vedovato. Nitric oxide synthesis is reduced in subjects with type 2 diabetes and nephropathy. *Diabetes*, 59(9):2152–2159, 2010.
- [5] David D. Chaplin. Overview of the immune response. *Journal of Allergy and Clinical Immunology*, 125(2, Supplement 2):S3–S23, 2010.
- [6] Balázs Hauser, Peter Radermacher, Christoph Thiemermann, and Martin Matejovic. Nitric oxide, bacteria, and host defense in sepsis: Who needs what? *Shock*, 22(6):588–590, 2004.
- [7] Nicholas P. Tucker, Nick E. Le Brun, Ray Dixon, and Matthew I. Hutchings. There's NO stopping NsrR, a global regulator of the bacterial NO stress response. *Trends in Microbiology*, 18(4):149–156, 2010.
- [8] Penelope J Andrew and Bernd Mayer. Enzymatic function of nitric oxide synthases. *Cardiovascular Research*, 43(3):521–531, 1999.
- [9] Bernd Mayer and Benjamin Hemmens. Biosynthesis and action of nitric oxide in mammalian cells. *Trends in Biochemical Sciences*, 22(12):477–481, 1997.
- [10] Nathalie Gonska, David Young, Riki Yuki, Takuya Okamoto, Tamao Hisano, Svetlana Antonyuk, S. Samar Hasnain, Kazumasa Muramoto, Yoshitsugu Shiro, Takehiko Tosha, and Pia Ädelroth. Characterization of the quinol-dependent nitric oxide reductase from the pathogen *Neisseria meningitidis*, an electrogenic enzyme. *Scientific Reports*, 8(1), 2018.
- [11] Ian M. Wasser, Simon de Vries, Pierre Moënne-Loccoz, Imke Schröder, and Kenneth D. Karlin. Nitric Oxide in Biological Denitrification: Fe/Cu Metalloenzyme and Metal Complex NO Redox Chemistry. *Chemical Reviews*, 102(4):1201–1234, 2002.

- [12] Rob J.M. van Spanning, David J. Richardson, and Stuart J. Ferguson. Introduction to the biochemistry and molecular biology of denitrification. In *Biology of the Nitrogen Cycle*, pages 3–20. Elsevier, 2007.
- [13] Daniel N. Wilson. Ribosome-targeting antibiotics and mechanisms of bacterial resistance. *Nature Reviews Microbiology*, 12(1):35–48, 2013.
- [14] Global Antimicrobial Surveillance System of World Health Organization <https://www.who.int/news/item/29-01-2018-high-levels-of-antibiotic-resistance-found-worldwide-new-data-shows>.
- [15] Jessica M. A. Blair, Mark A. Webber, Alison J. Baylay, David O. Ogbolu, and Laura J. V. Piddock. Molecular mechanisms of antibiotic resistance. *Nature Reviews Microbiology*, 13(1):42–51, 2014.
- [16] Taku Nishimura, Haruhiko Teramoto, Alain A. Vertes, Masayuki Inui, and Hideaki Yukawa. ArnR, a Novel Transcriptional Regulator, Represses Expression of the narKGHI Operon in *Corynebacterium glutamicum*. *Journal of Bacteriology*, 190(9):3264–3273, 2008.
- [17] Paul R. Gardner, Anne M. Gardner, Lori A. Martin, and Andrew L. Salzman. Nitric oxide dioxygenase: An enzymic function for flavohemoglobin. *Proceedings of the National Academy of Sciences*, 95:10378–10383, 1998.
- [18] Marc R. Roussel. A delayed mass-action model for the transcriptional control of hmp, an NO detoxifying enzyme, by the iron-sulfur protein FNR. In *Delays and Interconnections: Methodology, Algorithms and Applications*, pages 215–230. Springer International Publishing, 2019.
- [19] Donald Voet and Judith G. Voet. *Biochemistry*, pages 1283–1301. Wiley, Hoboken, NJ, fourth edition, 2011.
- [20] Juli D. Klemm, Stuart L. Schreiber, and Gerald R. Crabtree. Dimerization as a regulatory mechanism in signal transduction. *Annual Review of Immunology*, 16(1):569–592, 1998. PMID: 9597142.
- [21] Grigoris D. Amoutzias, David L. Robertson, Yves Van de Peer, and Stephen G. Oliver. Choose your partners: dimerization in eukaryotic transcription factors. *Trends in Biochemical Sciences*, 33(5):220–229, 2008.
- [22] Yun Mou, Po-Ssu Huang, Fang-Ciao Hsu, Shing-Jong Huang, and Stephen L. Mayo. Computational design and experimental verification of a symmetric protein homodimer. *Proceedings of the National Academy of Sciences*, 112(34):10714–10719, 2015.
- [23] Jason C. Crack, Dimitri A. Svistunenko, John Munnoch, Andrew J. Thomson, Matthew I. Hutchings, and Nick E. Le Brun. Differentiated, promoter-specific response of [4Fe-4S] NsrR DNA binding to reaction with nitric oxide. *Journal of Biological Chemistry*, 291(16):8663–8672, 2016.

- [24] L Aravind, V Ananthraman, S Balaji, M Babu, and L Iyer. The many faces of the helix-turn-helix domain: Transcription regulation and beyond. *FEMS Microbiology Reviews*, 29(2):231–262, 2005.
- [25] John Munnoch, Ma Martinez, Dimitri Svistunenko, Jason Crack, Nick Le Brun, and Matthew Hutchings. Characterization of a putative NsrR homologue in *Streptomyces venezuelae* reveals a new member of the Rrf2 superfamily. *Scientific Reports*, 6:31597, 2016.
- [26] Steven Wilkinson and Anne Grove. Ligand-responsive transcriptional regulation by members of the MarR family of winged helix protein. *Current Issues in Molecular Biology*, 8:51–62, 2006.
- [27] Dmitry A Rodionov, Inna L Dubchak, Adam P Arkin, Eric J Alm, and Mikhail S Gelfand. Dissimilatory metabolism of nitrogen oxides in bacteria: Comparative reconstruction of transcriptional networks. *PLoS Computational Biology*, 1(5):e55, 2005.
- [28] Jason C. Crack, Laura J. Smith, Melanie R. Stapleton, Jamie Peck, Nicholas J. Watmough, Mark J. Buttner, Roger S. Buxton, Jeffrey Green, Vasily S. Oganessian, Andrew J. Thomson, and Nick E. Le Brun. Mechanistic insight into the nitrosylation of the [4Fe4S] cluster of WhiB-like proteins. *Journal of the American Chemical Society*, 133(4):1112–1121, 2011. PMID: 21182249.
- [29] Todd C. Harrop, Zachary J. Tonzetich, Erwin Reisner, and Stephen J. Lippard. Reactions of synthetic [2Fe-2S] and [4Fe-4S] clusters with nitric oxide and nitrosothiols. *Journal of the American Chemical Society*, 130(46):15602–15610, 2008. PMID: 18939795.
- [30] Jonathan L. Robinson and Mark P. Brynildsen. A kinetic platform to determine the fate of nitric oxide in *Escherichia coli*. *PLoS Computational Biology*, 9(5):e1003049, 2013.
- [31] Jonathan L. Robinson and Mark P. Brynildsen. Discovery and dissection of metabolic oscillations in the microaerobic nitric oxide response network of *Escherichia coli*. *Proceedings of the National Academy of Sciences*, 113:E1757–E1766, 2016.
- [32] Chapter 34 - actinomyces, propionibacterium propionicus, and *Streptomyces*. In Samuel Baron, editor, *Medical Microbiology*. University of Texas Medical Branch at Galveston, 1996.
- [33] Leonard A. Harris, Justin S. Hogg, José-Juan Tapia, John A. P. Sekar, Sanjana Gupta, Ilya Korsunsky, Arshi Arora, Dipak Barua, Robert P. Sheehan, and James R. Faeder. BioNetGen 2.2: advances in rule-based modeling. *Bioinformatics*, 32(21):3366–3368, 2016.
- [34] Bard Ermentrout. *Simulating, Analyzing, and Animating Dynamical Systems: A Guide to XPPAUT for Researchers and Students*. SIAM, Philadelphia, 2002.

- [35] Marc R Roussel. *Nonlinear Dynamics: A Hands-On Introductory Survey*. IOP Concise Physics. Morgan & Claypool, San Rafael, CA, 2019.
- [36] Stefan Hoops, Sven Sahle, Ralph Gauges, Christine Lee, Jürgen Pahle, Natalia Simus, Mudita Singhal, Liang Xu, Pedro Mendes, and Ursula Kummer. COPASI—a COMplex PATHway SIMulator. *Bioinformatics*, 22(24):3067–3074, 2006.
- [37] M. Hucka, A. Finney, H. M. Sauro, H. Bolouri, J. C. Doyle, H. Kitano, A. P. Arkin, B. J. Bornstein, D. Bray, A. Cornish-Bowden, A. A. Cuellar, S. Dronov, E. D. Gilles, M. Ginkel, V. Gor, I. I. Goryanin, W. J. Hedley, T. C. Hodgman, J.-H. Hofmeyr, P. J. Hunter, N. S. Juty, J. L. Kasberger, A. Kremling, U. Kummer, N. Le Novère, L. M. Loew, D. Lucio, P. Mendes, E. Minch, E. D. Mjolsness, Y. Nakayama, M. R. Nelson, P. F. Nielsen, T. Sakurada, J. C. Schaff, B. E. Shapiro, T. S. Shimizu, H. D. Spence, J. Stelling, K. Takahashi, M. Tomita, J. Wagner, J. Wang, and the rest of the SBML Forum: The systems biology markup language (SBML): a medium for representation and exchange of biochemical network models. *Bioinformatics*, 19(4):524–531, 2003.
- [38] Sarah M Keating, Dagmar Waltemath, Matthias König, Fengkai Zhang, Andreas Dräger, Claudine Chaouiya, Frank T Bergmann, Andrew Finney, Colin S Gillespie, Tomáš Helikar, Stefan Hoops, Rahuman S Malik-Sheriff, Stuart L Moodie, Ion I Moraru, Chris J Myers, Aurélien Naldi, Brett G Olivier, Sven Sahle, James C Schaff, Lucian P Smith, Maciej J Swat, Denis Thieffry, Leandro Watanabe, Darren J Wilkinson, Michael L Blinov, Kimberly Begley, James R Faeder, Harold F Gómez, Thomas M Hamm, Yuichiro Inagaki, Wolfram Liebermeister, Allyson L Lister, Daniel Lucio, Eric Mjolsness, Carole J Proctor, Karthik Raman, Nicolas Rodriguez, Clifford A Shaffer, Bruce E Shapiro, Joerg Stelling, Neil Swainston, Naoki Tanimura, John Wagner, Martin Meier-Schellersheim, Herbert M Sauro, Bernhard Palsson, Hamid Bolouri, Hiroaki Kitano, Akira Funahashi, Henning Hermjakob, John C Doyle, Michael Hucka, and SBML Level 3 Community members. Sbm level 3: an extensible format for the exchange and reuse of biological models. *Molecular Systems Biology*, 16(8):e9110, 2020.
- [39] Jason C. Crack, John Munnoch, Erin L. Dodd, Felicity Knowles, Mahmoud M. Al Bassam, Saeed Kamali, Ashley A. Holland, Stephen P. Cramer, Chris J. Hamilton, Michael K. Johnson, Andrew J. Thomson, Matthew I. Hutchings, and Nick E. Le Brun. NsrR from *Streptomyces coelicolor* is a nitric oxide-sensing 4Fe-4S cluster protein with a specialized regulatory function. *Journal of Biological Chemistry*, 290:12689–12704, 2015.
- [40] Hubertus J. E. Beaumont, Sylvia I. Lens, Willem N. M. Reijnders, Hans V. Westerhoff, and Rob J. M. van Spanning. Expression of nitrite reductase in *Nitrosomonas europaea* involves NsrR, a novel nitrite-sensitive transcription repressor. *Molecular Microbiology*, 54:148–158, 2004.
- [41] Iel-Soo Bang, Limin Liu, Andrés Vazquez-Torres, Marie-Laure Crouch, Jonathan S. Stamler, and Ferric C. Fang. Maintenance of nitric oxide and redox homeosta-

- sis by the *Salmonella* flavohemoglobin Hmp\*. *Journal of Biological Chemistry*, 281(38):28039–28047, 2006.
- [42] Yasuyuki Sasaki, Haruka Oguchi, Takuya Kobayashi, Shinichiro Kusama, Ryo Sugiura, Kenta Moriya, Takuya Hirata, Yuriya Yukioka, Naoki Takaya, Shunsuke Yajima, Shinsaku Ito, Kiyoshi Okada, Kanju Ohsawa, Haruo Ikeda, Hideaki Takano, Kenji Ueda, and Hirofumi Shoun. Nitrogen oxide cycle regulates nitric oxide levels and bacterial cell signaling. *Scientific Reports*, 6:22038, 2016.
- [43] Anne M. Gardner, Lori A. Martin, Paul R. Gardner, Yi Dou, and John S. Olson. Steady-state and transient kinetics of *Escherichia coli* nitric-oxide dioxygenase (flavohemoglobin). *Journal of Biological Chemistry*, 275:12581–12589, 2000.
- [44] Kanhaiya Kumar and Per Bruheim. Nutrient-dependent metabolic switching during batch cultivation of *Streptomyces coelicolor* explored with absolute quantitative mass spectrometry-based metabolite profiling. *3 Biotech*, 12:80, 2022.
- [45] Dagmara Jakimowicz and Gilles Wezel. Cell division and DNA segregation in *Streptomyces*: How to build a septum in the middle of nowhere? *Molecular Microbiology*, 85:393–404, 2012.
- [46] Chien-Chin Yang, Chih-Hung Huang, Chien-Yi Li, Yeou-Guang Tsay, Sheng-Chung Lee, and Carton Chen. The terminal proteins of linear *Streptomyces* chromosomes and plasmids: A novel class of replication priming proteins. *Molecular Microbiology*, 43:297 – 305, 2002.
- [47] Hyun-Jin Kim, Michael J. Calcutt, Francis J. Schmidt, and Keith F. Chater. Partitioning of the linear chromosome during sporulation of *Streptomyces coelicolor* A3(2) involves an *oriC*-Linked *parAB* locus. *Journal of Bacteriology*, 182(5):1313–1320, 2000.
- [48] Aparna Gunjal and Devidas S. Bhagat. Chapter 7 - diversity of actinomycetes in western ghats. In Aparna Gunjal and Sonali Shinde, editors, *Microbial Diversity in Hotspots*, pages 117–133. Academic Press, 2022.
- [49] M Loferer-Krössbacher, J Klima, and Roland Psenner. Determination of bacterial cell dry mass by transmission electron microscopy and densitometric image analysis. *Applied and Environmental Microbiology*, 64:688–94, 1998.
- [50] Hans Degn. Bistability caused by substrate inhibition of peroxidase in an open reaction system. *Nature*, 217(5133):1047–1050, 1968.
- [51] F. F. Seelig and B. Denzel. Hysteresis without autocatalysis: Simple enzyme systems as possible binary memory elements. *FEBS Letters*, 24(3):283–286, 1972.
- [52] Baltazar D. Aguda. Emergent properties of coupled enzyme reaction systems 1. switching and clustering behaviour. *Biophysical Chemistry*, 61(1):1–7, 1996.

- [53] Michael C. Reed, Anna Lieb, and H. Frederik Nijhout. The biological significance of substrate inhibition: A mechanism with diverse functions. *BioEssays*, 32(5):422–429, 2010.
- [54] Elizabeth A. M. Trofimenkoff and Marc R. Roussel. Small binding-site clearance delays are not negligible in gene expression modeling. *Mathematical Biosciences*, 325:108376, 2020.
- [55] Zhe Wang, Qiang-Qiang Han, Mao-Tian Zhou, Xi Chen, and Lin Guo. Protein turnover analysis in *Salmonella* Typhimurium during infection by dynamic SILAC, Topograph, and quantitative proteomics. *Journal of Basic Microbiology*, 56:801–811, 2016.
- [56] Beth A. Lazazzera, Helmut Beinert, Natalia Khoroshilova, Mary Claire Kennedy, and Patricia J. Kiley. DNA binding and dimerization of the Fe–S-containing FNR protein from *Escherichia coli* are regulated by oxygen. *Journal of Biological Chemistry*, 271:2762–2768, 1996.
- [57] Jason C. Crack, Melanie R. Stapleton, Jeffrey Green, Andrew J. Thomson, and Nick E. Le Brun. Mechanism of [4Fe-4S](Cys)<sub>4</sub> cluster nitrosylation is conserved among NO-responsive regulators. *Journal of Biological Chemistry*, 288:11492–11502, 2013.
- [58] Erik T. Yukl, Mohamed A. Elbaz, Michiko M. Nakano, and Pierre Moënne-Loccoz. Transcription factor NsrR from *Bacillus subtilis* senses nitric oxide with a 4Fe–4S cluster. *Biochemistry*, 47:13084–13092, 2008.
- [59] Tim W. Overton, Marta C. Justino, Ying Li, Joana M. Baptista, Ana M. P. Melo, Jeffrey A. Cole, and Lígia M. Saraiva. Widespread distribution in pathogenic bacteria of di-iron proteins that repair oxidative and nitrosative damage to iron-sulfur centers. *Journal of Bacteriology*, 190(6):2004–2013, 2008.
- [60] William S. Hlavacek, James R. Faeder, Michael L. Blinov, Richard G. Posner, Michael Hucka, and Walter Fontana. Rules for modeling signal-transduction systems. *Science's STKE : Signal Transduction Knowledge Environment*, 2006:re6, 2006.
- [61] Thomas G. Kurtz. The relationship between stochastic and deterministic models for chemical reactions. *The Journal of Chemical Physics*, 57:2976–2978, 1972.
- [62] Karel Melzoch, M. Joost Teixeira de Mattos, and Oense M. Neijssel. Production of actinorhodin by *Streptomyces coelicolor* A3(2) grown in chemostat culture. *Biotechnology and Bioengineering*, 54:577–582, 1997.
- [63] Keith J. Laidler and John H. Meiser. *Physical Chemistry*, pages 908–909. Houghton Mifflin, Boston, third edition, 1999.
- [64] Michael H. Abraham, Joelle M. R. Gola, J. Enrique Cometto-Muntz, and William S. Cain. The solvation properties of nitric oxide. *Journal of the Chemical Society, Perkin Transactions 2*, pages 2067–2070, 2000.

- [65] Nicole Yang and Marlon Hinner. Getting across the cell membrane: An overview for small molecules, peptides, and proteins. *Methods in Molecular Biology*, 1266:29–53, 2015.
- [66] Takeshi Shimizu, Akio Matsumoto, and Masatoshi Noda. Cooperative roles of nitric oxide-metabolizing enzymes to counteract nitrosative stress in enterohemorrhagic *Escherichia coli*. *Infection and Immunity*, 87(9), 2019.
- [67] R. Sander. Compilation of Henry’s law constants (version 4.0) for water as solvent. *Atmospheric Chemistry and Physics*, 15:4399–4981, 2015.
- [68] S. K. Sheppard and D. Lloyd. Direct mass spectrometric measurement of gases in soil monoliths. *Journal of Microbiological Methods*, 50:175–188, 2002.
- [69] Vincent M. Isabella, John D. Lapek Jr, Edward M. Kennedy, and Virginia L. Clark. Functional analysis of NsrR, a nitric oxide-sensing Rrf2 repressor in *Neisseria gonorrhoeae*. *Molecular Microbiology*, 71:227–239, 2009.
- [70] Yanmin Hu, Philip Butcher, Joseph Mangan, Marie-Adele Rajandream, and Anthony Coates. Regulation of hmp gene transcription in *Mycobacterium tuberculosis*: Effects of oxygen limitation and nitrosative and oxidative stress. *Journal of Bacteriology*, 181:3486–3493, 1999.
- [71] Jack K. Hale and Hüseyin Koçak. *Dynamics and Bifurcations*, volume 3 of *Texts in Applied Mathematics*. Springer, New York, 1991.
- [72] Mathieu Desroches, John Guckenheimer, Bernd Krauskopf, Christian Kuehn, Hinke M. Osinga, and Martin Wechselberger. Mixed-mode oscillations with multiple time scales. *SIAM Review.*, 54:211–288, 2012.
- [73] Anne Volbeda, Erin L. Dodd, Claudine Darnault, Jason C. Crack, Oriane Renoux, Matthew I. Hutchings, Nick E. Le Brun, and Juan C. Fontecilla-Camps. Crystal structures of the NO sensor NsrR reveal how its iron-sulfur cluster modulates DNA binding. *Nature Communications*, 8:15052, 2017.
- [74] Karla Esquilin-Lebron, Sarah Dubrac, Frédéric Barras, and Jeffrey M. Boyd. Bacterial approaches for assembling iron-sulfur proteins. *American Society for Microbiology*, 12:e02425–21, 2021.
- [75] Jason C. Crack, Basema K. Balasiny, Sophie P. Bennett, Matthew D. Rolfe, Afonso Froes, Fraser MacMillan, Jeffrey Green, Jeffrey A. Cole, and Nick E. Le Brun. The di-iron protein YtfE is a nitric oxide-generating nitrite reductase involved in the management of nitrosative stress. *Journal of the American Chemical Society*, 144:7129–7145, 2022.
- [76] Harish Shankaran and H. Steven Wiley. Smad signaling dynamics: Insights from a parsimonious model. *Science Signaling*, 1:pe41, 2008.

- [77] Juanliang Cai and Ethylin Wang Jacobs. A twisted hand: bHLH protein phosphorylation and dimerization regulate limb development. *BioEssays : news and reviews in molecular, cellular and developmental biology*, 27:1102–1106, 2005.
- [78] Kresimir Josic, José López, William Ott, Liejune Shiau, and Matthew Bennett. Stochastic delay accelerates signaling in gene networks. *PLoS Computational Biology*, 7:e1002264, 2011.
- [79] Marc R. Roussel. The use of delay differential equations in chemical kinetics. *The Journal of Physical Chemistry*, 100:8323–8330, 1996.
- [80] Iel-Soo Bang, Limin Liu, Andrés Vazquez-Torres, Marie-Laure Crouch, Jonathan S. Stamler, and Ferric C. Fang. Maintenance of nitric oxide and redox homeostasis by the *Salmonella* flavohemoglobin hmp. *Journal of Biological Chemistry*, 281(38):28039–28047, 2006.
- [81] Dulce Maria Delgadillo, D Pérez, Consuelo Gómez, Arturo Ponce, Francisco Paz, Cecilia Bañuelos, Leobardo Mendoza, Cesar Lopez-Camarillo, and Esther Orozco. The *Entamoeba histolytica* EhPgp5 (MDR-like) protein induces swelling of the trophozoites and alters chloride-dependent currents in *Xenopus laevis* oocytes. *Microbial Drug Resistance*, 8:15–26, 2002.
- [82] Fabiola Bello, Esther Orozco, Claudia G. Benítez-Cardoza, Absalom Zamorano-Carrillo, César A. Reyes-López, D. Guillermo Pérez-Ishiwara, and Consuelo Gómez-García. The novel EhHSTF7 transcription factor displays an oligomer state and recognizes a heat shock element in the *Entamoeba histolytica* parasite. *Microbial Pathogenesis*, 162:105349, 2022.

# Appendix A

## BioNetGen code

### A.1 Monomer (MM)

```
begin model
begin parameters
  kAB 4.52 # /micromol.s
  kBC 0.113 # /micromol.s
  kCD 1.34e-2 # /micromol.s
  kDE 7.48e-3 # /micromol.s
  kEF 0.43e-3 #/micromol.s
  kr 0.009
  NsrR_init 2.5 # micromolar
  NO_init 10 # micromolar
  NOext_init 0.1
  O2_init 200
  ke1 0.03
  kp 0
  k1 8
  k_1 1.4
  k2 2.5e+3
  k_2 6.2e-4
  k_3 6.2e+2
  k4 80
  k_4 6.2e-4
  k5 0.014
  k6 2.4e-4
  ProhmpA1_init 6.22e-3
  ProhmpA2_init 6.22e-3
  kd 0.71
  ke 0.83
  kA 10
  k_A 0.35
  kB 10
  k_B 0.4
  kC 10
  k_C 0.45
```

```
end parameters

begin molecule types
  NsrR(a)
  NsrRB(a)
  NsrRC(a)
  NsrRD(a)
  NsrRE(a)
  NsrRF(a)
  NO(a)
  NOext()
  Hmp(n,o)
  O2(a)
  ProhmpA2(b)
  ProhmpA1(b)
  RBS()
  NO3(a)
end molecule types

begin species
  NsrR(a) NsrR_init
  NO(a) NO_init
  ProhmpA2(b) ProhmpA2_init
  ProhmpA1(b) ProhmpA1_init
  $O2(a) O2_init
  $NOext() NOext_init
end species

begin observables

  #Species ProhmpA2 ProhmpA2(b)
  #Species ProhmpA1 ProhmpA1(b)
  Species No NO(a)
  #Species Hmp_NO Hmp(n!+)
  #Species RBS RBS()

end observables

begin reaction rules
  # Hmp/NO dynamics
  # Permeation and intracellular production
  NOext() <-> NO(a) kel,kel
  0 -> NO(a) kp
  # Enzyme kinetics
```

```

Hmp(n,o) + O2(a) <-> Hmp(n,o!1).O2(a!1) k1,k_1
Hmp(n,o!1).O2(a!1) + NO(a) <-> Hmp(n!0,o!1).O2(a!1).NO(a!0) k2,k_2
Hmp(n!0,o!1).O2(a!1).NO(a!0) -> Hmp(n,o) + NO3(a) k_3
Hmp(n,o) + NO(a) <-> Hmp(n!1,o).NO(a!1) k4,k_4

# Production/decay of mRNA (ribosome binding sites) and of Hmp
ProhmpA2(b) -> ProhmpA2(b) + RBS() kd
ProhmpA1(b) -> ProhmpA1(b) + RBS() kd
RBS() -> RBS() + Hmp(n,o) ke
RBS() -> 0 k5

# Decay of Hmp and its complexes
Hmp(n,o) -> 0 k6
Hmp(n,o!1).O2(a!1) -> O2(a) + 0 k6
Hmp(n!0,o!1).O2(a!1).NO(a!0) -> O2(a) + NO(a) k6
Hmp(n!1,o).NO(a!1) -> NO(a) k6

# Reactions of NsrR with NO
NsrR(a) + NO(a) -> NsrRB(a) kAB
NsrRB(a) + NO(a) -> NsrRC(a) kBC
NsrRC(a) + NO(a) -> NsrRD(a) kCD
NsrRD(a) + NO(a) -> NsrRE(a) kDE
NsrRE(a) + NO(a) -> NsrRF(a) kEF

# Binding equilibria
ProhmpA1(b) + NsrR(a) <-> ProhmpA1(b!1).NsrR(a!1) kA,k_A
ProhmpA1(b) + NsrRB(a) <-> ProhmpA1(b!1).NsrRB(a!1) kB,k_B
ProhmpA1(b) + NsrRC(a) <-> ProhmpA1(b!1).NsrRC(a!1) kC,k_C
ProhmpA2(b) + NsrR(a) <-> ProhmpA2(b!1).NsrR(a!1) kA,k_A
ProhmpA2(b) + NsrRB(a) <-> ProhmpA2(b!1).NsrRB(a!1) kB,k_B

# Reactions of NsrR in complex with promoters with NO
ProhmpA1(b!1).NsrR(a!1) + NO(a) -> ProhmpA1(b!1).NsrRB(a!1) kAB
ProhmpA1(b!1).NsrRB(a!1) + NO(a) -> ProhmpA1(b!1).NsrRC(a!1) kBC
ProhmpA1(b!1).NsrRC(a!1) + NO(a) -> ProhmpA1(b) + NsrRD(a) kCD
ProhmpA2(b!1).NsrR(a!1) + NO(a) -> ProhmpA2(b!1).NsrRB(a!1) kAB
ProhmpA2(b!1).NsrRB(a!1) + NO(a) -> ProhmpA2(b) + NsrRC(a) kBC

# NsrR recycling
NsrRB(a) -> NsrR(a) kr
NsrRC(a) -> NsrR(a) kr
NsrRD(a) -> NsrR(a) kr
NsrRE(a) -> NsrR(a) kr
NsrRF(a) -> NsrR(a) kr
end reaction rules

```

```
end model

generate_network({overwrite=>1})
#writeSBML()

#parameter_scan({parameter=>"NO_init",par_min=>0,par_max=>100,n_scan_pts=>100,\
#method=>"ode",t_end=>10})

#Varying kp
bifurcate({parameter=>"kp",par_min=>0,par_max=>100,n_scan_pts=>200,\
method=>"ode",t_end=>1e7})

#writeLatex()
```

## A.2 Dimer model 1 (DM1)

```
begin model
begin parameters
  kAB 4.52 # /micromol.s
  kBC 0.113 # /micromol.s
  kCD 1.34e-2 # /micromol.s
  kDE 7.48e-3 # /micromol.s
  kEF 0.43e-3 #/micromol.s
  kr 0.001
  NsrR_init 2.5
  logNO -4
  NO_init 10^logNO
  NOext_init 0
  O2_init 200
  km 750
  kp 0
  k1 3.5
  k_1 0.44
  k2 850
  k_2 2e-4
  k_3 200
  k4 26
  k_4 2e-4
  k5 0.014
  k6 1.8e-4
  ProhmpA1_init 6e-3
  ProhmpA2_init 6e-3
  kd 0.71
  ke 0.83
  kA 10
```

```

k_A 0.35
kB 10
k_B 0.4
kC 10
k_C 0.45
end parameters

begin molecule types
  NsrR(b,dim,s~0~1~2~3~4~5)
  NO(a)
  NOext()
  Hmp(n,o)
  O2(a)
  ProhmpA2(b,b)
  ProhmpA1(b,b)
  RBS()
  NO3(a)
end molecule types

begin species
  NsrR(b,dim!1,s~0).NsrR(b,dim!1,s~0) NsrR_init
  $NO(a) NO_init
  ProhmpA2(b,b) ProhmpA2_init
  ProhmpA1(b,b) ProhmpA1_init
  $O2(a) O2_init
  $NOext() NOext_init

end species

begin observables

  #Species Hmp_NO Hmp(b,c!1).NO(a!1)
  #Species Hmp_O2_NO Hmp(b!0,c!1).O2(a!0).NO(a!1)
  #Species Hmp_O2 Hmp(b,c!1).O2(a!1)
  Species NO NO(a)
  Species ProhmpA2 ProhmpA2(b)
  Species ProhmpA1 ProhmpA1(b)
  #Species Hmp Hmp(c,c)
  #Species RBS RBS()

  #Species NsrRC_NsrR NsrR(s~2).NsrR(s~0)
  #Species NsrRC_NsrRB NsrR(s~2).NsrR(s~1)
  #Species NsrRC_NsrRC NsrR(s~2).NsrR(s~2)
  #Species NsrRC_NsrRD NsrR(s~2).NsrR(s~3)
  #Species NsrRC_NsrRE NsrR(s~2).NsrR(s~4)

```

```

#Species NsrRC_NsrRF    NsrR(s~2).NsrR(s~5)

#Species NsrR_NsrR    NsrR(b,s~0).NsrR(b,s~0)
#Species NsrRB_NsrRB  NsrR(b,s~1).NsrR(b,s~1)
#Species NsrRC_NsrRC  NsrR(s~2).NsrR(s~2)
#Species NsrRD_NsrRD  NsrR(s~3).NsrR(s~3)
#Species NsrRE_NsrRE  NsrR(s~4).NsrR(s~4)
#Species NsrRF_NsrRF  NsrR(s~5).NsrR(s~5)

end observables

begin reaction rules
  # Hmp/NO dynamics
  # Permeation and intracellular production
  NOext() <-> NO(a) km,km
  0 -> NO(a) kp
  # Enzyme kinetics
  Hmp(n,o) + O2(a) <-> Hmp(n,o!1).O2(a!1) k1,k_1
  Hmp(n,o!1).O2(a!1) + NO(a) <-> Hmp(n!0,o!1).O2(a!1).NO(a!0) k2,k_2
  Hmp(n!0,o!1).O2(a!1).NO(a!0) -> Hmp(n,o) + NO3(a) k_3
  Hmp(n,o) + NO(a) <-> Hmp(n!1,o).NO(a!1) k4,k_4

  # Production/decay of mRNA (ribosome binding sites) and of Hmp
  ProhmpA2(b,b) -> ProhmpA2(b,b) + RBS() kd
  ProhmpA1(b,b) -> ProhmpA1(b,b) + RBS() kd
  RBS() -> RBS() + Hmp(n,o) ke
  RBS() -> 0 k5

  # Decay of Hmp and its complexes
  Hmp(n,o) -> 0 k6
  Hmp(n,o!1).O2(a!1) -> O2(a) + 0 k6
  Hmp(n!0,o!1).O2(a!1).NO(a!0) -> O2(a) + NO(a) k6
  Hmp(n!1,o).NO(a!1) -> NO(a) k6

  # Reactions of NsrR with NO
  {MatchOnce}NsrR(b,s~0).NsrR(b,s) + NO(a) -> NsrR(b,s~1).NsrR(b,s) kAB
  {MatchOnce}NsrR(b,s~1).NsrR(b,s) + NO(a) -> NsrR(b,s~2).NsrR(b,s) kBC
  {MatchOnce}NsrR(b,s~2).NsrR(b,s) + NO(a) -> NsrR(b,s~3).NsrR(b,s) kCD
  {MatchOnce}NsrR(b,s~3).NsrR(b,s) + NO(a) -> NsrR(b,s~4).NsrR(b,s) kDE
  {MatchOnce}NsrR(b,s~4).NsrR(b,s) + NO(a) -> NsrR(b,s~5).NsrR(b,s) kEF

  # Binding equilibria using as simple a binding rule as possible
  {MatchOnce}ProhmpA1(b,b) + {MatchOnce}NsrR(b,s~0).NsrR(b,s) <-> \
  {MatchOnce}ProhmpA1(b!1,b!2).NsrR(b!1,s~0).NsrR(b!2,s) kA,k_A
  {MatchOnce}ProhmpA1(b,b) + {MatchOnce}NsrR(b,s~1).NsrR(b,s) <-> \

```

```

{MatchOnce}ProhmpA1 (b!1,b!2) .NsrR (b!1,s~1) .NsrR (b!2,s) kB,k_B
{MatchOnce}ProhmpA1 (b,b) + {MatchOnce}NsrR (b,s~2) .NsrR (b,s) <-> \
{MatchOnce}ProhmpA1 (b!1,b!2) .NsrR (b!1,s~2) .NsrR (b!2,s) kC,k_C

{MatchOnce}ProhmpA2 (b,b) + {MatchOnce}NsrR (b,s~0) .NsrR (b,s) <-> \
{MatchOnce}ProhmpA2 (b!1,b!2) .NsrR (b!1,s~0) .NsrR (b!2,s) kA,k_A
{MatchOnce}ProhmpA2 (b,b) + {MatchOnce}NsrR (b,s~1) .NsrR (b,s) <-> \
{MatchOnce}ProhmpA2 (b!1,b!2) .NsrR (b!1,s~1) .NsrR (b!2,s) kB,k_B

# Reactions of NsrR in complex with promoters with NO
{MatchOnce}ProhmpA1 (b!1,b!2) .NsrR (b!1,s~0) .NsrR (b!2,s) + NO(a) -> \
ProhmpA1 (b!1,b!2) .NsrR (b!1,s~1) .NsrR (b!2,s) kAB
{MatchOnce}ProhmpA1 (b!1,b!2) .NsrR (b!1,s~1) .NsrR (b!2,s) + NO(a) -> \
ProhmpA1 (b!1,b!2) .NsrR (b!1,s~2) .NsrR (b!2,s) kBC
{MatchOnce}ProhmpA1 (b!1,b!2) .NsrR (b!1,s~2) .NsrR (b!2,s) + NO(a) -> \
ProhmpA1 (b,b) + NsrR (b,s~3) .NsrR (b,s) kCD

{MatchOnce}ProhmpA2 (b!1,b!2) .NsrR (b!1,s~0) .NsrR (b!2,s) + NO(a) -> \
ProhmpA2 (b!1,b!2) .NsrR (b!1,s~1) .NsrR (b!2,s) kAB
{MatchOnce}ProhmpA2 (b!1,b!2) .NsrR (b!1,s~1) .NsrR (b!2,s) + NO(a) -> \
ProhmpA2 (b,b) + NsrR (b,s~2) .NsrR (b,s) kBC

# NsrR recycling
NsrR (b,s~0) .NsrR (b,s) -> NsrR (b,s~0) .NsrR (b,s~0) kr
NsrR (b,s~1) .NsrR (b,s) -> NsrR (b,s~1) .NsrR (b,s~0) kr
NsrR (b,s~2) .NsrR (b,s) -> NsrR (b,s~2) .NsrR (b,s~0) kr
NsrR (b,s~3) .NsrR (b,s) -> NsrR (b,s~3) .NsrR (b,s~0) kr
NsrR (b,s~4) .NsrR (b,s) -> NsrR (b,s~4) .NsrR (b,s~0) kr
NsrR (b,s~5) .NsrR (b,s) -> NsrR (b,s~5) .NsrR (b,s~0) kr

end reaction rules
end model

generate_network({overwrite=>1})
bifurcate({parameter=>"kp",par_min=>0,par_max=>150,n_scan_pts=>200,\
method=>"ode",t_end=>1e7})
#parameter_scan({parameter=>"km",par_min=>0,par_max=>1,n_scan_pts=>500,\
#method=>"ode",t_end=>100})
#writeSBML()

#writeLatex()

```

### A.3 Dimer model 2 (DM2)

```
begin model
```

```
begin parameters
  kAB 4.52 # /micromol.s
  kBC 0.113 # /micromol.s
  kCD 1.34e-2 # /micromol.s
  kDE 7.48e-3 # /micromol.s
  kEF 0.43e-3 #/micromol.s
  kr 0.001
  NsrR_init 2.5
  NO_init 0
  NOext_init 0
  O2_init 200
  km 750
  kp 0
  k1 3.5
  k_1 0.44
  k2 850
  k_2 2e-4
  k_3 200
  k4 26
  k_4 2e-4
  k5 0.014
  k6 1.8e-4
  ProhmpA1_init 6e-3
  ProhmpA2_init 6e-3
  kd 0.71
  ke 0.83
  kA 10
  k_A 0.35
  kB 10
  k_B 0.4
  kC 10
  k_C 0.45
end parameters

begin molecule types
  NsrR(b,dim,s~0~1~2~3~4~5)
  NO(a)
  NOext()
  Hmp(n,o)
  O2(a)
  ProhmpA2(b,b)
  ProhmpA1(b,b)
  RBS()
  NO3(a)
end molecule types
```

```

begin species
  NsrR(b,dim!1,s~0).NsrR(b,dim!1,s~0) NsrR_init
  ProhmpA2(b,b) ProhmpA2_init
  ProhmpA1(b,b) ProhmpA1_init
  # Note: O2 and NOext are fixed.
  $O2(a) O2_init
  $NOext() NOext_init
  $NO(a) NO_init
end species

begin observables

  #Species Hmp_NO Hmp(b,c!1).NO(a!1)
  #Species Hmp_O2_NO Hmp(b!0,c!1).O2(a!0).NO(a!1)
  #Species Hmp_O2 Hmp(b,c!1).O2(a!1)
  Species ProhmpA2 ProhmpA2(b)
  Species ProhmpA1 ProhmpA1(b)
  #Species No NO(a)
  #Species Hmp Hmp(c,c)
  #Species RBS RBS()

  #Species NsrRC_NsrR NsrR(s~2).NsrR(s~0)
  #Species NsrRC_NsrRB NsrR(s~2).NsrR(s~1)
  #Species NsrRC_NsrRC NsrR(s~2).NsrR(s~2)
  #Species NsrRC_NsrRD NsrR(s~2).NsrR(s~3)
  #Species NsrRC_NsrRE NsrR(s~2).NsrR(s~4)
  #Species NsrRC_NsrRF NsrR(s~2).NsrR(s~5)

end observables

begin reaction rules
  # Hmp/NO dynamics
  # Permeation and intracellular production
  NOext() <-> NO(a) km,km
  0 -> NO(a) kp
  # Enzyme kinetics
  Hmp(n,o) + O2(a) <-> Hmp(n,o!1).O2(a!1) k1,k_1
  Hmp(n,o!1).O2(a!1) + NO(a) <-> Hmp(n!0,o!1).O2(a!1).NO(a!0) k2,k_2
  Hmp(n!0,o!1).O2(a!1).NO(a!0) -> Hmp(n,o) + NO3(a) k_3
  Hmp(n,o) + NO(a) <-> Hmp(n!1,o).NO(a!1) k4,k_4

  # Production/decay of mRNA (ribosome binding sites) and of Hmp
  ProhmpA2(b,b) -> ProhmpA2(b,b) + RBS() kd

```

```

ProhmpA1(b,b) -> ProhmpA1(b,b) + RBS() kd
RBS() -> RBS() + Hmp(n,o) ke
RBS() -> 0 k5

# Decay of Hmp and its complexes
Hmp(n,o) -> 0 k6
Hmp(n,o!1).O2(a!1) -> O2(a) + 0 k6
Hmp(n!0,o!1).O2(a!1).NO(a!0) -> O2(a) + NO(a) k6
Hmp(n!1,o).NO(a!1) -> NO(a) k6

# Reactions of NsrR with NO
{MatchOnce}NsrR(b,s~0).NsrR(b,s) + NO(a) -> NsrR(b,s~1).NsrR(b,s) kAB
{MatchOnce}NsrR(b,s~1).NsrR(b,s) + NO(a) -> NsrR(b,s~2).NsrR(b,s) kBC
{MatchOnce}NsrR(b,s~2).NsrR(b,s) + NO(a) -> NsrR(b,s~3).NsrR(b,s) kCD
{MatchOnce}NsrR(b,s~3).NsrR(b,s) + NO(a) -> NsrR(b,s~4).NsrR(b,s) kDE
{MatchOnce}NsrR(b,s~4).NsrR(b,s) + NO(a) -> NsrR(b,s~5).NsrR(b,s) kEF

# Binding equilibria using the rule that binding strength is determined by
# the weakest binding part of a dimer
{MatchOnce}ProhmpA1(b,b) + NsrR(b,s~0).NsrR(b,s~0) <-> \
ProhmpA1(b!1,b!2).NsrR(b!1,s~0).NsrR(b!2,s~0) kA,k_A
{MatchOnce}ProhmpA1(b,b) + NsrR(b,s~1).NsrR(b,s~1) <-> \
ProhmpA1(b!1,b!2).NsrR(b!1,s~1).NsrR(b!2,s~1) kB,k_B
{MatchOnce}ProhmpA1(b,b) + NsrR(b,s~1).NsrR(b,s~0) <-> \
ProhmpA1(b!1,b!2).NsrR(b!1,s~1).NsrR(b!2,s~0) kB,k_B
{MatchOnce}ProhmpA1(b,b) + NsrR(b,s~2).NsrR(b,s~2) <-> \
ProhmpA1(b!1,b!2).NsrR(b!1,s~2).NsrR(b!2,s~2) kC,k_C
{MatchOnce}ProhmpA1(b,b) + NsrR(b,s~2).NsrR(b,s~1) <-> \
ProhmpA1(b!1,b!2).NsrR(b!1,s~2).NsrR(b!2,s~1) kC,k_C
{MatchOnce}ProhmpA1(b,b) + NsrR(b,s~2).NsrR(b,s~0) <-> \
ProhmpA1(b!1,b!2).NsrR(b!1,s~2).NsrR(b!2,s~0) kC,k_C

{MatchOnce}ProhmpA2(b,b) + NsrR(b,s~0).NsrR(b,s~0) <-> \
ProhmpA2(b!1,b!2).NsrR(b!1,s~0).NsrR(b!2,s~0) kA,k_A
{MatchOnce}ProhmpA2(b,b) + NsrR(b,s~1).NsrR(b,s~1) <-> \
ProhmpA2(b!1,b!2).NsrR(b!1,s~1).NsrR(b!2,s~1) kB,k_B
{MatchOnce}ProhmpA2(b,b) + NsrR(b,s~1).NsrR(b,s~0) <-> \
ProhmpA2(b!1,b!2).NsrR(b!1,s~1).NsrR(b!2,s~0) kB,k_B

# Reactions of NsrR in complex with promoters with NO
{MatchOnce}ProhmpA1(b!1,b!2).NsrR(b!1,s~0).NsrR(b!2,s) + NO(a) -> \
ProhmpA1(b!1,b!2).NsrR(b!1,s~1).NsrR(b!2,s) kAB
{MatchOnce}ProhmpA1(b!1,b!2).NsrR(b!1,s~1).NsrR(b!2,s) + NO(a) -> \
ProhmpA1(b!1,b!2).NsrR(b!1,s~2).NsrR(b!2,s) kBC
{MatchOnce}ProhmpA1(b!1,b!2).NsrR(b!1,s~2).NsrR(b!2,s) + NO(a) -> \

```

```

ProhmpA1 (b,b) + NsrR (b,s~3) .NsrR (b,s) kCD

{MatchOnce}ProhmpA2 (b!1,b!2) .NsrR (b!1,s~0) .NsrR (b!2,s) + NO(a) -> \
ProhmpA2 (b!1,b!2) .NsrR (b!1,s~1) .NsrR (b!2,s) kAB
{MatchOnce}ProhmpA2 (b!1,b!2) .NsrR (b!1,s~1) .NsrR (b!2,s) + NO(a) -> \
ProhmpA2 (b,b) + NsrR (b,s~2) .NsrR (b,s) kBC

# NsrR recycling
NsrR (b,s~0) .NsrR (b,s) -> NsrR (b,s~0) .NsrR (b,s~0) kr
NsrR (b,s~1) .NsrR (b,s) -> NsrR (b,s~1) .NsrR (b,s~0) kr
NsrR (b,s~2) .NsrR (b,s) -> NsrR (b,s~2) .NsrR (b,s~0) kr
NsrR (b,s~3) .NsrR (b,s) -> NsrR (b,s~3) .NsrR (b,s~0) kr
NsrR (b,s~4) .NsrR (b,s) -> NsrR (b,s~4) .NsrR (b,s~0) kr
NsrR (b,s~5) .NsrR (b,s) -> NsrR (b,s~5) .NsrR (b,s~0) kr

end reaction rules
end model

generate_network ({overwrite=>1})
bifurcate ({parameter=>"kp",par_min=>0,par_max=>150,n_scan_pts=>200,\
method=>"ode",t_end=>1e7})
#parameter_scan ({parameter=>"km",par_min=>0,par_max=>1,n_scan_pts=>500,\
#method=>"ode",t_end=>100})
#writeSBML()

#writeLatex()

```

# Appendix B

## Differential equations

### B.1 Monomer (MM)

MM has 22 species and 42 reactions.

$$\begin{aligned} \dot{x}_1 &= -p_{26}x_4x_1 - p_{26}x_3x_1 - p_1x_1x_2 + p_{27}x_8 \\ &\quad + p_{27}x_9 + p_6x_{10} + p_6x_{14} + p_6x_{18} + p_6x_{20} \\ &\quad + p_6x_{22} \\ \dot{x}_2 &= +p_{12}x_6 - p_{12}x_2 - p_1x_1x_2 - p_1x_8x_2 \\ &\quad - p_1x_9x_2 - p_2x_{10}x_2 - 2p_{18}x_{11}x_2 - p_2x_{12}x_2 - p_2x_{13}x_2 \\ &\quad - p_3x_{14}x_2 - p_{15}x_{15}x_2 + p_{19}x_{16} + p_{21}x_{16} - p_3x_{17}x_2 \\ &\quad - p_4x_{18}x_2 + p_{16}x_{19} + p_{21}x_{19} - p_5x_{20}x_2 \\ \dot{x}_3 &= -p_{26}x_3x_1 + p_{27}x_9 - p_{28}x_3x_{10} + p_{29}x_{13} \\ &\quad + p_2x_{13}x_2 \\ \dot{x}_4 &= -p_{26}x_4x_1 + p_{27}x_8 - p_{28}x_4x_{10} + p_{29}x_{12} \\ &\quad - p_{30}x_4x_{14} + p_{31}x_{17} + p_3x_{17}x_2 \\ \dot{x}_5 &= -2p_{13}x_{11}x_5 + p_{14}x_{15} + p_{21}x_{15} + p_{21}x_{19} \\ \dot{x}_6 &= -p_{12}x_6 + p_{12}x_2 \\ \dot{x}_7 &= +p_{24}x_3 + p_{24}x_4 - p_{20}x_7 \\ \dot{x}_8 &= +p_{26}x_4x_1 - p_{27}x_8 - p_1x_8x_2 \\ \dot{x}_9 &= +p_{26}x_3x_1 - p_{27}x_9 - p_1x_9x_2 \\ \dot{x}_{10} &= +p_1x_1x_2 - p_{28}x_4x_{10} - p_{28}x_3x_{10} - p_2x_{10}x_2 \\ &\quad - p_6x_{10} + p_{29}x_{12} + p_{29}x_{13} \\ \dot{x}_{11} &= +p_{25}x_7 - 2p_{13}x_{11}x_5 - 2p_{18}x_{11}x_2 - p_{21}x_{11} \\ &\quad + p_{14}x_{15} + p_{19}x_{16} + p_{17}x_{19} \\ \dot{x}_{12} &= +p_{28}x_4x_{10} + p_1x_8x_2 - p_{29}x_{12} - p_2x_{12}x_2 \\ \dot{x}_{13} &= +p_{28}x_3x_{10} + p_1x_9x_2 - p_{29}x_{13} - p_2x_{13}x_2 \\ \dot{x}_{14} &= +p_2x_{10}x_2 - p_{30}x_4x_{14} + p_2x_{13}x_2 - p_3x_{14}x_2 \\ &\quad - p_6x_{14} + p_{31}x_{17} \\ \dot{x}_{15} &= +2p_{13}x_{11}x_5 - p_{14}x_{15} - p_{15}x_{15}x_2 - p_{21}x_{15} \end{aligned}$$

$$\begin{aligned}
& +p_{16}x_{19} \\
x_{16} & = +2p_{18}x_{11}x_2 - p_{19}x_{16} - p_{21}x_{16} \\
x_{17} & = +p_{30}x_4x_{14} + p_2x_{12}x_2 - p_{31}x_{17} - p_3x_{17}x_2 \\
x_{18} & = +p_3x_{14}x_2 + p_3x_{17}x_2 - p_4x_{18}x_2 - p_6x_{18} \\
x_{19} & = +p_{15}x_{15}x_2 - p_{16}x_{19} - p_{17}x_{19} - p_{21}x_{19} \\
x_{20} & = +p_4x_{18}x_2 - p_5x_{20}x_2 - p_6x_{20} \\
x_{21} & = +p_{17}x_{19} \\
x_{22} & = +p_5x_{20}x_2 - p_6x_{22}
\end{aligned}$$

BioNetGen generates a .net file to show the meanings of the parameters and variables in each model. The relevant sections of the .net file for MM are:

```

# Created by BioNetGen 2.5.1
begin parameters
  1 kAB          4.52 # Constant
  2 kBC          0.113 # Constant
  3 kCD          1.34e-2 # Constant
  4 kDE          7.48e-3 # Constant
  5 kEF          0.43e-3 # Constant
  6 kr           0.001 # Constant
  7 NsrR_init    2.5 # Constant
  8 logNO        -0.4 # Constant
  9 NO_init      10.0^logNO # ConstantExpression
 10 NOext_init   0 # Constant
 11 O2_init      200 # Constant
 12 km           750 # Constant
 13 k1           3.5 # Constant
 14 k_1          0.44 # Constant
 15 k2           850 # Constant
 16 k_2          2e-4 # Constant
 17 k_3          200 # Constant
 18 k4           26 # Constant
 19 k_4          2e-4 # Constant
 20 k5           0.014 # Constant
 21 k6           1.8e-4 # Constant
 22 ProhmpA1_init 6e-3 # Constant
 23 ProhmpA2_init 6e-3 # Constant
 24 kd           0.71 # Constant
 25 ke           0.83 # Constant
 26 kA           10 # Constant
 27 k_A          0.35 # Constant
 28 kB           10 # Constant
 29 k_B          0.4 # Constant

```

```

30 kC          10 # Constant
31 k_C         0.45 # Constant
end parameters
begin species
  1 NsrR(a) NsrR_init
  2 $NO(a) NO_init
  3 ProhmpA2(b) ProhmpA2_init
  4 ProhmpA1(b) ProhmpA1_init
  5 $O2(a) O2_init
  6 $NOext() NOext_init
  7 RBS() 0
  8 NsrR(a!1).ProhmpA1(b!1) 0
  9 NsrR(a!1).ProhmpA2(b!1) 0
10 NsrRB(a) 0
11 Hmp(c,c) 0
12 NsrRB(a!1).ProhmpA1(b!1) 0
13 NsrRB(a!1).ProhmpA2(b!1) 0
14 NsrRC(a) 0
15 Hmp(c!1,c).O2(a!1) 0
16 Hmp(c!1,c).NO(a!1) 0
17 NsrRC(a!1).ProhmpA1(b!1) 0
18 NsrRD(a) 0
19 Hmp(c!1,c!2).NO(a!2).O2(a!1) 0
20 NsrRE(a) 0
21 NO3(a) 0
22 NsrRF(a) 0
end species

```

## B.2 Dimer model 1 (DM1)

DM1 has 58 species and 168 reactions.

$$\begin{aligned}
 \dot{x}_1 &= -p_1x_1x_2 - p_{26}x_4x_1 - p_{26}x_3x_1 + p_{27}x_9 \\
 &\quad + p_{27}x_{10} + p_6x_8 + p_6x_{13} + p_6x_{19} + p_6x_{27} \\
 &\quad + p_6x_{35} \\
 \dot{x}_2 &= +p_{11}x_6 - p_{11}x_2 + p_{12} - p_1x_1x_2 \\
 &\quad - p_1x_8x_2 - p_2x_8x_2 - p_1x_9x_2 - p_1x_{10}x_2 - p_{18}x_{11}x_2 \\
 &\quad - p_1x_{13}x_2 - p_2x_{12}x_2 - p_3x_{13}x_2 - p_1x_{14}x_2 - p_2x_{14}x_2 \\
 &\quad - p_1x_{15}x_2 - p_2x_{15}x_2 - p_{15}x_{16}x_2 + p_{19}x_{17} + p_{21}x_{17} \\
 &\quad - p_1x_{19}x_2 - p_2x_{18}x_2 - p_3x_{18}x_2 - p_4x_{19}x_2 - p_1x_{20}x_2 \\
 &\quad - p_2x_{21}x_2 - p_3x_{20}x_2 - p_1x_{22}x_2 - p_2x_{23}x_2 + p_{16}x_{24} \\
 &\quad + p_{21}x_{24} - p_1x_{27}x_2 - p_2x_{25}x_2 - p_3x_{26}x_2 - p_4x_{25}x_2
 \end{aligned}$$

$$\begin{aligned}
 & -p_5x_{27}x_2 - p_1x_{28}x_2 - p_2x_{29}x_2 - p_3x_{29}x_2 - p_1x_{30}x_2 \\
 & -p_2x_{31}x_2 - p_1x_{35}x_2 - p_2x_{33}x_2 - p_3x_{34}x_2 - p_4x_{34}x_2 \\
 & -p_5x_{33}x_2 - p_1x_{36}x_2 - p_2x_{37}x_2 - p_3x_{38}x_2 - p_1x_{39}x_2 \\
 & -p_2x_{40}x_2 - p_2x_{41}x_2 - p_3x_{42}x_2 - p_4x_{43}x_2 - p_5x_{42}x_2 \\
 & -p_1x_{44}x_2 - p_2x_{45}x_2 - p_3x_{46}x_2 - p_1x_{47}x_2 - p_2x_{48}x_2 \\
 & -p_3x_{49}x_2 - p_4x_{50}x_2 - p_5x_{50}x_2 - p_2x_{51}x_2 - p_3x_{52}x_2 \\
 & -p_2x_{53}x_2 - p_4x_{54}x_2 - p_5x_{55}x_2 - p_3x_{56}x_2 - p_5x_{57}x_2 \\
 \dot{x}_3 = & -p_{26}x_3x_1 - p_{26}x_3x_8 + p_{27}x_{10} - p_{28}x_3x_8 \\
 & -p_{26}x_3x_{13} + p_{27}x_{15} - p_{28}x_3x_{12} + p_{29}x_{15} + p_{2x_{15}x_2} \\
 & -p_{26}x_3x_{19} + p_{27}x_{22} - p_{28}x_3x_{18} + p_{29}x_{23} + p_{2x_{23}x_2} \\
 & -p_{26}x_3x_{27} + p_{27}x_{30} - p_{28}x_3x_{25} + p_{29}x_{31} + p_{2x_{31}x_2} \\
 & -p_{26}x_3x_{35} + p_{27}x_{39} - p_{28}x_3x_{33} + p_{29}x_{40} + p_{2x_{40}x_2} \\
 & + p_{27}x_{47} - p_{28}x_3x_{41} + p_{29}x_{48} + p_{2x_{48}x_2} + p_{29}x_{53} \\
 & + p_{2x_{53}x_2} \\
 \dot{x}_4 = & -p_{26}x_4x_1 - p_{26}x_4x_8 + p_{27}x_9 - p_{28}x_4x_8 \\
 & -p_{26}x_4x_{13} + p_{27}x_{14} - p_{28}x_4x_{12} + p_{29}x_{14} - p_{30}x_4x_{13} \\
 & -p_{26}x_4x_{19} + p_{27}x_{20} - p_{28}x_4x_{18} + p_{29}x_{21} - p_{30}x_4x_{18} \\
 & + p_{31}x_{20} + p_{3x_{20}x_2} - p_{26}x_4x_{27} + p_{27}x_{28} - p_{28}x_4x_{25} \\
 & + p_{29}x_{29} - p_{30}x_4x_{26} + p_{31}x_{29} + p_{3x_{29}x_2} - p_{26}x_4x_{35} \\
 & + p_{27}x_{36} - p_{28}x_4x_{33} + p_{29}x_{37} - p_{30}x_4x_{34} + p_{31}x_{38} \\
 & + p_{3x_{38}x_2} + p_{27}x_{44} - p_{28}x_4x_{41} + p_{29}x_{45} - p_{30}x_4x_{42} \\
 & + p_{31}x_{46} + p_{3x_{46}x_2} + p_{29}x_{51} - p_{30}x_4x_{49} + p_{31}x_{52} \\
 & + p_{3x_{52}x_2} + p_{31}x_{56} + p_{3x_{56}x_2} \\
 \dot{x}_5 = & -p_{13}x_{11}x_5 + p_{14}x_{16} + p_{21}x_{16} + p_{21}x_{24} \\
 \dot{x}_6 = & -p_{11}x_6 + p_{11}x_2 \\
 \dot{x}_7 = & +p_{24}x_3 + p_{24}x_4 - p_{20}x_7 \\
 \dot{x}_8 = & +p_1x_1x_2 - p_1x_8x_2 - p_2x_8x_2 - p_{26}x_4x_8 \\
 & -p_{28}x_4x_8 - p_{26}x_3x_8 - p_{28}x_3x_8 - p_6x_8 + p_{27}x_{14} \\
 & + p_{29}x_{14} + p_{27}x_{15} + p_{29}x_{15} + 2p_6x_{12} + p_6x_{18} \\
 & + p_6x_{25} + p_6x_{33} + p_6x_{41} \\
 \dot{x}_9 = & +p_{26}x_4x_1 - p_{27}x_9 - p_1x_9x_2 \\
 \dot{x}_{10} = & +p_{26}x_3x_1 - p_{27}x_{10} - p_1x_{10}x_2 \\
 \dot{x}_{11} = & +p_{25}x_7 - p_{13}x_{11}x_5 - p_{18}x_{11}x_2 - p_{21}x_{11} \\
 & + p_{14}x_{16} + p_{19}x_{17} + p_{17}x_{24} \\
 \dot{x}_{12} = & +p_1x_8x_2 - p_2x_{12}x_2 - p_{28}x_4x_{12} - p_{28}x_3x_{12} \\
 & - 2p_6x_{12} + p_{29}x_{21} + p_{29}x_{23} \\
 \dot{x}_{13} = & +p_2x_8x_2 - p_1x_{13}x_2 - p_3x_{13}x_2 - p_{26}x_4x_{13}
 \end{aligned}$$

$$\begin{aligned}
 & -p_{30}x_4x_{13} - p_{26}x_3x_{13} + p_2x_{15}x_2 - p_6x_{13} + p_{27}x_{20} \\
 & + p_{31}x_{20} + p_{27}x_{22} + p_6x_{18} + 2p_6x_{26} + p_6x_{34} \\
 & + p_6x_{42} + p_6x_{49} \\
 x_{14} & = +p_{26}x_4x_8 + p_{28}x_4x_8 + p_1x_9x_2 - p_{27}x_{14} \\
 & - p_{29}x_{14} - p_1x_{14}x_2 - p_2x_{14}x_2 \\
 x_{15} & = +p_{26}x_3x_8 + p_{28}x_3x_8 + p_1x_{10}x_2 - p_{27}x_{15} \\
 & - p_{29}x_{15} - p_1x_{15}x_2 - p_2x_{15}x_2 \\
 x_{16} & = +p_{13}x_{11}x_5 - p_{14}x_{16} - p_{15}x_{16}x_2 - p_{21}x_{16} \\
 & + p_{16}x_{24} \\
 x_{17} & = +p_{18}x_{11}x_2 - p_{19}x_{17} - p_{21}x_{17} \\
 x_{18} & = +p_1x_{13}x_2 + p_2x_{12}x_2 - p_2x_{18}x_2 - p_3x_{18}x_2 \\
 & - p_{28}x_4x_{18} - p_{30}x_4x_{18} - p_{28}x_3x_{18} + p_2x_{23}x_2 - p_6x_{18} \\
 & - p_6x_{18} + p_{29}x_{29} + p_{31}x_{29} + p_{29}x_{31} \\
 x_{19} & = +p_3x_{13}x_2 - p_1x_{19}x_2 - p_4x_{19}x_2 - p_{26}x_4x_{19} \\
 & - p_{26}x_3x_{19} + p_3x_{20}x_2 - p_6x_{19} + p_{27}x_{28} + p_{27}x_{30} \\
 & + p_6x_{25} + p_6x_{34} + 2p_6x_{43} + p_6x_{50} + p_6x_{54} \\
 x_{20} & = +p_{26}x_4x_{13} + p_{30}x_4x_{13} + p_2x_{14}x_2 - p_{27}x_{20} \\
 & - p_{31}x_{20} - p_1x_{20}x_2 - p_3x_{20}x_2 \\
 x_{21} & = +p_{28}x_4x_{12} + p_1x_{14}x_2 - p_{29}x_{21} - p_2x_{21}x_2 \\
 x_{22} & = +p_{26}x_3x_{13} - p_{27}x_{22} - p_1x_{22}x_2 \\
 x_{23} & = +p_{28}x_3x_{12} + p_1x_{15}x_2 - p_{29}x_{23} - p_2x_{23}x_2 \\
 x_{24} & = +p_{15}x_{16}x_2 - p_{16}x_{24} - p_{17}x_{24} - p_{21}x_{24} \\
 x_{25} & = +p_1x_{19}x_2 + p_3x_{18}x_2 - p_2x_{25}x_2 - p_4x_{25}x_2 \\
 & - p_{28}x_4x_{25} - p_{28}x_3x_{25} + p_3x_{29}x_2 - p_6x_{25} - p_6x_{25} \\
 & + p_{29}x_{37} + p_{29}x_{40} \\
 x_{26} & = +p_2x_{18}x_2 - p_3x_{26}x_2 - p_{30}x_4x_{26} + p_2x_{31}x_2 \\
 & - 2p_6x_{26} + p_{31}x_{38} \\
 x_{27} & = +p_4x_{19}x_2 - p_1x_{27}x_2 - p_5x_{27}x_2 - p_{26}x_4x_{27} \\
 & - p_{26}x_3x_{27} - p_6x_{27} + p_{27}x_{36} + p_{27}x_{39} + p_6x_{33} \\
 & + p_6x_{42} + p_6x_{50} + 2p_6x_{55} + p_6x_{57} \\
 x_{28} & = +p_{26}x_4x_{19} - p_{27}x_{28} - p_1x_{28}x_2 \\
 x_{29} & = +p_{28}x_4x_{18} + p_{30}x_4x_{18} + p_1x_{20}x_2 + p_2x_{21}x_2 \\
 & - p_{29}x_{29} - p_{31}x_{29} - p_2x_{29}x_2 - p_3x_{29}x_2 \\
 x_{30} & = +p_{26}x_3x_{19} - p_{27}x_{30} - p_1x_{30}x_2 \\
 x_{31} & = +p_{28}x_3x_{18} + p_1x_{22}x_2 - p_{29}x_{31} - p_2x_{31}x_2 \\
 x_{32} & = +p_{17}x_{24} \\
 x_{33} & = +p_1x_{27}x_2 + p_4x_{25}x_2 - p_2x_{33}x_2 - p_5x_{33}x_2
 \end{aligned}$$

$$\begin{aligned}
 & -p_{28}x_4x_{33} - p_{28}x_3x_{33} - p_6x_{33} - p_6x_{33} + p_{29}x_{45} \\
 & + p_{29}x_{48} \\
 x_{\dot{34}} = & + p_2x_{25}x_2 + p_3x_{26}x_2 - p_3x_{34}x_2 - p_4x_{34}x_2 \\
 & - p_{30}x_4x_{34} + p_3x_{38}x_2 + p_2x_{40}x_2 - p_6x_{34} - p_6x_{34} \\
 & + p_{31}x_{46} \\
 x_{\dot{35}} = & + p_5x_{27}x_2 - p_1x_{35}x_2 - p_{26}x_4x_{35} - p_{26}x_3x_{35} \\
 & - p_6x_{35} + p_{27}x_{44} + p_{27}x_{47} + p_6x_{41} + p_6x_{49} \\
 & + p_6x_{54} + p_6x_{57} + 2p_6x_{58} \\
 x_{\dot{36}} = & + p_{26}x_4x_{27} - p_{27}x_{36} - p_1x_{36}x_2 \\
 x_{\dot{37}} = & + p_{28}x_4x_{25} + p_1x_{28}x_2 - p_{29}x_{37} - p_2x_{37}x_2 \\
 x_{\dot{38}} = & + p_{30}x_4x_{26} + p_2x_{29}x_2 - p_{31}x_{38} - p_3x_{38}x_2 \\
 x_{\dot{39}} = & + p_{26}x_3x_{27} - p_{27}x_{39} - p_1x_{39}x_2 \\
 x_{\dot{40}} = & + p_{28}x_3x_{25} + p_1x_{30}x_2 - p_{29}x_{40} - p_2x_{40}x_2 \\
 x_{\dot{41}} = & + p_1x_{35}x_2 + p_5x_{33}x_2 - p_2x_{41}x_2 - p_{28}x_4x_{41} \\
 & - p_{28}x_3x_{41} - p_6x_{41} - p_6x_{41} + p_{29}x_{51} + p_{29}x_{53} \\
 x_{\dot{42}} = & + p_2x_{33}x_2 + p_4x_{34}x_2 - p_3x_{42}x_2 - p_5x_{42}x_2 \\
 & - p_{30}x_4x_{42} + p_2x_{48}x_2 - p_6x_{42} - p_6x_{42} + p_{31}x_{52} \\
 x_{\dot{43}} = & + p_3x_{34}x_2 - p_4x_{43}x_2 + p_3x_{46}x_2 - 2p_6x_{43} \\
 x_{\dot{44}} = & + p_{26}x_4x_{35} - p_{27}x_{44} - p_1x_{44}x_2 \\
 x_{\dot{45}} = & + p_{28}x_4x_{33} + p_1x_{36}x_2 - p_{29}x_{45} - p_2x_{45}x_2 \\
 x_{\dot{46}} = & + p_{30}x_4x_{34} + p_2x_{37}x_2 - p_{31}x_{46} - p_3x_{46}x_2 \\
 x_{\dot{47}} = & + p_{26}x_3x_{35} - p_{27}x_{47} - p_1x_{47}x_2 \\
 x_{\dot{48}} = & + p_{28}x_3x_{33} + p_1x_{39}x_2 - p_{29}x_{48} - p_2x_{48}x_2 \\
 x_{\dot{49}} = & + p_2x_{41}x_2 + p_5x_{42}x_2 - p_3x_{49}x_2 - p_{30}x_4x_{49} \\
 & + p_2x_{53}x_2 - p_6x_{49} - p_6x_{49} + p_{31}x_{56} \\
 x_{\dot{50}} = & + p_3x_{42}x_2 + p_4x_{43}x_2 - p_4x_{50}x_2 - p_5x_{50}x_2 \\
 & + p_3x_{52}x_2 - p_6x_{50} - p_6x_{50} \\
 x_{\dot{51}} = & + p_{28}x_4x_{41} + p_1x_{44}x_2 - p_{29}x_{51} - p_2x_{51}x_2 \\
 x_{\dot{52}} = & + p_{30}x_4x_{42} + p_2x_{45}x_2 - p_{31}x_{52} - p_3x_{52}x_2 \\
 x_{\dot{53}} = & + p_{28}x_3x_{41} + p_1x_{47}x_2 - p_{29}x_{53} - p_2x_{53}x_2 \\
 x_{\dot{54}} = & + p_3x_{49}x_2 + p_5x_{50}x_2 - p_4x_{54}x_2 + p_3x_{56}x_2 \\
 & - p_6x_{54} - p_6x_{54} \\
 x_{\dot{55}} = & + p_4x_{50}x_2 - p_5x_{55}x_2 - 2p_6x_{55} \\
 x_{\dot{56}} = & + p_{30}x_4x_{49} + p_2x_{51}x_2 - p_{31}x_{56} - p_3x_{56}x_2 \\
 x_{\dot{57}} = & + p_4x_{54}x_2 + p_5x_{55}x_2 - p_5x_{57}x_2 - p_6x_{57} \\
 & - p_6x_{57} \\
 x_{\dot{58}} = & + p_5x_{57}x_2 - 2p_6x_{58}
 \end{aligned}$$

The relevant sections of the .net file for DM1 are:

```
# Created by BioNetGen 2.5.1
begin parameters
  1 kAB          4.52 # Constant
  2 kBC          0.113 # Constant
  3 kCD          1.34e-2 # Constant
  4 kDE          7.48e-3 # Constant
  5 kEF          0.43e-3 # Constant
  6 kr           0.1 # Constant
  7 NsrR_init    2.5 # Constant
  8 NO_init      0 # Constant
  9 NOext_init   0 # Constant
 10 O2_init      200 # Constant
 11 km           750 # Constant
 12 kp           0 # Constant
 13 k1           3.5 # Constant
 14 k_1          0.44 # Constant
 15 k2           850 # Constant
 16 k_2          2e-4 # Constant
 17 k_3          200 # Constant
 18 k4           26 # Constant
 19 k_4          2e-4 # Constant
 20 k5           0.014 # Constant
 21 k6           1.8e-4 # Constant
 22 ProhmpA1_init 6e-3 # Constant
 23 ProhmpA2_init 6e-3 # Constant
 24 kd           0.71 # Constant
 25 ke           0.83 # Constant
 26 kA           10 # Constant
 27 k_A          0.35 # Constant
 28 kB           10 # Constant
 29 k_B          0.4 # Constant
 30 kC           10 # Constant
 31 k_C          0.45 # Constant
end parameters
begin species
  1 NsrR(b,dim!1,s~0).NsrR(b,dim!1,s~0) NsrR_init
  2 NO(a) NO_init
  3 ProhmpA2(b,b) ProhmpA2_init
  4 ProhmpA1(b,b) ProhmpA1_init
  5 $O2(a) O2_init
  6 $NOext() NOext_init
```

```

7 RBS() 0
8 NsrR(b,dim!1,s~0).NsrR(b,dim!1,s~1) 0
9 NsrR(b!1,dim!2,s~0).NsrR(b!3,dim!2,s~0).ProhmpA1(b!1,b!3) 0
10 NsrR(b!1,dim!2,s~0).NsrR(b!3,dim!2,s~0).ProhmpA2(b!1,b!3) 0
11 Hmp(n,o) 0
12 NsrR(b,dim!1,s~1).NsrR(b,dim!1,s~1) 0
13 NsrR(b,dim!1,s~0).NsrR(b,dim!1,s~2) 0
14 NsrR(b!1,dim!2,s~0).NsrR(b!3,dim!2,s~1).ProhmpA1(b!1,b!3) 0
15 NsrR(b!1,dim!2,s~0).NsrR(b!3,dim!2,s~1).ProhmpA2(b!1,b!3) 0
16 Hmp(n,o!1).O2(a!1) 0
17 Hmp(n!1,o).NO(a!1) 0
18 NsrR(b,dim!1,s~1).NsrR(b,dim!1,s~2) 0
19 NsrR(b,dim!1,s~0).NsrR(b,dim!1,s~3) 0
20 NsrR(b!1,dim!2,s~0).NsrR(b!3,dim!2,s~2).ProhmpA1(b!1,b!3) 0
21 NsrR(b!1,dim!2,s~1).NsrR(b!3,dim!2,s~1).ProhmpA1(b!1,b!3) 0
22 NsrR(b!1,dim!2,s~0).NsrR(b!3,dim!2,s~2).ProhmpA2(b!1,b!3) 0
23 NsrR(b!1,dim!2,s~1).NsrR(b!3,dim!2,s~1).ProhmpA2(b!1,b!3) 0
24 Hmp(n!1,o!2).NO(a!1).O2(a!2) 0
25 NsrR(b,dim!1,s~1).NsrR(b,dim!1,s~3) 0
26 NsrR(b,dim!1,s~2).NsrR(b,dim!1,s~2) 0
27 NsrR(b,dim!1,s~0).NsrR(b,dim!1,s~4) 0
28 NsrR(b!1,dim!2,s~0).NsrR(b!3,dim!2,s~3).ProhmpA1(b!1,b!3) 0
29 NsrR(b!1,dim!2,s~1).NsrR(b!3,dim!2,s~2).ProhmpA1(b!1,b!3) 0
30 NsrR(b!1,dim!2,s~0).NsrR(b!3,dim!2,s~3).ProhmpA2(b!1,b!3) 0
31 NsrR(b!1,dim!2,s~1).NsrR(b!3,dim!2,s~2).ProhmpA2(b!1,b!3) 0
32 NO3(a) 0
33 NsrR(b,dim!1,s~1).NsrR(b,dim!1,s~4) 0
34 NsrR(b,dim!1,s~2).NsrR(b,dim!1,s~3) 0
35 NsrR(b,dim!1,s~0).NsrR(b,dim!1,s~5) 0
36 NsrR(b!1,dim!2,s~0).NsrR(b!3,dim!2,s~4).ProhmpA1(b!1,b!3) 0
37 NsrR(b!1,dim!2,s~1).NsrR(b!3,dim!2,s~3).ProhmpA1(b!1,b!3) 0
38 NsrR(b!1,dim!2,s~2).NsrR(b!3,dim!2,s~2).ProhmpA1(b!1,b!3) 0
39 NsrR(b!1,dim!2,s~0).NsrR(b!3,dim!2,s~4).ProhmpA2(b!1,b!3) 0
40 NsrR(b!1,dim!2,s~1).NsrR(b!3,dim!2,s~3).ProhmpA2(b!1,b!3) 0
41 NsrR(b,dim!1,s~1).NsrR(b,dim!1,s~5) 0
42 NsrR(b,dim!1,s~2).NsrR(b,dim!1,s~4) 0
43 NsrR(b,dim!1,s~3).NsrR(b,dim!1,s~3) 0
44 NsrR(b!1,dim!2,s~0).NsrR(b!3,dim!2,s~5).ProhmpA1(b!1,b!3) 0
45 NsrR(b!1,dim!2,s~1).NsrR(b!3,dim!2,s~4).ProhmpA1(b!1,b!3) 0
46 NsrR(b!1,dim!2,s~2).NsrR(b!3,dim!2,s~3).ProhmpA1(b!1,b!3) 0
47 NsrR(b!1,dim!2,s~0).NsrR(b!3,dim!2,s~5).ProhmpA2(b!1,b!3) 0
48 NsrR(b!1,dim!2,s~1).NsrR(b!3,dim!2,s~4).ProhmpA2(b!1,b!3) 0
49 NsrR(b,dim!1,s~2).NsrR(b,dim!1,s~5) 0
50 NsrR(b,dim!1,s~3).NsrR(b,dim!1,s~4) 0
51 NsrR(b!1,dim!2,s~1).NsrR(b!3,dim!2,s~5).ProhmpA1(b!1,b!3) 0

```

```

52 NsrR(b!1, dim!2, s~2) .NsrR(b!3, dim!2, s~4) .ProhmpA1 (b!1, b!3) 0
53 NsrR(b!1, dim!2, s~1) .NsrR(b!3, dim!2, s~5) .ProhmpA2 (b!1, b!3) 0
54 NsrR(b, dim!1, s~3) .NsrR(b, dim!1, s~5) 0
55 NsrR(b, dim!1, s~4) .NsrR(b, dim!1, s~4) 0
56 NsrR(b!1, dim!2, s~2) .NsrR(b!3, dim!2, s~5) .ProhmpA1 (b!1, b!3) 0
57 NsrR(b, dim!1, s~4) .NsrR(b, dim!1, s~5) 0
58 NsrR(b, dim!1, s~5) .NsrR(b, dim!1, s~5) 0
end species

```

### B.3 Dimer model 2 (DM2)

DM2 has 41 species and 109 reactions.

$$\begin{aligned}
 \dot{x}_1 &= -p_1x_1x_2 - p_{26}x_4x_1 - p_{26}x_3x_1 + p_{27}x_9 \\
 &\quad + p_{27}x_{10} + p_6x_8 + p_6x_{13} + p_6x_{19} + p_6x_{26} \\
 &\quad + p_6x_{31} \\
 \dot{x}_2 &= +p_{11}x_6 - p_{11}x_2 + p_{12} - p_1x_1x_2 \\
 &\quad - p_1x_8x_2 - p_2x_8x_2 - p_1x_9x_2 - p_1x_{10}x_2 - p_{18}x_{11}x_2 \\
 &\quad - p_1x_{13}x_2 - p_2x_{12}x_2 - p_3x_{13}x_2 - p_1x_{14}x_2 - p_2x_{14}x_2 \\
 &\quad - p_1x_{15}x_2 - p_2x_{15}x_2 - p_{15}x_{16}x_2 + p_{19}x_{17} + p_{21}x_{17} \\
 &\quad - p_1x_{19}x_2 - p_2x_{18}x_2 - p_3x_{18}x_2 - p_4x_{19}x_2 - p_1x_{21}x_2 \\
 &\quad - p_2x_{20}x_2 - p_3x_{21}x_2 - p_2x_{22}x_2 + p_{16}x_{23} + p_{21}x_{23} \\
 &\quad - p_1x_{26}x_2 - p_2x_{24}x_2 - p_3x_{25}x_2 - p_4x_{24}x_2 - p_5x_{26}x_2 \\
 &\quad - p_2x_{27}x_2 - p_3x_{27}x_2 - p_1x_{31}x_2 - p_2x_{29}x_2 - p_3x_{30}x_2 \\
 &\quad - p_4x_{30}x_2 - p_5x_{29}x_2 - p_3x_{32}x_2 - p_2x_{33}x_2 - p_3x_{34}x_2 \\
 &\quad - p_4x_{35}x_2 - p_5x_{34}x_2 - p_3x_{36}x_2 - p_4x_{37}x_2 - p_5x_{37}x_2 \\
 &\quad - p_4x_{38}x_2 - p_5x_{39}x_2 - p_5x_{40}x_2 \\
 \dot{x}_3 &= -p_{26}x_3x_1 + p_{27}x_{10} - p_{28}x_3x_8 - p_{28}x_3x_{12} \\
 &\quad + p_{29}x_{15} + p_2x_{15}x_2 + p_{29}x_{22} + p_2x_{22}x_2 \\
 \dot{x}_4 &= -p_{26}x_4x_1 + p_{27}x_9 - p_{28}x_4x_8 - p_{28}x_4x_{12} \\
 &\quad + p_{29}x_{14} - p_{30}x_4x_{13} + p_{29}x_{20} - p_{30}x_4x_{18} + p_{31}x_{21} \\
 &\quad + p_3x_{21}x_2 - p_{30}x_4x_{25} + p_{31}x_{27} + p_3x_{27}x_2 + p_{31}x_{32} \\
 &\quad + p_3x_{32}x_2 \\
 \dot{x}_5 &= -p_{13}x_{11}x_5 + p_{14}x_{16} + p_{21}x_{16} + p_{21}x_{23} \\
 \dot{x}_6 &= -p_{11}x_6 + p_{11}x_2 \\
 \dot{x}_7 &= +p_{24}x_3 + p_{24}x_4 - p_{20}x_7 \\
 \dot{x}_8 &= +p_1x_1x_2 - p_1x_8x_2 - p_2x_8x_2 - p_{28}x_4x_8 \\
 &\quad - p_{28}x_3x_8 - p_6x_8 + p_{29}x_{14} + p_{29}x_{15} + 2p_6x_{12} \\
 &\quad + p_6x_{18} + p_6x_{24} + p_6x_{29} + p_6x_{33}
 \end{aligned}$$

$$\begin{aligned}
 \dot{x}_9 &= +p_{26}x_4x_1 - p_{27}x_9 - p_1x_9x_2 \\
 \dot{x}_{10} &= +p_{26}x_3x_1 - p_{27}x_{10} - p_1x_{10}x_2 \\
 \dot{x}_{11} &= +p_{25}x_7 - p_{13}x_{11}x_5 - p_{18}x_{11}x_2 - p_{21}x_{11} \\
 &\quad + p_{14}x_{16} + p_{19}x_{17} + p_{17}x_{23} \\
 \dot{x}_{12} &= +p_1x_8x_2 - p_2x_{12}x_2 - p_{28}x_4x_{12} - p_{28}x_3x_{12} \\
 &\quad - 2p_6x_{12} + p_{29}x_{20} + p_{29}x_{22} \\
 \dot{x}_{13} &= +p_2x_8x_2 - p_1x_{13}x_2 - p_3x_{13}x_2 - p_{30}x_4x_{13} \\
 &\quad + p_2x_{15}x_2 - p_6x_{13} + p_{31}x_{21} + p_6x_{18} + 2p_6x_{25} \\
 &\quad + p_6x_{30} + p_6x_{34} + p_6x_{36} \\
 \dot{x}_{14} &= +p_{28}x_4x_8 + p_1x_9x_2 - p_{29}x_{14} - p_1x_{14}x_2 \\
 &\quad - p_2x_{14}x_2 \\
 \dot{x}_{15} &= +p_{28}x_3x_8 + p_1x_{10}x_2 - p_{29}x_{15} - p_1x_{15}x_2 \\
 &\quad - p_2x_{15}x_2 \\
 \dot{x}_{16} &= +p_{13}x_{11}x_5 - p_{14}x_{16} - p_{15}x_{16}x_2 - p_{21}x_{16} \\
 &\quad + p_{16}x_{23} \\
 \dot{x}_{17} &= +p_{18}x_{11}x_2 - p_{19}x_{17} - p_{21}x_{17} \\
 \dot{x}_{18} &= +p_1x_{13}x_2 + p_2x_{12}x_2 - p_2x_{18}x_2 - p_3x_{18}x_2 \\
 &\quad - p_{30}x_4x_{18} + p_2x_{22}x_2 - p_6x_{18} - p_6x_{18} + p_{31}x_{27} \\
 \dot{x}_{19} &= +p_3x_{13}x_2 - p_1x_{19}x_2 - p_4x_{19}x_2 + p_3x_{21}x_2 \\
 &\quad - p_6x_{19} + p_6x_{24} + p_6x_{30} + 2p_6x_{35} + p_6x_{37} \\
 &\quad + p_6x_{38} \\
 \dot{x}_{20} &= +p_{28}x_4x_{12} + p_1x_{14}x_2 - p_{29}x_{20} - p_2x_{20}x_2 \\
 \dot{x}_{21} &= +p_{30}x_4x_{13} + p_2x_{14}x_2 - p_{31}x_{21} - p_1x_{21}x_2 \\
 &\quad - p_3x_{21}x_2 \\
 \dot{x}_{22} &= +p_{28}x_3x_{12} + p_1x_{15}x_2 - p_{29}x_{22} - p_2x_{22}x_2 \\
 \dot{x}_{23} &= +p_{15}x_{16}x_2 - p_{16}x_{23} - p_{17}x_{23} - p_{21}x_{23} \\
 \dot{x}_{24} &= +p_1x_{19}x_2 + p_3x_{18}x_2 - p_2x_{24}x_2 - p_4x_{24}x_2 \\
 &\quad + p_3x_{27}x_2 - p_6x_{24} - p_6x_{24} \\
 \dot{x}_{25} &= +p_2x_{18}x_2 - p_3x_{25}x_2 - p_{30}x_4x_{25} - 2p_6x_{25} \\
 &\quad + p_{31}x_{32} \\
 \dot{x}_{26} &= +p_4x_{19}x_2 - p_1x_{26}x_2 - p_5x_{26}x_2 - p_6x_{26} \\
 &\quad + p_6x_{29} + p_6x_{34} + p_6x_{37} + 2p_6x_{39} + p_6x_{40} \\
 \dot{x}_{27} &= +p_{30}x_4x_{18} + p_1x_{21}x_2 + p_2x_{20}x_2 - p_{31}x_{27} \\
 &\quad - p_2x_{27}x_2 - p_3x_{27}x_2 \\
 \dot{x}_{28} &= +p_{17}x_{23} \\
 \dot{x}_{29} &= +p_1x_{26}x_2 + p_4x_{24}x_2 - p_2x_{29}x_2 - p_5x_{29}x_2 \\
 &\quad - p_6x_{29} - p_6x_{29}
 \end{aligned}$$

$$\begin{aligned}
\dot{x}_{30} &= +p_2x_{24}x_2 + p_3x_{25}x_2 - p_3x_{30}x_2 - p_4x_{30}x_2 \\
&\quad + p_3x_{32}x_2 - p_6x_{30} - p_6x_{30} \\
\dot{x}_{31} &= +p_5x_{26}x_2 - p_1x_{31}x_2 - p_6x_{31} + p_6x_{33} \\
&\quad + p_6x_{36} + p_6x_{38} + p_6x_{40} + 2p_6x_{41} \\
\dot{x}_{32} &= +p_3x_4x_{25} + p_2x_{27}x_2 - p_3x_{32} - p_3x_{32}x_2 \\
\dot{x}_{33} &= +p_1x_{31}x_2 + p_5x_{29}x_2 - p_2x_{33}x_2 - p_6x_{33} \\
&\quad - p_6x_{33} \\
\dot{x}_{34} &= +p_2x_{29}x_2 + p_4x_{30}x_2 - p_3x_{34}x_2 - p_5x_{34}x_2 \\
&\quad - p_6x_{34} - p_6x_{34} \\
\dot{x}_{35} &= +p_3x_{30}x_2 - p_4x_{35}x_2 - 2p_6x_{35} \\
\dot{x}_{36} &= +p_2x_{33}x_2 + p_5x_{34}x_2 - p_3x_{36}x_2 - p_6x_{36} \\
&\quad - p_6x_{36} \\
\dot{x}_{37} &= +p_3x_{34}x_2 + p_4x_{35}x_2 - p_4x_{37}x_2 - p_5x_{37}x_2 \\
&\quad - p_6x_{37} - p_6x_{37} \\
\dot{x}_{38} &= +p_3x_{36}x_2 + p_5x_{37}x_2 - p_4x_{38}x_2 - p_6x_{38} \\
&\quad - p_6x_{38} \\
\dot{x}_{39} &= +p_4x_{37}x_2 - p_5x_{39}x_2 - 2p_6x_{39} \\
\dot{x}_{40} &= +p_4x_{38}x_2 + p_5x_{39}x_2 - p_5x_{40}x_2 - p_6x_{40} \\
&\quad - p_6x_{40} \\
\dot{x}_{41} &= +p_5x_{40}x_2 - 2p_6x_{41}
\end{aligned}$$

The relevant sections of the .net file for DM2 are:

```

# Created by BioNetGen 2.5.1
begin parameters
  1 kAB          4.52 # Constant
  2 kBC          0.113 # Constant
  3 kCD          1.34e-2 # Constant
  4 kDE          7.48e-3 # Constant
  5 kEF          0.43e-3 # Constant
  6 kr           0.1 # Constant
  7 NsrR_init    2.5 # Constant
  8 NO_init      0 # Constant
  9 NOext_init   0 # Constant
 10 O2_init      200 # Constant
 11 km           750 # Constant
 12 kp           0 # Constant
 13 k1           3.5 # Constant
 14 k_1          0.44 # Constant
 15 k2           850 # Constant

```

```

16 k_2          2e-4 # Constant
17 k_3          200 # Constant
18 k4           26 # Constant
19 k_4          2e-4 # Constant
20 k5           0.014 # Constant
21 k6           1.8e-4 # Constant
22 ProhmpA1_init 6e-3 # Constant
23 ProhmpA2_init 6e-3 # Constant
24 kd           0.71 # Constant
25 ke           0.83 # Constant
26 kA           10 # Constant
27 k_A          0.35 # Constant
28 kB           10 # Constant
29 k_B          0.4 # Constant
30 kC           10 # Constant
31 k_C          0.45 # Constant
end parameters
begin species
  1 NsrR(b,dim!1,s~0).NsrR(b,dim!1,s~0) NsrR_init
  2 NO(a) NO_init
  3 ProhmpA2(b,b) ProhmpA2_init
  4 ProhmpA1(b,b) ProhmpA1_init
  5 $O2(a) O2_init
  6 $NOext() NOext_init
  7 RBS() 0
  8 NsrR(b,dim!1,s~0).NsrR(b,dim!1,s~1) 0
  9 NsrR(b!1,dim!2,s~0).NsrR(b!3,dim!2,s~0).ProhmpA1(b!1,b!3) 0
 10 NsrR(b!1,dim!2,s~0).NsrR(b!3,dim!2,s~0).ProhmpA2(b!1,b!3) 0
 11 Hmp(n,o) 0
 12 NsrR(b,dim!1,s~1).NsrR(b,dim!1,s~1) 0
 13 NsrR(b,dim!1,s~0).NsrR(b,dim!1,s~2) 0
 14 NsrR(b!1,dim!2,s~0).NsrR(b!3,dim!2,s~1).ProhmpA1(b!3,b!1) 0
 15 NsrR(b!1,dim!2,s~0).NsrR(b!3,dim!2,s~1).ProhmpA2(b!3,b!1) 0
 16 Hmp(n,o!1).O2(a!1) 0
 17 Hmp(n!1,o).NO(a!1) 0
 18 NsrR(b,dim!1,s~1).NsrR(b,dim!1,s~2) 0
 19 NsrR(b,dim!1,s~0).NsrR(b,dim!1,s~3) 0
 20 NsrR(b!1,dim!2,s~1).NsrR(b!3,dim!2,s~1).ProhmpA1(b!1,b!3) 0
 21 NsrR(b!1,dim!2,s~0).NsrR(b!3,dim!2,s~2).ProhmpA1(b!3,b!1) 0
 22 NsrR(b!1,dim!2,s~1).NsrR(b!3,dim!2,s~1).ProhmpA2(b!1,b!3) 0
 23 Hmp(n!1,o!2).NO(a!1).O2(a!2) 0
 24 NsrR(b,dim!1,s~1).NsrR(b,dim!1,s~3) 0
 25 NsrR(b,dim!1,s~2).NsrR(b,dim!1,s~2) 0
 26 NsrR(b,dim!1,s~0).NsrR(b,dim!1,s~4) 0
 27 NsrR(b!1,dim!2,s~1).NsrR(b!3,dim!2,s~2).ProhmpA1(b!3,b!1) 0

```

```
28 NO3(a) 0
29 NsrR(b, dim!1, s~1) .NsrR(b, dim!1, s~4) 0
30 NsrR(b, dim!1, s~2) .NsrR(b, dim!1, s~3) 0
31 NsrR(b, dim!1, s~0) .NsrR(b, dim!1, s~5) 0
32 NsrR(b!1, dim!2, s~2) .NsrR(b!3, dim!2, s~2) .ProhmpA1(b!1, b!3) 0
33 NsrR(b, dim!1, s~1) .NsrR(b, dim!1, s~5) 0
34 NsrR(b, dim!1, s~2) .NsrR(b, dim!1, s~4) 0
35 NsrR(b, dim!1, s~3) .NsrR(b, dim!1, s~3) 0
36 NsrR(b, dim!1, s~2) .NsrR(b, dim!1, s~5) 0
37 NsrR(b, dim!1, s~3) .NsrR(b, dim!1, s~4) 0
38 NsrR(b, dim!1, s~3) .NsrR(b, dim!1, s~5) 0
39 NsrR(b, dim!1, s~4) .NsrR(b, dim!1, s~4) 0
40 NsrR(b, dim!1, s~4) .NsrR(b, dim!1, s~5) 0
41 NsrR(b, dim!1, s~5) .NsrR(b, dim!1, s~5) 0
end species
```